Prediction of Transient Stability Status and Coherent Generator Groups

KNUST

By

Emmanuel AsumingFrimpong

A Thesis submitted to the Department of Electrical and Electronic Engineering, Kwame Nkrumah University of Science and Technology in partial fulfilment for the degree of

Doctor of Philosophy

College of Engineering Department of Electrical and Electronic Engineering

August 2015

DECLARATION

I hereby declare that this submission is my own work towards the Doctor of Philosophy (PhD) and that, to the best of my knowledge, it contains no material previously published by another person nor material which has been accepted for the award of any other degree of the University, except where due acknowledgement has been made in the text.

……	……..	……..……
Student Name & ID	Signature	Date

Certified by:

……	……..	……..……
Supervisor 1	Signature	Date

……	……..	……..……
Supervisor 2	Signature	Date

Certified by:

……	……..	……..……
Head of Department	Signature	Date

ACKNOWLEDGEMENTS

The doctoral study at the Kwame Nkrumah University of Science and Technology (KNUST) has provided a solid foundation for my professional career. The study was fully funded by KNUST through the staff development programme initiated by Prof. William Otoo Ellis, the Vice Chancellor of the University. I am grateful to Prof. W. O. Ellis for providing this opportunity. I am highly indebted to my supervisors: Prof. Johnson Asumadu of Western Michigan University, USA,and Prof. Philip Yaw Okyere of KNUST. These distinguished scholars spent time and energy towards assisting me chart my research directions, reviewing my articles and supporting my study progress. Through the time spent with them, I have gained more knowledge about the power industry, learned how to think creatively and analytically, and built confidence to tackle complex engineering problems.

I will forever be grateful to my elder brother, Prof. Richard FrimpongOppong for his encouragement and for providing access to journal articles. I would also like to express my appreciation to Mr. Isaac DjanOtchere, my former student who provided me access to journal articles. I am also grateful to my wife, RubbyNtiamoahBoafo for her immense moral support.

My gratitude also goes to Elder Philip Agyapong, of Kwamo, Ghana for his encouragement.

ABSTRACT

The prediction of transient stability status and instability scenarios such as coherent generator groups has become extremely important for the improvement of power system performance in the event of large disturbances. This research workis aimed at developing various schemes for providing advance information on the stability status of power systems following a transient disturbance. The work also focuses on predicting coherent generator groups that are likely to be formed when a system is predicted to become transient unstable. Power System Simulator for Engineers (PSSE) software is employed to model a test system and carry out simulations. MATLAB® software is used for the analysis and development of the prediction schemes. Three schemes for predicting transient stability status and one scheme for predicting coherent generator groups have been developed. Rotor speed deviation following a disturbance was found to be an excellent input parameter for the schemes. The first proposed method for predicting transient stability status employs the Daubechies 4 mother wavelet to decompose rotor speed deviation data obtained for three consecutive cycles after the tripping of a line or bus. The wavelet entropies subsequently obtained are then used as input to an algorithm which predicts the transient stability status of a power system. The prediction accuracy of this method was found to be 91.2%. The second transient stability status prediction schemeuses the sum of the maximum rotor speed deviations of system generators obtained within the first cycle after the tripping of a bus or line following a transient disturbance for its prediction. The obtained sum is then used as input data to a trained multilayer perceptron neural network (MLPNN) which is used for the prediction. This method was found to be 100% accurate. The third scheme developed is anchored onstability status prediction of each generator based the maximum rotor speed deviation (MSD) of that generator, obtained within the first cycle after the tripping of a line or bus. The MSD of each generator has

also been used as input to a trained MLPNN assigned to that generator forits transient stability prediction. The method has been found to return 98.05% accuracy in generator transient stability predictions.The final scheme developed is aimed at identifying coherent generator groups only after successful prediction of system transient instability. This final scheme has been realized via two MLPNNs each of which is equipped with three input neurons. Herein, the input data to the three input neurons are: (1) MSD of a reference generator in a predicted coherent group, (2) MSD of a generator to be placed in a group, and (3) the difference between the two MSDs. The proposed coherency prediction scheme has been tested exhaustively and found to be90.43% accurate. The proposed schemes which rely principally on MSD are computationally fast and efficient in their respective predictive capabilities; and can therefore be easily implemented on-line in real systems with the availability of phasor measurement units.

KNUST

NYANSAPƆ W ƆSANE NO BADWENMA

TABLE OF CONTENT

LIST OF TABLES

Page

KNUST

LIST OF FIGURES

Pag

KNUST

LIST OF ABBREVIATIONS

KNUST

ANN – Artificial Neural Network

AR – Autoregressive

COI – Centre of Inertial Angle

CWT – Continuous Wavelet Transform

DWT – Discrete Wavelet Transform

FIS – Fuzzy Inference System

GCPT – Geometrical Characteristics of Post-fault Trajectory

IMFs – Intrinsic Mode Functions

PSSE – Power System Simulator for Engineers

MLP – Multilayer Perceptron

MLPNN – Multilayer Perceptron Neural Network

MSD – Maximum Rotor Speed Deviation

NN – Neural Network

OMIB – One Machine Infinite Bus Transform

OS – Out-of-Step

PMU – Phasor Measurement Unit

RBF – Radial Basis Function

RBFNN – Radial Basis Function Neural Network

SMSD – Sum of Maximum Rotor Speed Deviation

WT – Wavelet Transform

KNUST

Chapter 1

INTRODUCTION

1.1 Overview

The rapid growth in industrialization, modernization, and population all over the world has increased the demand for electric power. The high cost of building new transmission lines to handle the increased demand, coupled with the difficulty in securing right-of-ways has resulted in larger power being transmitted through existing lines. This reduces stability margins and endangers power system stability, especially under large disturbance conditions [1].

Due to the complexity and geographical vastness of a practical power network, instability of power systems has been divided into various categories. The first stage of the categorisation, partitions power system instability into two categories: load driven and generator driven instabilities. Load driven instabilities mainly include voltage instability and voltage collapse problems. Generator driven instability is also known as rotor angle instability. Rotor angle stability is mainly due to synchronism of generators, that is, ability of generating units to work together at prescribed synchronous frequency. The angle stability is divided into short-term and long-term periods. The short-term angle stability is known as transient stability; an important subset of power system stability. The long-term angle stability consists of small signal and frequency stability [2]. This work is in the area of transient stability which is defined as the ability of synchronous machines to remain in synchronism after being subjected to severe disturbances.

Power systems are subjected to wide range of abnormal conditions such as faults, generator tripping, line switching, loss of excitation, or load shedding. These severe disturbances may cause large separation of generator rotor angles, large swings of power flows, large fluctuations of voltages, and currents at generator or transmission line terminals. The occurrence of any of these may eventually lead to loss of synchronism or what is called out-of-step (OS) operation between a generator and the rest of the power system, or between interconnected power systems.

Loss of synchronism leads to blackouts [3]. For example, 2003 saw separate blackouts in Italy, Sweden/Denmark, and USA/Canada, affecting millions of customers. Also, the wide area disturbance in 2006 to the Union for the Co-ordination of Transmission of Electricity (UCTE) system caused the system to split in an uncontrollable way, forming three islands [4].Furthermore, the Ghana power system suffered one system collapse in 2011 and three system collapses in 2012 [5]. The system collapse in 2011 was due to the explosion of a circuit breaker leading to the loss of a generating unit. The first system collapse in 2012 was due to the tripping of two generating units as a result of a bus fault. The second collapse was a result of the tripping of the inter tie line between Ghana and Cote d'Ivoire owing to the loss of a generator in the Cote d'Ivoire power system. The third system failure occurred because of the tripping of a generator due to transformer in-rush current.

Indeed, an OS condition may result in torsional resonance and pulsating torques that are severely harmful to the generator-turbine shaft. If such OS condition occurs, it is imperative that the asynchronous generator(s) is/are isolated to avoid widespread outages, flashovers and equipment damage[3].

A solution to OS problems is the use of schemes that analyse transient disturbances to determine critical clearing times, predict possible transient instability and offer techniques for improvement of transient stability [1, 6].To this end, research is on-going and a number of schemes for evaluating (that is determining critical clearing times) [7-13], detecting transient instability [3, 14-18], predicting transient stability or otherwise [6, 19-32], and improving transient stability [1, 33-35] have been developed. These proposed methods have addressed the problem of transient instability with varying levels of successby using different power system inputs such as rotor angle, mechanical input power, generator kinetic energy deviation, average acceleration during fault, angular velocity, bus voltage, line current, and rotor speed. Signal processing tools such as discrete Fourier transforms, wavelet transform, and k-means clustering have been used. Decision making tools such as neural networks, fuzzy logic, and decision trees have been employed. A detailed review of the schemes is presented in Chapter 2 of this thesis.

An OS scheme must operate on-line, act speedily and accurately. It must also be robust and simple to implement. All these desired features are yet to be found in a single scheme. For example, rotor angles which are the most widely used input parameter for OS studies have implementation challenges. The practical use of rotor angles in algorithm require centre of inertia reference values which also require continuous updates using real time measurements [19]. This introduces extra pre-processing and significant errors. Hence, an input parameter which does not need to be expressed with reference to any other and which can be easily captured is required [19].

A transient instability issue that needs to be addressed is islanding in power systems [2].When system islanding becomes inevitable, it has to be controlled. Controlled or intelligent islanding is a critical way of preventing large disturbances from adversely affecting system stability and hence

reliability. Successful intelligent islanding results in the maintenance of suitable island frequency and voltage, both transiently and in post disturbance steady state. This allows faster system recovery [37]. An important requirement for successful controlled islanding is the determination of the island boundaries. The criterion for determining these boundaries is largely dependent on generator coherency[38]. In order to achieve the foregoing, a number of off-line [39,40] and on-line [41-51] generator coherency identification methods have been proposed. The off-line schemes generally put system generators into fixed coherent groups whereas most of the on-line schemes are adaptive in their coherent grouping. This makes the on-line schemes a preferred choice in coherency identification. However, the existing online schemes are either complex, have reduced accuracy or slow in identifying coherent groups.

1.2 Aim of Study

This study focused on improving the control of power systems during transient instability. The specific objectives were to develop on-line schemesto: (i) predict transient stability status, and

(ii) identify coherent generator groups.

1.3 Work Done

Three schemes for predicting transient stability status and one method for predicting coherent generator groups have been developed. The schemes are:

(a) Speed deviation and wavelet analysis based generator out-of-step prediction scheme

(b) Speed deviation and multilayer perceptron neural network (MLPNN) based generator out-of-step prediction scheme

(c) Speed deviation and MLPNN based system transient stability status prediction scheme

(d) Speed deviation and MLPNN based coherent generator groups prediction scheme

This research has made use of rotor speed deviation as the key power system input data. Rotor speed deviations of generators unlike rotor angles do not need to be referenced to any value. Thus there is no computational burden and practical implementation difficulties. Rotor speed deviation of each generating unit can be obtained with the help of phasor measurement units (PMUs)[52,53].

The signal processing tool employed in the study was the discrete wavelet transform (DWT). DWT is a mathematical technique and has a special feature of variable time-frequency localization, which is different from the windowed Fourier transform [54]. It processes data at different scales so that they may provide multiple resolutions in frequency and time [54]. Wavelet analysis is capable of revealing aspects of data that other signal analysis techniques miss; aspects such as trends, breakdown points, discontinuities in higher derivatives, and self– similarity. Wavelet is able to compress and de–noise a signal without appreciable degradation [55].

The multilayer perceptron artificial neural network (MLPNN) was employed as a decision making tool. MLPNN is apopular neural network architecture [56-58]. Artificial Neural Networks (ANNs) represent a modern and sophisticated approach to problem solving widely explored also for power system protection and control applications. The ANNs perform actions similar to human reasoning, which relies upon experience gathered during a training process. Advantages of ANNs computing methodologies over conventional approaches include faster computation, learning ability, adaptive features, robustness, and noise rejection [30]. The MLP can be trained by a back- propagation

algorithm. Typically, the MLP is organized as a set of interconnected layers of artificial neurons; input, hidden, and output layers [59].

The Daubechies 4 (db4) mother wavelet was employed to develop a generator out-of-step prediction scheme. The scheme uses rotor speed deviations as power system input data. The speed deviations wereobtained withinthe first 3 cycles after the tripping of a line or bus. The rotor speed deviations were processed using wavelet analysis. Wavelet entropies of level 8 detailed coefficients obtained in three successive cycles were used to predict the generators that go out of step, with the help of a decision logic. Test results of the scheme show 100% prediction accuracy for out of step conditions involving one or two generators. 91.2% prediction accuracy was recorded for the prediction of stable generator conditions.

An improved generator out-of-step prediction scheme was further developed using rotor speed deviations and a multilayer perceptron neural network (MLPNN). The input data fed into the MLPNN was the maximum rotor speed deviation (MSD) obtained within the first cycle after the tripping of a line or bus. Prediction accuracy of the MLPNN-MSD based generator out of step prediction scheme was 100% accurate for all out-of-step cases. The prediction accuracy for stable generator conditions was 98.05%.

Also, a scheme for predicting the transient stability status of a system was developed. The scheme uses the sum of the maximum rotor speed deviations of the generators of the system as input data. Here too, a multilayer perceptron neural network was employed as a decision making tool. Test

results of the scheme show 100% prediction accuracy for both transient stable and transient unstable conditions.

A method for predicting coherent generator groups was also developed. The coherency prediction scheme uses the maximum rotor speed deviation obtained in the fifth cycle after the tripping of a line or bus following a disturbance. A multilayer perceptron neural network was again trained for the group prediction. Test results of the scheme show 90.43% prediction accuracy.

1.5 Thesis Outline

A review of pertinent literature is presented in chapter 2. In this chapter, anumber of methods for detecting and predicting out-of-step conditions are reviewed. Also, schemes for identifying coherent generator groups are reviewed. The review discusses the input data used, and the signal processing and or decision making toolsemployed. The strengths and weaknesses of the schemes are also pointed out.

Chapter 3 discusses the concept of power system stability and data acquisition for transient stability studies. The theory of wavelet analysis; a signal processing tool used in this work is also presented in this chapter. The chapter also discusses the theory of artificial neural networks; the decision making tool utilised in this work.

Chapter 4describes the methodologies developed for predicting transient stability status and coherent generator groups. The input data to the schemes and the operational algorithms are also presented. The test systems used and the simulations carried are also described in the chapter.

Chapter 5 presents results of simulations done as well as test results of the proposed schemes.

Chapter 6 presents the conclusion and provides discussion for future work.

KNUST

Chapter 2

LITERATURE REVIEW

KNUST

2.1 Introduction

Under normal operating conditions, an electrical power system is near equilibrium, with only minor deviations from true steady-state conditions caused by small, nearly continuous, changes in load. When a large disturbance such as a three-phase short circuit occurs in a power network, there are significant, nearly instantaneous rise in power requirement from some generators. Instead of the power system returning to a steady-state condition after the disturbance one or more generators may encounter sufficient variations in rotational speed that they could lose synchronism and as a result must be taken off-line to avoid catastrophic failures. Strictly speaking, sudden removal of such generators will decrease the available capacity on-line, thereby increasing transient energy imbalance in the system. The hypothesized system transient scenario, in the absence of emergence control action, could lead to cascaded unit shutdowns, culminating ultimately in system-wide blackouts [60, 61]. Consequently, emergency control strategiessuch as out-of-step blocking and tripping, fast-valve control of turbines, dynamic braking, superconducting magnetic energy storage system, system switching, modulation of high voltage direct current (HVDC) link power flow and load shedding are employed to mitigate the effect of cascading system failures [6]. The effectiveness of the aforementioned control actions are improved with the detection or prediction of transient instability [6]. As a corollary, researchers have come up with a number of transient instability detectionand prediction schemes. Some of these methods are reviewed in this chapter.

When a system becomes transient unstable, the major step taken is to split the system into various islands [62]. Subsequently, the generation and load of these islands are controlled. The primary

motive of controlled islanding is to limit the source of the disturbance and the affected areas to a minimum region, as soon as possible [62]. A reasonable approach to islanding can result in significant benefits to the corrective control actions that follow the islanding procedure [39, 63]. The criteria for determining the boundaries of the islands are stability within individual islands and minimum load-generation unbalance [62]. In determining the islands, the inherent structural characteristics of the system should be considered and the choice of these islands should not be disturbance dependent [39, 63]. Subsequently, the boundaries of the islands may be decided on the basis of coherency of generators [63]. This study has also reviewed a number of methods for identifying the coherency of generators

2.2 Methods for Detecting Transient Stability Status

Researchers have come up with a number of methods for detecting out of step conditions in power systems. Some of these methods have been reviewed in sub-sections 2.2.1 to 2.2.5. The strengths and weaknesses of the various methods have been pointed out. Generally,the detection schemes have a common disadvantage of detecting out of step conditions when they have alreadyoccurred and this does not augur well for improved system performance.

2.2.1 *Adaptive Out of Step Detection using Artificial Neural Network*

An out-of step detection scheme based on five inputs and an artificial neural network has been proposed in [14]. The scheme detects the out-of-step status of a particular machine with respect to other machines in the power system. The scheme was developed and validated using a 3generator, 9-bus test system. The inputs used are: mechanical input power (or pre-fault loading on generator), generator kinetic energy deviation, average acceleration during fault, and power flow on two

adjacent lines. The inputs are fed into a feed forward neural network trained with the stochastic backpropagation algorithm.

The scheme of [14] can only be employed in a system with the same topology. Thus its adaptability to a system of different topology will face serious challenges. Also, a long processing time will be required in a system with several generators since each generator has to be compared with the remaining others to predict whether or not that generator goes out of step.

Additionally, the time frame when the input data are captured was not specified.

2.2.2 *Transient Instability Detection by Identifying the Characteristics of a Surface on which a Post-Fault System Trajectory Lies*

A method for detecting transient instability based on generator rotor angles, angular velocities, and their rates of change has been presented in [15].An index is calculated by solving the intersectionpoint between a tangent plane and a straight line. The developed index detects system instability or out-of-step condition by identifying the characteristics-concave or convex-of a surface on which the post-fault system trajectorylies. An index value less than 1 or being discontinuous implies that the surface is convex, which implies system instability.The developed scheme was validated using the IEEE 39-bus test system.This scheme is computationally simple and reliable.

2.2.3 *Impedance and Prony Analysis-Based OS Detection*

In [3**]**, an OS detection method using an impedance-based relay and prony analysis is presented. The study was done using a system which comprises a single transmission line with a generator each at both ends. The input data required by the scheme is the voltage and current signals at the

relaying point. Prony analysis is used to track the actual system frequencies by decomposing the measured voltage and current signals into their modal components: amplitude, frequency, damping factor, and phase angle. Once the actual system modes are determined, the instantaneous apparent impedance seen by the relay is calculated. The instantaneous apparent impedance loci are then used to qualitatively describe the power system behaviour during the OS operation.

The method is not based on any developed indices. A qualitative description, unlike an indexbased one, makes the implementation of the scheme complex, especially for a large system.
Also, the scheme is unable to tell the specific generator that goes out of step.

2.2.4 *Transient Instability Detection based on Wide Area Measurement System*

The method for detecting power system transient instability presented in [16,17]employs techniques of the generalized one machine infinite bus (OMIB) transform. The detection of a loss of synchronism is made based on the geometrical characteristics of the post-fault trajectory (GCPT) of the generalized one-machine equivalent system at each time step. The study system used was the IEEE 145-bus test system. Simulations were also carried out on a real power system to verify the method. The scheme uses rotor angle, speed, and prime mover power input signals. For a given disturbance, the salient steps of the instability detection algorithm aredescribed as follows: The instability detection process involves ranking the machines according to their angles and calculating the equivalent trajectory of a candidate pattern by an OMIB transform. The algorithm then evaluates whether the trajectory is stable at the current instant using a geometric characteristic index of the post-fault trajectory and the discrete form of a uniform criteria. If the geometric characteristic index of the post-fault trajectory is less than zero or the discrete form of the uniform

criteria is less than zero, then the system is stable. When the geometric characteristic index of the post-fault trajectory and the discrete form of the uniform criteria are greater than zero then the algorithm uses the least squares approximation method to estimate parameters of equivalent system. The algorithm evaluates whether the parameter variation of the candidate OMIB increases or decreases the stability margin of the OMIB at current instants. If the change in unbalance power corresponding to OMIB parameters is larger than zero for positive speed or less than zero for negative speed, instability is indicated. In some peculiar cases, although the parameter variation is increasing the stability margin of OMIB system, the system could still be unstable if the discrete form of the uniform criterion is greater than zero. To avoid this peculiar instance, a condition is prescribed where if the conventional equal area criterion condition is less than zero, a new set of measurement is obtained at the next sampling instant and the procedure starts all over again.

The foregoing method requires complex computation and its practical implementation will be difficult.

2.2.5 *Transient Instability Detection based on Partial Centre of Inertia*

A method for detecting instability of multi-machine power systems using partial centre of inertia information has been proposed in [18]. The scheme is premised on the fact that a system's ability to maintain transient stability is based on its ability to convert its kinetic energy during a disturbance into another form of energy. Consequently, the method first determines the kinetic energy of each system generator at an arbitrary time. Subsequently, the obtained kinetic energies are summed to give the kinetic energy of the system at that arbitrary time.The maximum kinetic energy of the individual kinetic energies of the generators is obtained. The generator with the

maximum kinetic energy is then noted. The disturbed state of each generator is then obtained. A generator is classified as being disturbed if the ratio of its kinetic energy to the maximum kinetic energy is greater than 0.03.A stability index is then computed for all severely disturbed generators. A system is classified as transient unstable when the stability index obtained for all severely disturbed generators is greater than zero for four continuous samplings.

The proposed method is reliable in its ability to distinguish between stable and unstable swings.However, it is computationally demanding and also takes a long time to detect unstable swings.

2.3 **Methods for Predicting Transient Stability Status**

Control measures employed during transient instability will be more effective if they are implemented before instability sets in [6]. In pursuance of this, a number of schemes for predicting transient instability have been proposed [6, 19-32]. In the sub-sections that follow, a number of these schemes are reviewed.

2.3.1 ***Transient Stability Prediction by a Hybrid Intelligent System***

The scheme presented in [6] uses three input quantities obtained from each generating unit. The input quantities measured from each generator are: rotor angle measured 3 cycles after fault clearance, rotor angle measured 6 cycles after fault clearance, and angular velocity. The inputs are fed into a proposed hybrid intelligent system. The hybrid intelligent system comprises a preprocessor, an array of neural networks (NN), and an interpreter. The scheme was developed and validated using the PSB4 and IEEE 39-bus test systems.

Each NN has a multilayer perceptron (MLP) structure andLevenberg-Marquardt learning algorithm, which is one of themost efficient training mechanisms for estimation tasks.The instability criterion is based on the difference between any two generator angles. The scheme divides the whole set of synchronous machines into smaller groups, each group having only two machines. This task is performed by a pre-processor. The pre-processorconsiders all twosome combinations of the machines so that all asynchronous possibilities can be evaluated.The preprocessorassigns each couple to one subnet (NN). All NNs have the same number of input features. An interpreter gathers outputs of all NNs. If all the outputs are 1, then all generators are in the synchronous state, that is, transient stability is saved. Otherwise, transient stability is lost.

The technique reduces computational burden of the training phase, covers unknown and incorrect responses of the NNs, and determines tripped generators and islanded parts.Although the hybrid intelligent system requires short training times for the considered test systems, this time can rapidly grow for large power systems. This is a result of the large input data requirement of the scheme. Rotor angles used as inputs need to be expressed relative to a common reference. This reference cannot be based on a single generator, since any instability in the reference generator makes the relative angles meaningless. In order to overcome this difficulty, the concept of system centre of inertia (COI) angle is used to derive a reference angle
[19]. However, COI values in practice require continuous updates using real time measurements. This requires extra pre-processing and has significant errors. Also, the authors did not demonstrate how tripped generators and islanded parts are identified by the proposed method.

2.3.2 *Transient Stability Prediction by Committee Neural Networks*

A method for predicting the transient stability status of a power system has been proposed in [2022]. The study systems used werethe IEEE 9-bus and IEEE 14-bus test systems. This schemeuses the following input data: relative rotor angles of generators, generator speed, real and reactive power flows of generators, real and reactive power flows on transmission line, real and reactive power flows in transformers, and bus voltages. The inputs are fed into a trained dynamic structure of artificial neural networks called mixture of experts[20], multilayer perceptron neural network[21] or probabilistic neural network[22].

The proposed technique is reported to be 100% accurate in its predictions. However, its implementation does not seem to be feasible. This is because of the diverse and excessive number of input data required. For example, the input data set required for making any prediction in the IEEE14-bus test system that was used for the study is 107. The volume of data that has to be handled in a real system with hundreds and even thousands of busbarswill be prohibitive and will require an unacceptably long processing time.

2.3.3 *Out-of-Step Prediction based on Autoregressive Model*

An autoregressive (AR)model based out-of-step prediction scheme has been presented in [23]. The test system used the 10-generator western Japan 60Hz power system model. This scheme uses as input data, the phase difference of the voltage between buses, and rotor angle relative to the phase of the terminal voltage in each generator. Prediction of out-of-step between interconnected systems is made in three steps. The first step involves the identification of the AR model that represents the oscillations of phase difference of the voltage between substations and assessment of the stability

of the power system from the sign of the real part of the characteristic roots. A positive real part of the characteristic root represents stable status and a negative real part of the characteristic root represents unstable status. The second stage involves the identification of the AR model that represents the oscillation of the rotor angle relative to the phase of the terminal voltage in each generator if it is predicted in the first stage that the interconnected power systems will fall into instability. The last stage is the decision stage. Here, the system falls out-of-step on the condition that the frequency calculated from the characteristic root with a negative sign in the first stage is identical to that calculated in the second stage.

The period of occurrence of out of step after a fault was assumed to be 14s. The time frame of interest in transient stability studies is usually 3 to 5 seconds following a disturbance. It may extend to 10–20 seconds for very large systems with dominant inter-area swings [24]. Thus the period of 14s appears to be too long for the 10-generator test system used. It is not likely that this scheme when implemented in practical systems will yield good results. The authors indicated that the scheme is able to tell the specific generators which go out of step. This is however not demonstrated in the paper.

2.3.4 ***Transient Instability Prediction using Post-Disturbance Voltage Trajectories***

A rotor angle stability prediction scheme based on voltage trajectories following a disturbance has been presented in [19]. The IEEE 39-bus test system was used for the study. The proposed transient stability prediction system uses as inputs voltage magnitudes at key buses in the system. When a fault is detected, the system starts evaluating the proximity of the evolving voltage to pre-identified templates. These proximity values are then fed into a support vector machine classifier, which predicts the stability status of the power system.

The scheme has over 90.91% accuracy and is faster and simpler to implement compared with rotor angle-based schemes. However, the scheme uses predetermined voltage templates which depend on system loading and fault conditions. Therefore, the scheme may not respond appropriately to disturbances occurring during loading and fault conditions different from the conditions for which the voltage templates were obtained. The scheme is also unable to identify the specific generators which will go out of step.

2.3.5 *Support Vector Machine-Based Algorithm for Post-Fault Transient Stability Status Prediction*

The work presented in[25] demonstrates that the transient stabilitystatus of a power system following a large disturbance can be predicted on the basis of themeasured post-fault values of the generator voltages, speeds, or rotor angles. This method is an improvement over the one presented in [19].Synchronously sampled values provided by phasor measurement units of the generator voltages, frequencies, or rotor angles collected immediately after clearing a fault are used as inputs to a support vector machine classifier which predicts the transient stability status. The use of bus voltage magnitudes produced the most accurate andthe fastest predictions. Studies with the New England 39-bus test system and the Venezuelan power network indicated that the method is fast and accurate. Here too, the specific machines which will go out of step are not predicted.

2.3.6 *Neuro-Fuzzy approach to Transient Stability Prediction*

Atwo-layer fuzzy hyperrectangular composite neural network for real-time transient stability prediction using synchronized phasor measurements has been proposed in [26]. The study system

employed was the IEEE 39-bus test system. Stability prediction is based on an eight cycle window of phasor measurements which begins at fault clearing time. Three consecutive measurements of rotor angles, four cycles apart, are taken for each of the generators. Additionally, two velocities and one acceleration are computed from the generator angles. Thus a total of six input data is taken for each generator. Theneuro-fuzzy network is trained off-line and then used to make on-line predictions.

The technique is able to make fast predictions.The large volume of input data required for the off-line training of the proposed neuro-fuzzy network makesit difficult for the scheme to be implementedon-line in a practical power system with a large number of generators. The method will also suffer practical implementation challenges since it is based on rotor angles.

2.3.7 *Decision Tree Method for Transient Stability Prediction*

A method for predicting transient stability using decision trees has been presented in [27]. The method was tested using the IEEE 39-bus test system. The input data employed for stability prediction is the rotor angles of the 10 generators of the system. Stability prediction is based on an eight cycle window of phasor measurements which begins at fault clearing time. Three consecutive measurements, four cycles apart, are taken from each of the ten generator angles. The generator angles, measured in radians and in the centre of angle coordinates, are first written to a file in FORTRAN format. The written data is truncated to three digits after the decimal. In addition to the measured rotor angles, two velocities and one acceleration are computed from the truncated generator angles. Thus a total of six input data is obtained for each generator.The input data taken

from the 10 generators of the system are then used as inputs to a decision tree which has already been trained off-line using various generated fault cases.

This scheme has high accuracy, in excess of 95%. However, a large volume of training data is required for developing a single decision tree. For a system with large number of generators, building a single decision tree will be extremely difficult. Decision trees are only applicable for transient stability prediction in very small power systems due to the exponential growth of possible states with the number of generators and system buses [2]. This method also suffers from the setbacks associated with the use of rotor angles as input data.

2.3.8 *Transient Stability Prediction using Fuzzy Neural Network*

The scheme in [2] predicts transient stability status using generator rotor angles as inputs, and a fuzzy neural network as decision making tool. The prediction technique was tested using simulations carried out on the PSB4, IEEE 14-bus and IEEE 39-bus test systems. This scheme uses a six-cycle window of generator rotor angles. The window begins at the fault clearing time and contains three consecutive measurements. These measurements are taken three cycles apartfor each generator rotor angle. The generator rotor angles are measured in radians and in centre of angle coordinates. Two velocities and one acceleration are then derived from the three angle measurements to provide a total of six predictors per generator.

Only test results for the PSB4 test system are shown in [2].No results were presented for the IEEE 14-bus and IEEE 39-bus test systems, which are relatively large systems compared with the PSB4. Results presented for the PSB4 system show high accuracy. This method, like others which use

generator rotor angles will suffer implementation challenges due to difficulties in obtaining the centre of inertia angle in real time.

2.3.9 *Out-of-Step Prediction using Angular Velocity*

An OS prediction scheme using angular velocity data measured directly from power system generators has been designed and implemented in [28]. The angular velocities are measured by electromagnetic sensors and gears fastened to rotors of the generators. The angular velocity data of each generator is used to determine the generator's phase-angle shift after a system disturbance. This is done by integrating the angular velocity data. The phase angle calculation is initiated by detecting sudden changes of output power in each generator, which may have been triggered by a power system disturbance.An out-of-step between two generators is predicted by the phase angle difference between them using the following criteria:

i. The predicted phase angle difference between the two generators exceeds a predetermined threshold value which is 180 electrical degrees.
ii. The predicted phase angle difference is still increasing.

An out-of-step between two generator groups is predicted using a matrix.Field tests of this scheme were carried out using the Kansai Electric Power Co., Inc.hydroelectric power station. The station has four-generators coupled to a single bus. Test results showed that the developed scheme is accurate and can be practically implemented.

Measurement error gives limitations in applyingthe developed scheme. Angular-velocity measurement errors, especially, are enlarged by the integrating calculation process, and it limits the time length that the control is effective after initiating the calculation. Also having to compute

the phase angle difference between the various generators of a large system will be complicated and time consuming. These limitations will make the use of this scheme in large systems difficult.

2.3.10 *Out-of-Step Protection with AI Methods*

An OS prediction method which utilizes a multilayer perceptron artificial neural network(ANN) has been presented in [29, 30]. Additionally, a fuzzy inference system (FIS) was employed in [29]. The schemes were developed using a simple three-generator power systemconnected to an infinite bus. All the generators were coupled to a single bus. The schemes employ the following power input signals: machine angular frequency deviation, impedance angle, active power, reactive power as well as resistance and reactance measured at the generator terminals from machine phase currents and voltages.The six inputs are further pre-processed by a Fuzzy

Inference System (FIS) module in [29]yielding nine input features which are fed into the ANN.

In [30], different input data combinations and artificial neural network architectures were experimented. The developed hybrid OS detector [29] is able to recognize OS conditions 1001000ms before they actually occur.

Reference [29]did notprovide details of the nine outputs of the FIS module. The digital processing of phase voltages and currents to obtain input signals such as components of generator power and impedance vector (seen from machine terminals) increases the overall processing time of the scheme especially for a large system. Additionally, nine input features employed for a single-bus system will mean excessively large number of input data for a large system.

2.3.11 *Transient Instability Prediction using Decision Tree Technique*

Reference [31] has presented a decision tree based method for out-of-step prediction of synchronous generators. The method was developed using a 9-bus dynamic network. The proposed OS scheme uses five inputs for prediction. The inputs are: mechanical input power, kinetic energy deviation, average acceleration, electrical output power at the moment of fault clearing, and fault duration. These inputs are fed into a decision tree which indicates system stability or instability.

The proposed method is essentially a detection scheme rather than a prediction scheme. The method indicates transient instability whenit has already occurred. Also, it is computationally demanding. Additionally, the method does not indicate specific machines that go out of step in relation to others. Again, decision trees are not suitable for large systems due to the exponential growth of possible states with the dimension of the system [2].

2.3.12 *Fuzzy rule-based transient stability prediction*

The schemein [32] builds compact and transparent fuzzy rule-based classifiers for rapid stability assessment; the classifiers are initialized by large accurate decision trees. The approach starts by selecting strategic monitoring buses where phasor measurement units are placed to capture widearea response signals in real-time operation. These measurements are processed in the time and frequency domains for extracting selected decision features such as the peak spectral density of angle, frequency, and their dot product evaluated over the grid areas. Large-size decision trees are used to generate initial accurate classification boundaries for decision making. From the decision classification boundaries, fuzzy membership functions are developed and the corresponding fuzzy rule base is formulated parsimoniously by eliminating redundant membership functions and rules using a similarity measure.

Test results on a large database of detailed simulations of the Hydro-Quebec grid and actual measurements recorded with existing wide-area measurements show good results. The method requires1–2 s after fault clearance to make accurate predictions. This time taken to make prediction is rather long [36]. Some instability conditions can easily occur before this time.

2.4 **Generator Coherency Identification**

Generator coherency identification is establishing itself as an important task to circumvent cascading failures within wide-area power systems and as a necessary pre-processing stage in real-time control for transient stability [47].To achieve this, a number of off-line schemes have been developed to identify coherent groups of generators [39,40].Studies have shown that the use of predetermined boundaries may not always indicate the optimum islanding configuration for some disturbances[62]. Coherent generator groups may differ in response to various disturbances at different system operating conditions [41]. For instance, an event happening near a coherent group may cause its member generators to lose coherency during oscillation. Thus, for effective damping control for online operation of power systems, it is essential to have an online adaptive coherency grouping approach [41, 50]. Such a scheme will set the boundaries of islands based on the nature of the disturbance. In pursuance of this, a number of methods for detecting coherent generators online to facilitate system separation have been proposed. Some of these schemes [4151] are reviewed in sub-sections 2.4.1 to 2.4.10.

2.4.1 *K-harmonic Means Clustering Approach for Coherency Grouping*

The proposed coherency grouping scheme in [41] uses the inertia constant and speed deviation data of each generator as input data. The test system used for the study was the IEEE 68-bus 16machine test system. The K-harmonic means clusteringwhich is a global optimization technique is applied to the input data for the coherency grouping. The algorithm first receives all generator data and then initializes group centres. The distances between each generator and the group centres are obtained. The group centres are then updated in order to minimise a cost function. The group centres are updated until a metric used is satisfied or the maximum number of iterations is reached. Coherency grouping is achieved when the group centres become stable.

Test results of the scheme were not presented in the paper [41].Also, the algorithm is computationally time consuming.

2.4.2 *Coherency Identification using Hilbert-Haung Transform*

An online scheme for identifying coherent generator groups using Hilbert-Haung transform has been proposed in [42]. The Hilbert–Huang transform is an empirical mode decomposition along with Hilbert transform. Coherency between generators is tracked by examining the instantaneous phase differences among inter-area oscillations and swing curves in disturbed multi-area power systems.Huang's empirical mode decomposition is applied to extractdominant oscillatory modes from inter-area oscillations and swingcurves. Hilbert transform on these modes yields their instantaneousphase values. The instantaneous phase information is furtherutilized to identify the degree of coherency between inter-areaoscillations or disturbed machine pairs. Two generators are said to be coherent if the differencebetween the instantaneous phases of their swing curvesis zero

at any instant in time.In order to compute the instantaneous phase difference, the proposed algorithm first extracts the mono-component intrinsic mode functions (IMFs) from the swing curves/inter-area oscillations and then computes the instantaneous frequency of the extracted IMFs. An IMF is a waveform obtained by repeatedly shifting a distorted signal until no further baseline signals can be detected. The IMFs whose instantaneous frequencies match each other are then selected for computing the instantaneous phase difference. The instantaneous phase difference is obtained by taking the difference between the instantaneous phase angles of two generators.

Graphical analysis of swing curves show that the scheme is capable of identifying coherent generators. However, no quantitative result was provided to validate the algorithm.

2.4.3 *Coherency Identification using Fourier Analysis*

The proposed coherency identification scheme [43] applied Fourier analysis to wide area generator speed measurements.The study utilized the 68 bus Northeast Power Coordinating Council (NPCC) system. The discrete Fourier transform of generator speed is first obtained and thenumber of equally spaced spectral components is then calculated. A vector foreach time value which contains the Fourier coefficientsseparated by the spectral frequency resolution are then determined. The coefficients are complex and denote both the magnitude and phase of each oscillation mode.In order to determine the dominant inter-area mode, the Fourier coefficient with the largest amplitude is determined. The final establishment of a dominant inter-area mode is then carried out. Once a dominant inter-area mode has been identified, the phase of that mode is determined for the involved system generators and a vector is organized including all these phases. Finally, a phase comparison is performed where the phase angle of one of the generators is used as the reference angle.

Generator coherency is then defined by a given function where generators having (approximately) the same phase difference with respect to the reference angle represent a coherent group.

Test results presented indicate that the method is accurate.The scheme places generators with the same phase angle with respect to the reference angle, in the same coherent group, and places generators with different phase angles with respect to the reference angle, in another coherent group. This essentially means that the method classifies generators into two fixed coherent groups. Variations in system conditions during disturbance will reduce the accuracy of the scheme since not only two coherent groups will be formed all the time. Additionally, the proposed method is computationally complex and is also not fast. Furthermore, identifying the dominant inter-area mode from the Fourier transform coefficient amplitudes, in the presence of damped oscillations, may be error-prone especially when studying 'ringdown' signals [44].

2.4.4 *Coherency Identification using K-means Clustering*

The coherency identification scheme proposed in [45] made use of real-time information obtained from wide area measurement systems. The scheme was tested using the IEEE 39-bus test system. Generator angle, angular velocity, and unbalanced power constitute the input data used by the proposed algorithm. The scheme first formulates a matrix using the input data. The formulated matrix is then normalized and the K-means clustering algorithm applied to divide the normalized matrix into two groups. A coherency index is subsequently calculated to evaluate the clustering result.

The proposed coherency identification scheme requires little computation, has fast identification and high accuracy. However, the scheme has a disadvantage of dividing the generators into two coherent groups at all times. The number of coherent groups may differ in response to various events at different operating conditions.

KNUST

2.4.5 *Coherency Identification based on Correlation Characteristics of Generator Rotor Angles*

The method proposed in [44] recognizes coherent groups of generators based on the correlation characteristics of generator rotor angle oscillations. The study system used was the IEEE 39-bus test system. The algorithm starts by measuring generator rotor angle oscillations in a time window and then calculating correlation coefficients for all pairs of units. Negative correlation coefficients are discarded. The average correlation coefficient is then calculated from the remaining coefficients. The calculated average correlation coefficient serves as a reference value. The calculated correlation coefficients are then compared with the reference value. All generator pairs with correlation coefficients greater than the reference value are placed in one coherent group. For generators pairs with correlation coefficients less than the average value, a new average correlation coefficient is calculated. This new average correlation coefficient serves as a new reference value to classify the generators. The procedure is repeated until all generators are placed in coherent groups.

The proposed method is adaptive in the number of coherent groups classified. The classification is based on the system conditions during the disturbance. The method is also computationally simple and accurate. However, it is time consuming.

2.4.6 *A Wide Area Information based Online Recognition of Coherent Generators*

By using the power-angle information of generators measured by wide area measurement systems, anew method that enables online recognition of coherent generators in power system is proposed in [46]. Firstly, power-angle values are sampled. The sampled values are then fitted by trigonometric function to attain the primaryresult of coherency identification. The final result ofcoherency identification is achieved by calculating the discreteFréchet distance.

The proposed method is simple and not computationally demanding. It can also be applied to complex interconnected power grids. However, the proposed method is not fast.

2.4.7 *Coherency Identification using Multiflock-based Technique*

A novel multiflock-based technique to identify generator coherence within a short observation window has been presented in [47]. The measurement based approach transforms generator data from the observation space to an information space, whereby the generator frequencies and phases characterize the movement and dynamics of boids within multiple flocks. Analysis of the boids' trajectories enables the discrimination of multiple flocks corresponding to coherent generator clusters. The effectiveness of the proposed method was demonstrated using the 39-bus New England test system and a modified IEEE 118-Bus test system.

Although the proposed method is claimed to be fast and accurate, the authors did not state its practical implementation in respect of large power systems.

2.4.8 *CoherencyIdentification based on Nonlinear Koopman Modes*

The proposed coherency identification scheme in [48,49] employs Koopman modes derived through spectral analysis of the Koopman operator. The Koopman operator is a linear, infinitedimensional operatorthat is defined for any nonlinear dynamic system and capturesfull information of the system.Koopman modes analysis is applied on generator frequency data to characterize nonlinearoscillatory modes for coherency identification.

The method is computationally demanding and does not offer fast coherency identification.

2.4.9 *Generator Coherency Identification using the Continuation Method*

The paper [50], presents a generator coherency indices tracing approach using the continuation method. The tracing method involves modelling of appropriate power system dynamics and network representation to obtain aJacobian matrix, and a globally convergent technique to make the continuation method applicable. Using this approach, it is then possible to trace the loci of the generator coherency indices over a range of system operating conditions. The loci provide information about the grouping associated with the slow modes. The approach was appliedto the 10-generator 39-bus New England system, and the 29-generator179-bus model of the Western Electricity Coordinating Council (WECC) system**.**

This method essentially uses the notion of slow coherency arising from inter-area oscillations. It uses singular perturbation to assess time-scale separation of the inter-area and local modes, and implements an eigenvector-based method to identify coherent generator groups. This method is computationally inefficient when the inter-area oscillation is not sufficiently reduced [47].

2.4.10 ***Coherency Identification based on Independent Component Analysis***

The proposed approach presented in [51] is able to identify the cluster of generators and buses following a disturbance in a system. Coherency properties are extracted from wide-area generator speed and bus voltage angle signals. The mixing ratio of independent components extracted using the proposed independent component analysis method is used to cluster the generators and buses displaying the common features in the measured signals into their coherent areas. The coherency identification method was tested on a 16-machine 68-bus test system.

The method accurately identifies the coherent groups of generators even with the presence of noise in the measured data. However, the scheme is not fast.

KNUST

Chapter 3

THEORITICAL BACKGROUND

3.1 Power System Stability

Power systems are subjected to wide range of disturbances; small and large. Small disturbances in the form of load changes occur continually.Under such conditions, the system must be able to adjust to the changing conditions and operate satisfactorily. It must also be able to survive numerous disturbances of a severe nature, such as a short circuit on a transmission line or loss of a large generator. A large disturbance may lead to structural changes due to the isolation of the faulted elements [24].

Power system stability is the ability of an electric power system, for a given initial operating condition, to regain a state of operating equilibrium after being subjected to a physical disturbance, with most system variables bounded so that practically, the entire system remains intact. Power system stability may be classified as rotor angle stability or voltage stability [24, 64].

Voltage stability is the ability of a power system to maintain steady acceptable voltage at all the busses in the system under normal operating conditions and after the system has been subjected to disturbances. The system enters into a state of voltage instability when a change in system condition such as an increase in load causes progressive decrease in voltage. The main cause of voltage instability is the inability of the power system to meet the demand for reactive power [64, 65].

Rotor angle stability in a power system is the ability of interconnected synchronous machines to remain in step with each other following a disturbance in the power system. Rotor angle stability may be classified as small signal stability and transient stability. Small signal stability relates to small disturbances whereas transient stability relates to large disturbances [64, 65]. The focus of this research is in the area of transient stability.

3.1.1 *Transient Stability*

Transient stability is the ability of synchronous machines to remain in synchronism after being subjected to a severe disturbance. A severe disturbance may be a sudden application of load, loss of generation, loss of large load, or a fault on the system [65,66]. During normal operations of a generator, the output electric power from the generator produces an electric torque that balances the mechanical torque applied to the generator rotor shaft. The generator rotor therefore runs at a constant speed. When a fault reduces the amount of power transmitted, the electric torque that counters the mechanical torque is also decreased. If the mechanical power is not reduced during the period of the fault, the generator rotor will accelerate with a net surplus of torque input. When an unstable condition exists in apower system, one or more generators rotate at speeds different from the othergenerators of the system. Such an event is referred to as a loss of synchronism or an out-of-stepcondition. OS conditions may result in torsional resonance and pulsating torques that are severely harmful to generator-turbine shaft. When OS conditions occur, it is imperative that all asynchronous generators be isolated to avoid widespread outages, flashovers and equipment damage [3].

3.1.2 **Islanding in Power Systems**

Presently, power systems are being operated closer to stability limits than before in order to meet the requirements of a rapidly growing electricity market. Therefore, there is a higher probability that unexpected tripping of system elements may cause cascading outages or inter-area out of step in a power system which may in turn lead to unintentional system separation. When system separation is unavoidable, the control centrecan separate the system into electric islands in a controlled manner. The islands will have a better chance of surviving if in each island formed, generation and load imbalance as well as generator frequency swings are keptwithin acceptable limits [67].

Three issues are important for controlled separation in power systems [67]. These are:

(a) *Determination of separation interfaces to form the islands*

To determine separation interfaces, coherent generation groups, load/generation balance, and other security criteria such as avoiding overloading of any transmission line within islands, need to be considered. In addition, consideration should be given to whether the separation interfaces are topologically fixed or adaptive to changes in power-flow profiles or coherent generation groups.

Due to topological characteristics of the system, generators tend to form coherent groups oscillating with each other under disturbances. These coherent generation groups can be studied offline using techniques such as slow coherency analysis technology. However, actual out-ofstep groupsin real time may be different from those obtained offline. Therefore, the separation interfaces should be able to separate only actual out-of-step groups [67].

(b) *Determination of conditions/criteria for which action is required*

With regards to identifying the conditions/criteria for determining the need to take actions and what actions or what interface locations require separation, the control action will primarily be the result of differential synchrophasor measurements taken at two or more points in the system.

The measurements will reflect the emerging instability ("out of step') of coherent generation groups with regard to each other. The controlled separation criteria may involve rapid processing of differential angle rates or even accelerations of differential angles. As such, the approach may require dedicated distributed processing power at key locations [67].

(c) *Determination of when in the out of step cycle the separation needs to occur*

Generally, controlled separation could be implemented when out-of-step of coherent generation groups is credibly predicted. Synchrophasors can help monitor oscillations between coherent generation groups and predict the time when out of step may occur. Based on that information, the separation timing should be reasonably proactive in order to minimize adverse transient reactions and the chance for equipment damage. In the event that out of step conditions cannot be predicted ahead of time, the best time for separation during the out of step cycle needs to be determined[67].

3.2 **Data Acquisition for Power System Studies**

Using Phasor Measurement Units (PMUs) to measurephasors across a power system at a point in time has the potential to solve power system problems[52]. PMUs rely on a global positioning satellite (GPS) time signal for extremely accurate time-stamping of power system information.

The GPS satellite receiver provides a precise timing pulse, which is correlated with the sampled data. Modern PMUs use one pulse per second signals provided by the GPS receivers. The accuracy of the GPS timing pulse is better than 1μs, which for a 50 Hz system corresponds to about 0.018

degrees. This accuracy is more than enough to ensure that the measurements obtained by such clocks will be simultaneous for the purpose of estimation and analysis of the power system state [53].

With the advent of phasor measurement units (PMUs) capable of tracking the dynamics of an electric power system, and with modern telecommunication abilities, utilities are able to respond intelligently to an event in progress. By synchronising sampling of microprocessor-based systems, phasor calculations can be placed on a common reference. The magnitudes and angles of these phasors comprise the state of the power system and are used in state estimation and transient stability analysis. By communicating time-tagged phasor measurements to a central location, the dynamic state of a system can be tracked in real time. An emerging application of this technology is to track the state of the system immediately following a transient event to select an appropriate remedial control action [68].

3.2.1 *CommonPower System data for Transient Stability Studies*

Researchers have utilized various power system data for transient stability studies [3-14, 19-35, 41-50]. The data include rotor angle,mechanical input power, generator kinetic energy deviation, average acceleration during fault, angular velocity, bus voltage, line current, and rotor speed. Others are real and reactive power flows of generators, real and reactive power flows on lines, real and reactive power flows in transformers, phase difference of the voltage between buses, rotor angle relative to the phase of generator terminal voltage, angular velocity deviation, impedance angle measured at generator terminals, and resistance and reactancemeasured at generator terminals.

Rotor angles are the most widely used power system data for transient stability studies. Rotor angle is a key parameter in the fundamental equation governing generator rotor dynamics.

Equation (3.1)shows the fundamental equation governing rotor dynamics.

$$M \frac{d^2\delta}{dt^2} = P_m - P_e \quad (3.1)$$

Where:M is the inertia coefficient, $\delta$is the rotor angle, P_m is the mechanical power and P_e is the electrical power.

This equation is commonly referred to as the swing equation [69]. Rotor angles need to be expressed relative to a common reference. This reference cannot be based on a single generator, since any instability in the reference generator makes the relative angles meaningless. In order to overcome this difficulty, the concept of system centre of inertia (COI) angle,δ_{co} is used to obtain a reference angle [19]. COI is given as:

$$\delta_{co} = \frac{\sum_{i=1}^{n} H_i \delta_i}{\sum_{in=1}^{n} H_i} \quad (3.2)$$

Where:δ_i and H_i are the rotor angle and inertia constant of the *ith* generator, respectively. The angle, δ_i is usually approximated by the phase angle of the respective generator bus voltage [19,70]. Many researchers however discourage the use of rotor angles in algorithms [19]. This is because the COI values, in practice require continuous updates using real time measurements. This

requires extra pre-processing and has significant errors [19]. Rotor angles, thus best serve as the reference parameter for telling stability status of a system in a simulation. Other electrical parameters whose use in algorithms, do not have practical constraints may then be employed for algorithm development.

The time derivative of rotor angle is the rotor speed deviation in electrical radians per second [66]. Mathematically,

$$\frac{d\Delta}{dt} \Delta\Delta\Delta\Delta\Delta\Delta\Delta\Delta_s \qquad (3.3)$$

Where $\Delta\Delta$ is the rotor speed deviation, Δ is the rotor speed at a particular time, and Δ_s is the synchronous speed.

Equation (3.3) shows that rotor speed deviation has the potential to assist in determining transient stability conditions following a large disturbance. Unlike rotor angles, rotor speed and for that matter rotor speed deviation of a particular generator need not be referenced to any particular machine.

3.3 **Wavelet Analysis**

Wavelet transform (WT)is a mathematical technique which has a special feature of variable time-frequency localization, different from the windowed Fourier transform. Wavelet algorithms process data at different scales so that they may provide multiple resolutions in frequency and time [54]. Wavelet analysis is capable of revealing aspects of data that other signal analysis techniques

miss; aspects such as trends, breakdown points, discontinuities in higher derivatives, and self-similarity. Wavelet is able to compress and de-noise a signal without appreciable degradation [55]. Wavelets have been used for several years in such areas as seismic, image compression, acoustics, and mechanical vibrations. Several papers have also been presented proposing the use of wavelets for power system studies [71,72]. The most popular wavelet transform applications in power systems are in the following areas: power system protection, power quality, power system transients, partial discharges, load forecasting, and power system measurement [72].

Wavelet analysis is done using mother wavelets. The process of breaking up a signal into scaled and shifted versions of the mother wavelet is called decomposition. The 'mother wavelet' determines the shape of the components of the decomposed signals. There are essentially two types of wavelet decomposition: Continuous Wavelet Transform (CWT) and Discrete Wavelet Transform (DWT). CWT is mainly used for theory research, but DWT is more popular in the field of engineering, because the observed time series are discrete in real world [55, 73]. DWT is a digitally implementable version of wavelet transforms[74]. There are many types of mother wavelets. They includeHaar, Meyer, Morlet, Daubechies 4, Daubechies 8, Coiflet3 and Symmlet[73, 75,76]. Haar is a square-wave wavelet.Daubechies 4 wavelet is a compactly supported orthonormal wavelet family. Coiflet3 is an orthonormal wavelet system where both father and mother have special vanishing moment properties. Symmlet8 is a nearly-symmetric orthogonal wavelet of compact support with 8 vanishing moments [73, 76].

The necessary and sufficient condition for wavelets is: it must be oscillatory, must decay quickly to zero, and must have an average value of zero[71, 75]. A particular type of wavelet is selected

depending on the particular type of application [75].The Daubechies wavelet family are the most widely used wavelets in power system studies [77].Among the Daubechies mother wavelets, Daubechies 4 and Daubechies 8 are found to be the most suitable for the analysis of power system transients [75, 78]. They are very effective in reconstructing power system transient signals. Daubechies 8 wavelet has the following advantages over Daubechies 4: It closely matches the signal to be processed, which is of utmost importance in wavelet applications. Moreover, Daubechies 8 wavelet is more localized,that is, it is compactly supported in time and hence is good for short and fast transient analysis as compared to Daubechies4 wavelet and provides almost perfect reconstruction. Also, Daubechies8 wavelet is found to be more suitable as compared to Daubechies4 wavelet in representing transient signals because it is smoother and more oscillatory in nature which is also the nature of the transient signals[77, 78].

However, Daubechies 4 has given more satisfactory results than Daubechies 8 mother wavelet in several other power system applications [77].

3.3.1 *Discrete Wavelet Transform*

A discrete wavelet transform (DWT) expands a signal not in terms of a trigonometric polynomial but by wavelet, generated using the translation and dilation of a fixed wavelet function. The wavelet function is localized in time and frequency yielding wavelet coefficients at different scales. This gives the wavelet transform much greater compact support for the analysis of signals with localized transient components[79]. The DWT output can be represented in a twodimensional grid but with very different divisions in time and frequency so that the windows are narrow at high frequencies and wide at low frequencies. The efficiency of wavelet analysis stems from its fast

pyramid algorithm. The algorithm has two phases: The forward algorithm which is used to decompose the signal into component wavelets (DWT) and the backward algorithm which is used to reconstruct the original signal from the component wavelets; inverse discrete wavelet transform (IDWT). The forward algorithm uses linear filters (low and high pass analogue devices) to decompose the signal into low- and high-frequency components, and combines these filters with downsampling operations (whichaccounts for the algorithm's speed). The backward algorithm simply inverts the process by combining an upsampling process with linear filtering operations [79].

The original signal passes through two complementary filters and emerges as two signals (lowpass and highpass components). The decomposition process can be iterated, with successive low-frequency components being decomposed, in turn, so that one signal is broken down intomany lower-resolution components. The low and highpassdecomposition filters (LD, HD), together with their associatedreconstruction filters (LR, HR), form a system of what is knownas quadrature mirror filters[79].

The wavelet filter,*W*, which is called the scaling filter (non-normalized), is of a finite impulse response (FIR) of length 2*N*, of sum 1, of norm 1/ sqrt(2), and is a lowpass filter. From filter *W*, fourFIR filters, of length 2*N* and of norm 1 are defined and organized as follows:

(a) Decomposition process: the low-frequency*LD* = *rev*(*LR*) and the high-frequency *HD* = *rev*(*HR*)

(b) Reconstruction process: the low-frequency*LR* = *W/norm*(*W*) and high-frequency *HR* = *qmf*(*LR*)

Where:*qmf* represents quadrature mirror filters, and *rev* representsreversing the vector.The decomposition and reconstruction processes are illustratedschematically in Figure 3.1 [79].

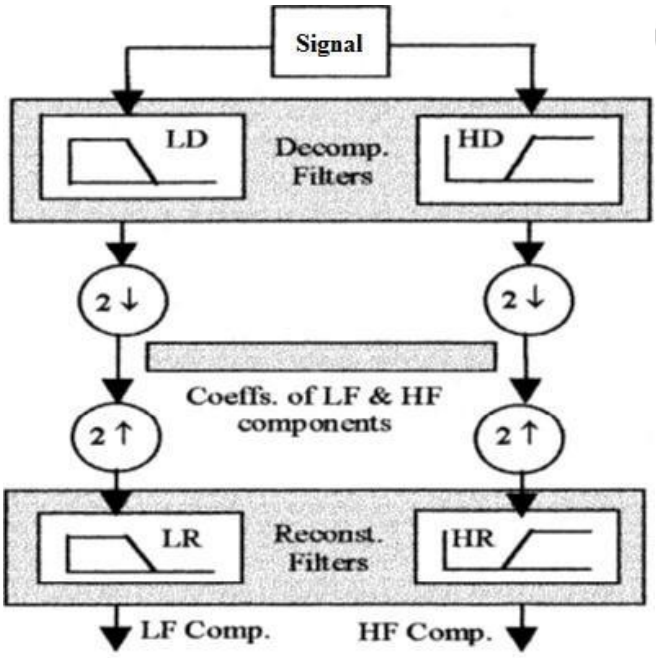

Figure 3.1: Discrete wavelet decomposition and reconstruction

The results of wavelet transform are called wavelet coefficients and this can be grouped into two: approximate and detailed coefficients. The approximations are the high-scale, low-frequency components of the signal and the details are the low-scale, high-frequency components [55].

The wavelet expansion of a signal, $f(x)$, is given as [59,80]:

$$f(x) = \sum_{i,j} a_{i,j} \psi_{i,j}(x) \qquad (3.4)$$

Where: i and j are integers, the functions $\psi_{i,j}(x)$ are the wavelet expansion functions and the two-parameter expansion coefficients $a_{i,j}$ are called the DWT coefficients of $f(x)$. The coefficients are given by:

$$a_{i,j} = \int f(x)\psi_{i,j}(x) \tag{3.5}$$

The coefficients can be computed from a function $\psi_{i,j}(x)$ called the generating or mother wavelet given by (3.6) through translation and scaling (dilation) parameters.

$$\psi_{i,j}(x) = 2^{i/2}\psi(2^i x - j) \tag{3.6}$$

Where: j is the translational parameter and i is the scaling parameter. Mother wavelet function is not unique and must satisfy a small set of conditions. One of them is multiresolution condition which is related to the two-scale difference equation

$$\phi(x) = \sqrt{2}\sum_k h(k)\phi(2x-k) \tag{3.7}$$

Where $\phi(x)$ is a scaling function and $h(k)$ must satisfy several conditions to make basis wavelet functions unique, orthonormal and have a certain degree of regularity. The mother wavelet is related to the scaling function as follows:

$$\psi(x) = \sqrt{2}\sum_k g(k)\phi(2x-k) \tag{3.8}$$

Where $g(k) = (-1)^k h(1-k)$. At this point, if valid $h(x)$ is available, one can obtain $g(x)$. h and g can be viewed as filter coefficients of half band low-pass and high-pass filters respectively. A $l$level wavelet decomposition can be computed as follows:

$$f(x) = \sum_k a_{0,k}\phi_{0,k}(x) + \sum_{l=0}^{l} \sum_k a_{l+1,k}\phi_{l+1,k}(x) + \sum_k d_{l+1,k}\psi_{l+1,k}(x) \quad (3.9)$$

Where coefficients $a_{0,k}$, $a_{l+1,n}$, and $d_{l+1,n}$ at scale $l+1$ are given and they can be obtained if coefficient at scale l is available:

$$a_{l+1,n} = \sum_k a_{l,k} h(k-2n)$$
$$d_{l+1,n} = \sum_k a_{l,k} g(k-2n) \quad (3.10)$$

Where a set of wavelet approximation coefficients, $a_{l+1,n}$ and detailed coefficients $d_{l+1,n}$ at scale l +1 are given.

3.3.2 ***Dilation Equation***

The dilation equation links a scaling function $\phi(x)$ and its translates $\phi(2x)$ [75]. The dilation equation is uniquely specified for each mother wavelet. For the Daubechies 4 wavelet, the dilation equation has theform [81]:

$$\phi(x) = c_0\phi(2x) + c_1\phi(2x-1) + c_2\phi(2x-2) + c_3\phi(2x-3) \quad (3.11)$$

Where: $c_0 = (1+\sqrt{3})/4$, $c_1 = (3+\sqrt{3})/4$, $c_2 = (3-\sqrt{3})/4$ and $c_3 = (1-\sqrt{3})/4$

Except for very few simple cases, it is not possible to solve directly for $\phi(x)$; the obvious approach is to solve for $\phi(x)$ iteratively until $\phi_j(x)$ is very nearly equal to $\phi_{j-1}(x)$.

$$\phi_j(x) = c_0\phi_{j-1}(2x) + c_1\phi_{j-1}(2x-1) + c_2\phi_{j-1}(2x-2) + c_3\phi_{j-1}(2x-3) \quad (3.12)$$

The function $\phi(x)$ is called the scaling function and the corresponding wavelet function is constructed from it. From the four-coefficient scaling functions, the dilation wavelet function is [81]:

$$W(x) = c_3\phi(2x) - c_2\phi(2x-1) + c_1\phi(2x-2) - c_0\phi(2x-3) \quad (3.13)$$

The same coefficients are used for $W(x)$ as for the definition of $\phi(x)$, but in reverse order and with alternate terms having their signs changed from plus to minus.

3.4 **Artificial Neural Networks**

Artificial Neural Networks (ANNs) represent a modern and sophisticated approach to problemsolving widely explored also for power system protection and control applications. ANNsperform actions similar to human reasoning, which relies upon experience gathered during a training process. Advantages of ANNs computing methodologies over conventional approachesinclude faster computation, learning ability, adaptive features, robustness and noise rejection [30].

ANNs are constructed to make use of some organizational principles resembling those of the human brain [80]. They represent a promising new generation of information processing systems. Neural networks are good at tasks such as pattern-matching and classification, function approximation, optimization and data clustering. Traditional computers, because of their architecture, are inefficient at these tasks, especially pattern-matching tasks [80].

ANNs are made up of a number of simple and highly interconnected processing elements, called neurons [59]. An artificial neuron is a computational model comparable to the natural neurons. Natural neurons receive signals through synapses located on the dendrites or membrane of the neuron. When the signals received are strong enough (surpass a certain threshold), the neuron is activated and emits a signal through the axon. This signal might be sent to another synapse, and might activate other neurons [82]. Figure 3.2 shows an artist's conception of a natural neuron[82].

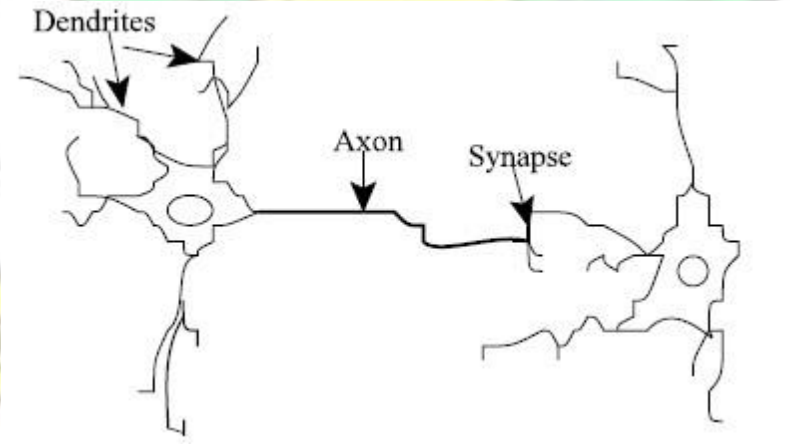

Figure3.2: A natural neuron

The complexity of real neurons is highly abstract when modelling artificial neurons. These basically consist of inputs (like synapses), which are multiplied by weights (strength of the respective signals), and then computed by a mathematical function which determines the activation of the neuron. Another function (which may be the identity) computes the output of the artificial neuron (sometimes based on a certain threshold). ANNs combine artificial neurons in order to process information [82].Figure 3.3 shows a mathematical model of an artificial neuron [83].

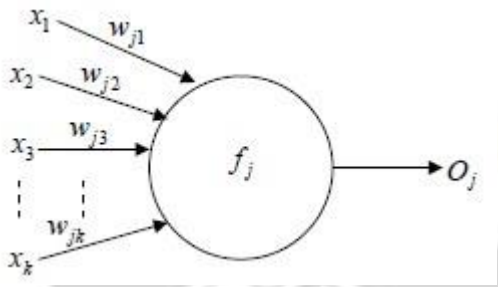

Figure 3.3: Mathematical model of an artificial neuron

The mathematical model of a neuron as shown in Figure 3.3 is expressed in (3.14)[59]:

$$O_j = f_j\left(\sum_{k=1}^{N} w_{jk} x_k\right) \quad (3.14)$$

Where: O_j is the output of a neuron, f_j is a transfer (activation) function which is differentiable and non-decreasing, w_{jk} is an adjustable weight that represents the connection strength, and x_k is the input of a neuron.

3.4.1 *Types of Artificial Neural Networks*

Various types of neural networks exist. These include multi-layer perceptrons, radial basis networks, Kohonen networks and recurrent networks [56]. Two commonly used neural networks areradial basis function (RBF) and multilayer perceptron (MLP) neural networks [56,57]. The main difference between the two architectures lies in the nature of the input–output relations of their nodes. RBF networks are three-layered networks, whose output nodes form a linear combination of the basis functions (usually of the Gaussian type) computed by the hidden layer nodes. Each node provides a significant non-zero response only when the input falls within a small localized region of the input space. MLP networks are basedon nonlinear sigmoid functions which give significant non-zero response in a wide region of the input space. Their approximations are smooth and continuous, far more accurate for increasing number of nodes in the hidden layers [83].

(a) *Radial basis function neural network*

Radial basis function neural network is an extremely powerful neural network [57]. A radial basis function neural network has a hidden layer of radial units and a linear-output layer unit.

The input nodes pass the inputs to the hidden nodes directly and the first layer connections are not weighted. The transfer functions in the hidden nodes are similar to the multivariate Gaussian density function [84]. Similar to biological receptor fields, an RBF neural network employs local receptor fields to perform function mappings [85]. Figure 3.4 shows a radial basis function neural network [85].

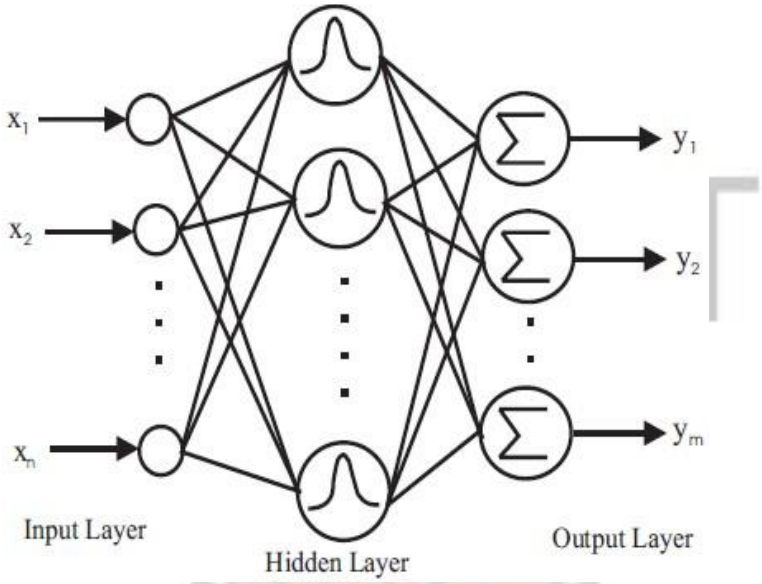

Figure 3.4: A RBF neural network

In an RBF neural network, a radial unit (that is, local receptor field) is defined by its centre point and a radius. The activation function of the *i*th radial unit is [85]:

$$h_i = R_i(x) = R_i\left(\frac{\|x - u_i\|}{\sigma_i}\right) \quad (3.15)$$

Where: x is the input vector, u_i is a vector with the same dimension as x denoting the centre, σ_i is the width of the function and R_i is the i-th radial basis function. Typically R_i is a Gaussian function:

$$R_i(x) = \exp\left(-\frac{\|x - u_i\|^2}{2\sigma_i^2}\right) \quad (3.16)$$

The i-th component of the final output y_i of an RBF neural network can be computed as the weighted sum of the outputs of the radial units as:

$$y_i = \sum_i w_i R_i(x) \quad (3.17)$$

Where: w_i is the connection weight between radial unit i and the output unit.

(b) ***Multilayer perceptron neural network***

Multi-Layer Perceptron is a popular neural network architecture[56-58]. They are a class of nonlinear models. The nonlinearity comes from the hidden layers of the neural network which can model very complex functions [86]. Typically, the MLP is organized as a set of interconnected layers of artificial neurons, input, hidden and output layers. When a neural group is provided with data through the input layer, the neurons in this first layer propagate the weighted data and randomly selected bias, through the hidden layers. Once the net sum at a hidden node is determined, an output response is provided at the node using a transfer function.

MLPs like any other neural network, has to be trained [86].

Two important characteristics of the MLP are its non-linear processing elements which have a non-linear activation function that must be smooth (the logistic function and the hyperbolic tangent are the most widely used), and its massive interconnectivity (that isany element of a given layer feeds all the elements of the next layer)[87]. In the multilayer perceptron, every hidden layer cantransfer its output to another hidden layer in an orderlymanner [86]. For example a two layer perceptron function couldbe expressed as follows:

$$O_j = f\left(\sum_k w_{jk(2)}\, g\left(\sum_i w_{ik(1)} x\right)\right) \qquad (3.18)$$

Where: j is the number of outputs or elements in outputvector, f is the output function,g is the activation (transfer) functionin hidden layer, and$w^{(1)}$ and$w^{(2)}$ are the weight vectors for the first and the second hidden layers respectively.

Commonly used transfer functions are: linear (*purelin*), log-sigmoid (*logsig*), hyperbolic tangent sigmoid (t*ansig*) transfer function [87, 88]. The output, *O*, of a purelin transfer function for a given input *x* is given in (3.19) [88]:

$$O = x \tag{3.19}$$

A plot of the linear transfer function is shown inFigure 3.5.

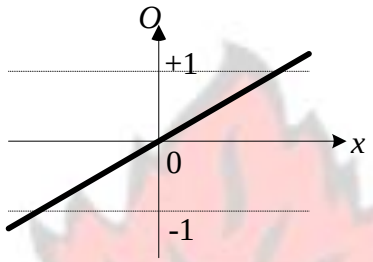

Figure 3.5: Linear transfer function

The output, *O*, of a log-sigmoid transfer function for a given input *x* is given as:

$$O = \frac{1}{1 + e^{-x}} \tag{3.20}$$

A plot of the log-sigmoid transfer function is shown inFigure 3.6.

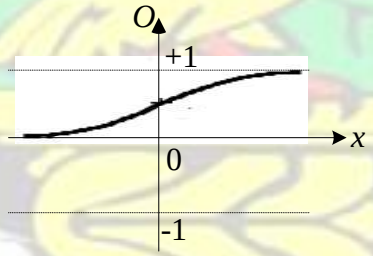

Figure 3.6: Log-sigmoid transfer function

The output, *O*, of a hyperbolic tangent sigmoid transfer function for a given input *x* is given as:

$$O = \frac{e^{2x} - 1}{e^{2x} + 1} \tag{3.21}$$

A plot of the hyperbolic tangent sigmoid transfer function is shown in Figure 3.7.

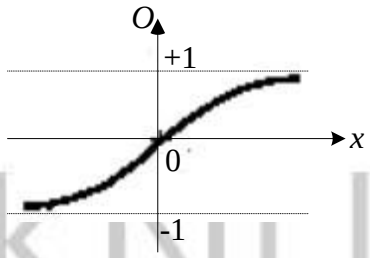

Figure 3.7: Tangent sigmoid transfer function

MLPs are mostly trained by the Levenberg-Marquardt back- propagation algorithm [87, 88].

The Levenberg–Marquardt algorithm, independently developed by Kenneth Levenberg and Donald Marquardt, provides a numerical solution to the problem of minimizing a nonlinear function. It is fast, and has stable convergence. This algorithm is suitable for training small and medium-sized networks. The update rule of the Levenberg-Marquardt algorithm is given in (3.22) [89]:

$$\boldsymbol{w}_{k+1} = \boldsymbol{w}_k - \left[\boldsymbol{J}_k^T \boldsymbol{J}_k + \mu \boldsymbol{I}\right]^{-1} \boldsymbol{J}_k \boldsymbol{e}_k \tag{3.22}$$

Where: $\boldsymbol{w}$ is the weight vector, k is the index of iteration, $\boldsymbol{J}$ is the Jacobian matrix, μ is the combination coefficient which is always positive, $\boldsymbol{I}$ is the identity matrix and $\boldsymbol{e}$ is the error vector.

The output O_j of a neuron j is calculated using

$$O_j = f_j(net_j) \tag{3.23}$$

Where: f_j is the activation function of neuron j, andnet value net_j is the sum of weighted input nodes of neuron j. The net value is given by:

$$net_j = \sum_{i}^{ni} w_{j,i} O_{j,i} \tag{3.24}$$

$i=1$

Where: $O_{j,i}$ is the ith input node of neuron j, weighted by $w_{j,i}$.

The training of a neural network using the Levenberg–Marquardt algorithm is organised into forward computation and backward computation. The forward computation for a three-layered multilayer perceptron neural network is as follows [89]:

Step 1: Calculate net value(net), output(O), and slope(s) for the neuron in the first layer:

$$net_1^1 = \sum_{i=1}^{ni} x_i w^1_{j,i} + w^1_{j,0} \quad (3.25)$$

$$O^1_j = f_j^1(net^1_j) \quad (3.26)$$

$$s^1_j = \frac{\partial f_{j1}}{\partial net_j} \quad (3.27)$$

Where: x_i are the network inputs, superscript '1' denotes first layer and subscript 'j' is the index of neurons in the first layer.

Step 2: Use the output of the first layer neuron as the inputs of all neurons in the second layer, do a similar calculation for net values, slopes, and outputs:

$$net^2_j = \sum_{i=1}^{ni} O_i^1 w^2_{j,1} + w^2_{j,0} \quad (3.28)$$

$$O^2_j = f_j^2(net^2_j) \quad (3.29)$$

$$s_{2j} = \frac{\partial f_{j22}}{\partial net_j} \quad (3.30)$$

Where: superscript '2' denotes second layer and subscript 'j' denotes *j*th neuron.

Step 3: Use the outputs of the second layer neurons as the inputs of the neuron in the output layer (third layer), do a similar calculation for net values, slopes, and outputs:

$$net_{3j} = \sum_{i=1}^{n2} O_{2j} w_{3j,i} + w_{3j,0} \quad (3.31)$$

$$o_j = f_j^3(net_j^3) \quad (3.32)$$

$$s_j^3 = \frac{\partial f_j^3}{\partial net_j} \quad (3.33)$$

Where: superscript '3' denotes third layer.

With the results from the forward computation, for a given output j, the backward computation can be organized as:

Step 4: Calculate error, e_j, at the output and initial , δ, as the slope of output :

$$e_j = d_j - O_j \quad (3.34)$$

$$\delta_{3j,j} = s_{3j} \quad (3.35)$$

$$\delta_{j,k}^3 = 0 \quad (3.36)$$

Where: d_j is the desired output at output *j*, O_j is the actual output at output neuron

obtained in the forward computation, $\delta^3_{j,j}$ is the self-backpropagation and $\delta^3_{j,k}$ is the backpropagation from other neurons in the same layer (output layer).

Step 5: Backpropagate δ from the input of the third layer to the outputs of the second layer

$$\delta_{2j,k} = w_{3j,k}\delta_{3j,j} \tag{3.37}$$

Where: k is the index of neurons in the second layer from 1 to n_2.

Step 6: Backpropagate δ from the outputs of the second layer to the inputs of the second layer

$$\delta_{2j,k} = \delta_{2j,k} s'_{k2} \tag{3.38}$$

Where: k is the index of neurons in the second layer.

Step 7: Backpropagate δ from the inputs of the second layer to the outputs of the first layer

$$\delta_{1_{j,k}} = \sum_{i=1}^{3} w_{2j,i}\delta_{2j,i} \tag{3.39}$$

Where: k is the index of neurons in the first layer, from 1 to n_1.

Step 8: Backpropagate δ from the outputs of the first layer to the input of the first layer

$$\delta_{1j,k} = \delta_{1j,k} s'_{1k} \tag{3.40}$$

Where: k is the index of neurons in the second layer, from 1 to n_1.

For the backpropagation process of other outputs, the steps 4 – 7 are repeated. By performing the forward computation and backward computation, the whole $\boldsymbol{\delta}$ array and O array canbe obtained for the given pattern. Then related row elements of a Jacobian matrix are calculated by using (3.41).

$$\frac{\partial e_{p,m}}{\partial w_{j,i}} = \delta_{m,j} O_{j,i} \tag{3.41}$$

Where:*p* is the desired pattern, *j* is the index of neurons, *i* is the index of neuron inputs, and *m* is index of neuron outputs.

KNUST

Chapter 4

PREDICTION SCHEMES FOR TRANSIENT STABILITY STATUS AND COHERENCY GROUPING

KNUST

4.1 Input Data Selection

From the second order model equation of a synchronous machine given by(3.3), the time derivative of rotor angle is the rotor speed deviation in electrical radians per second (that is, $\frac{d\delta}{dt} = \omega - \omega_s$).It can also be shown that [65],

$$\frac{d}{dt}\left(\frac{d\delta}{dt}\right) = \frac{\omega_0}{2H} P_a \qquad (4.1)$$

Where:H is the inertia constant and P_a is the difference between input mechanical power and output electromagnetic power. For stability to be attained after a disturbance,it is expected that $\frac{d\delta}{dt}$ will be zero in the first swing [66]. Thiscondition gives rise to the equal area criterion which is a well-known classical transient stability criterion.

From the above equations, it can also be deduced that

$$\frac{d\delta}{dt} = \left(\frac{\omega_0}{2H} P_a\right)^{\frac{1}{2}} \qquad (4.2)$$

Equation (4.2) suggests speed deviation as a good input parameter for the prediction of transient stability status.

The higher the rotor speed deviation following a disturbance, the more unstable the system becomes or the less likely the equal area criterion can be met [90].Thus, the maximum speed deviation at some time during a disturbance can be used to predict transient stability or otherwise. The best time is within the first swing, as indicated by the equal area criterion.This work proposes an algorithm for transient stability prediction using rotor speed deviation as power system input data.

Speed deviations of individual machines do not need to be expressed with reference to other machines; hence their use in algorithms eliminates the difficulties associated with the practical implementation of algorithms which use rotor angles as input. In a real power system, rotor speed deviation measurement of each generator can be provided by the phasor measurement unit (PMU), located on the EHV or HV bus of the generating plant [52, 53].

In this work, rotor speed deviation following a disturbance has been used in different ways for stability and coherency predictions.

4.2 **Use of Rotor Speed Deviation for Generator Out-of-Step Prediction**

The maximum rotor speed deviation of a generator, in the first swing following a transient disturbance, will be much lower if it maintains synchronism with the other generators than if it goes out of step with the others. Consequently, the maximum rotor speed deviation of each generator within the first swing is used as an input parameter to predict the synchronism status of each generator of a power system following a transient disturbance. Mathematically,

$$x_i = Max(\Delta\omega_{ij}) \qquad j = 1, 2, \ldots, m \tag{4.3}$$

Where: x_i is the input data of algorithm to predict the synchronism status of generator *i*,

$\Delta\omega_{ij}$ arethe several rotor speed deviations of generator *i* sampled within the 1st cycle after the tripping of a line or bus, and *m* is the number of samples.

KNUST

4.3 Use of Rotor Speed Deviation for the Prediction of Transient stability Status of Systems

The sum of the maximum speed deviations of system generators for an unstable swing is much greater than the sum of the maximum speed deviations for a stable swing. Thus, the sum of the maximum speed deviations of the individual generators of a system following a disturbance is employed as input data for predicting the transient stability status of a system. The sum of maximum rotor speed deviation, *x*, is obtained as follows:

$$x = \sum_{i=1}^{n} Max(\Delta\omega_{ij}), \; i = 1,2,3,\ldots,n, \quad j = 1,2,\ldots,m \tag{4.4}$$

Where: $\Delta\omega_{ij}$ is the *jth* sample of the rotor speed deviation of the *i*th generator captured in the 1st cycle after the tripping of a line or bus,

$Max(\Delta\omega_{ij})$ is the maximum rotor speed deviation of the m samples captured for generator *i*, *n* is the number of generators

of the system, and *m* is the number of samples.

4.4 **Use of Rotor Speed Deviation for the Prediction of Coherent Generator Groups**

Very often, individual generators or groups of generators tend to oscillate together for a particular fault. Their rotor angle swings are dependent on each other and they evolve together with time [91]. This can be expressed by:

$$\delta_i(t) - \delta_j(t) = K_{ij} \qquad 0 \le t \le t_{max} \qquad (4.5)$$

Where: i and j are pairs of generators, K_{ij} is a constant whose value may change with time. The value of K_{ij} will be small and nearly constant within a synchronous group. For a pair of generators which go out of step, the value of K_{ij} will be large and may also largely vary with time. It follows from (4.5) that

$$\frac{d\delta_i(t)}{dt} - \frac{d\delta_j(t)}{dt} = K_{2ij} \qquad (4.6)$$

From which

$$\omega_i - \omega_j = K_{2ij} \qquad (4.7)$$

K_{2ij} is another constant whose value may also change with time.

Equation (4.7) shows that following a disturbance, the difference in speed deviation of coherent generators will be small and nearly constant while the difference in speed deviation of pairs or group of generators that go out of step will be large and also vary. Also, generators that remain stable after a disturbance, keep their coherency.

In the light of the above discussions and also with reference to (4.3), the proposed algorithm for the prediction of coherent generator groups uses data sets each containing three input data namely,

$x_1 = Max(\Delta\omega_i)$ (4.8) $x_2 = Max(\Delta\omega_j)$ (4.9)

$$x_3 = \left| Max(\Delta\omega_i) - Max(\Delta\omega_j) \right| \quad (4.10)$$

Where: i is a reference generator in a coherent group and

j is a generator to be placed in a coherent group.

The reference generator is an unstable generator with the highest of $Max(\Delta\omega)$ values.

4.5 **Case Study**

Various power systems have been used as test systems for transient stability studies. These include a 3-generator, 9-bus test system [14], IEEE 145-bus[16, 17], PSB4 [2, 5], IEEE 39-bus [2, 6, 19, 26, 27], IEEE 9-bus [20-22], IEEE 14-bus [2, 20-22] and the 10-generator western Japan 60Hz power system model [23].

In this work, the IEEE 39-bus test system, also known as the New-England test system was used as a case study. This test system is widely used for steady state and transient stability studies. This is because data on this system is readily available. It represents a real system and can be handled by free versions of commercial power system software packages. The test system is shown inFigure 4.1.

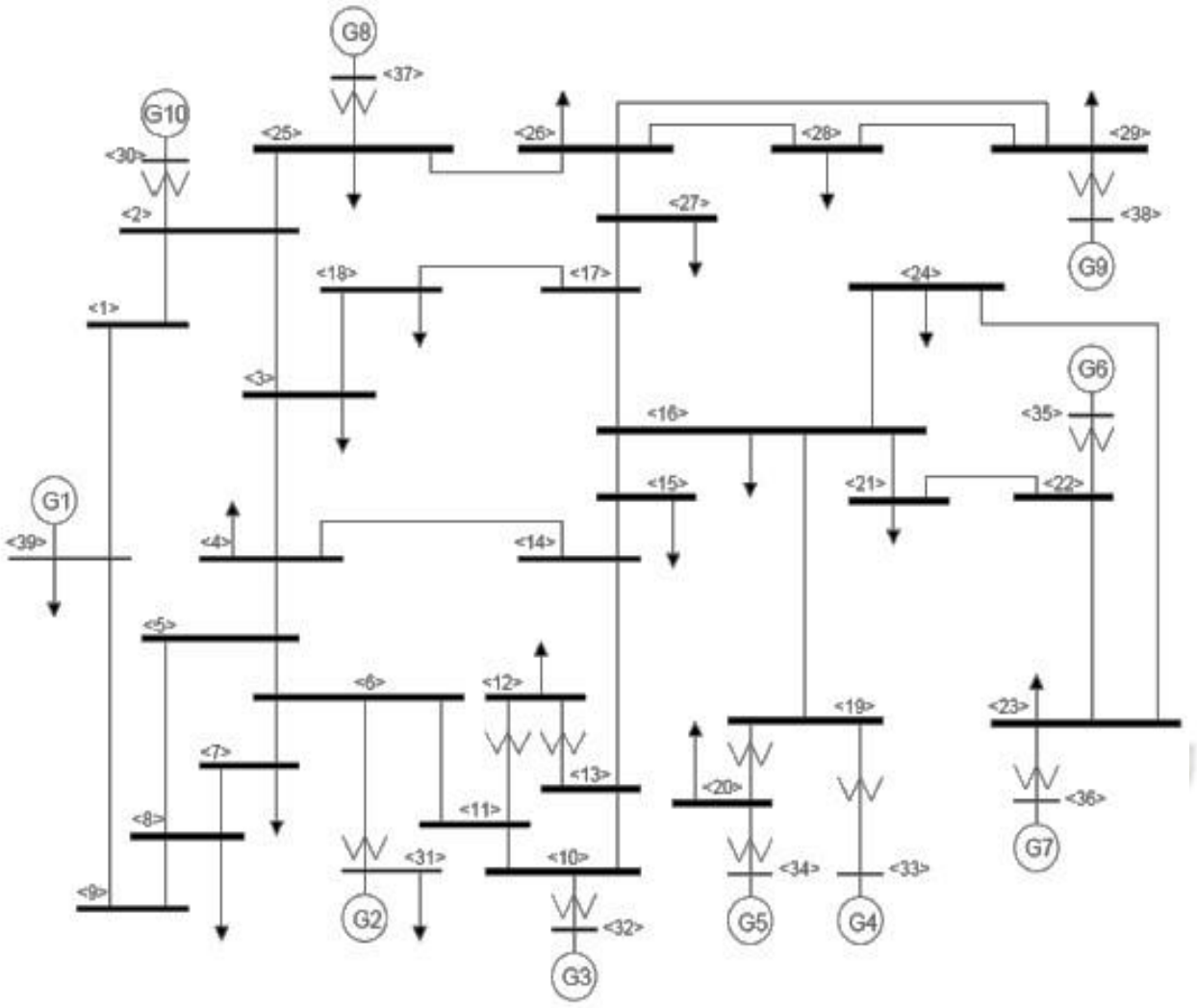

Figure 4.1: IEEE 39-bus test system

The system consists of 10 generators, one of which is a generator (G1) representing a large system. The system was modelled using the Power System Simulator for Engineers (PSSE) Software [92]. All the 10 generators were modelled using the GENROU (Round rotor synchronous machine with quadratic saturation in d-q axis) generator model. Each generator had IEEE Type 1 exciter, TGOV 1 (Steam Turbine Governor with reheat) turbine governor and PSS2A stabilizer. Data for the modelling of the test system isgiven in Appendix A [93].

The equations of the GENROU generator model and the IEEE type 1 exciter are also provided in Appendix A[94].

KNUST

4.6 **Generation of Transient Stable and Transient Unstable Cases for Algorithm Development and Testing**

The modelling and simulation of the test system to generate transient stable and transient unstable datawere carried out using the Power System Simulator for Engineers (PSSE) software. The data was generated at different loading levels. The levels are: base load, base load increased by 5%, base load increased by 7%, and base load increased by 10%. The load flow study was performed using the classical Newton-Raphson iterative method. The generators of the system, after the load flow study, were convertedusing the complex machine impedance (ZSORCE) option in the PSSE software.

The loads for the simulations were modelled as static loads with dependence on only bus voltage magnitude. The voltage dependency of load characteristics isrepresented by the exponential model[66]:

$$P = P_0 \left(\frac{V}{V_0} \right)^{2} \quad (4.11)$$

$$Q = Q_0 \left(\frac{V}{V_0} \right)^{2} \quad (4.12)$$

Where: P and Q are active and reactive components of the load when the bus voltage is V. The subscript‘0’ identifies the values of the respective variables at the initial operating condition. In

the static load model, active power wasrepresented as 100% constant current and reactive power as 100% constant admittance.

The network was initialized and run in steady state mode for 0.1 seconds after which various three-phase line and bus faults were separately applied. For each fault scenario, the fault was made to persist for some time (fault durations ranged from 0.1 to 1.5 seconds)after which the faulted line or bus was tripped. Simulations continued for some time with the line or bus tripped. The sampling frequency used was 6kHz.A summary of the simulation steps and processes are described in Figure 4.2.

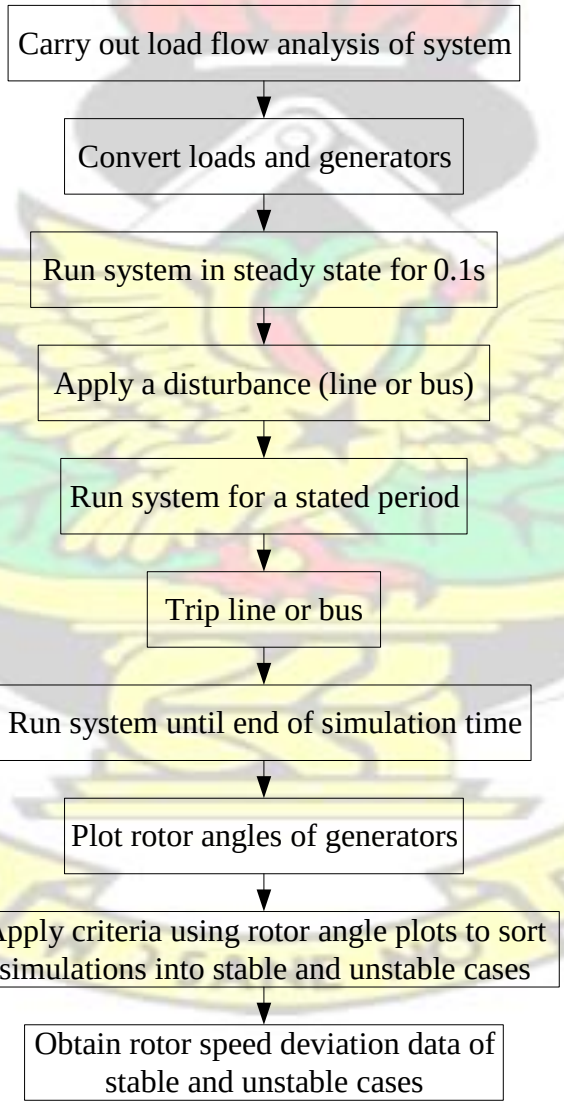

Figure 4.2: Flow chart of simulation process

The output data generated from the simulations were the rotor angles and rotor speed deviations of the various generators. The rotor angles were plotted to determine the simulations which resulted in transient stability and those which resulted in transient instability. The criteria used in this work for categorizing rotor angles was that a generator is unstable if the rotor angle difference between it and any other generator is more than 180^{o}, 1 second after the tripping of a line or bus following the application of a fault. Also the system is transient unstable if at least one of the generators is unstable [19, 27].

4.7 **Generator Out-of-Step Prediction using Wavelet Analysis**

Two stable and seven unstable fault conditions were simulated for the development of the wavelet-based generator OS prediction scheme. The analysis of the speed deviation data obtained from the simulations in PSSE software was done using the MATLAB® software [95]. In MATLAB, the speed deviations were further sampled every 20ms. Each sample represented a data cycle. Each data cycle was decomposed using the Daubechies 4 mother wavelet into 9 levels resulting in 1 approximate coefficient (a_9) and 9 detailed coefficients (d_1,d_2,d_3,d_4,d_5,d_6,d_7, d_8, and d_9). Figure 4.3 shows the 9-level decomposition of speed deviation signal. The 9-level decomposition of the rotor speed deviation signal,x, can be mathematically written as follows:

$$x = d_1 + a_1$$

$$= d_1 + [d_2 + a_2]$$

$$= d_1 + d_2 + [d_3 + a_3] + \ldots$$

$$= d_1 + d_2 + d_3 + d_4 + d_5 + d_6 + d_7 + d_8 + d_9 + a_9 \quad (4.13)$$

Where (d_j: j=1,2...9) are detailed coefficients and (a_j: j=1, 2...9) are approximate coefficients.

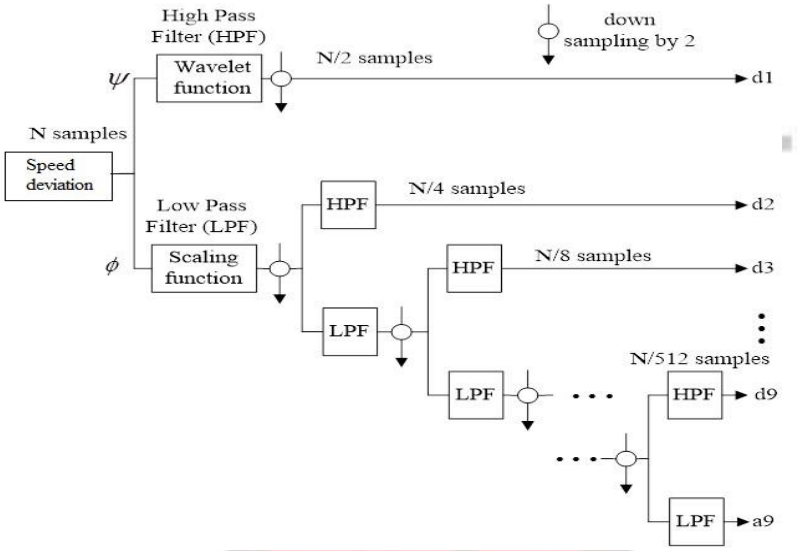

Figure 4.3: A 9-level decomposition of speed deviation

The frequency bands for the nine detailed coefficients corresponding to the 6000Hz sampling frequency are given in Table 4.1

Table 4.1: Frequency bands of detailed coefficients

Detailed coefficient	Frequency band (Hz)
d_1	6000 – 3000
d_2	3000 – 1500
d_3	1500 – 750
d_4	750 – 375
d_5	375 – 187.5
d_6	187.5 – 93.75
d_7	93.75 – 46.875
d_8	46.875 – 23.4375
d_9	23.4375 – 11.71875

The wavelet entropy(WE) of each of the detailed coefficients was subsequently obtained. The WE is a measure of the degree of disorder of a signal. Therefore, it can provide useful information about the underlying dynamical process associated with a signal [96, 97]. The WE,

E_j of a detailed coefficient, d_j, is given by [96-98] as follows:

$$E_j = |d_j|^2 \tag{4.14}$$

Analysis of the wavelet entropies of the detailed coefficients for each level revealed that the wavelet entropies (WEs) of detailed coefficient 8 (d_8) offered good characteristics for predicting generator OS conditions. A study of the extracted WEs revealed that in the first three cycles, generators which went out of step had their WEs decreasing throughout the data cycles while the stable ones had their WEs either remaining the same or increasing.

For example, Tables 4.2(a) – (c) provide the wavelet entropies of d8 for a three-phase fault on the line between bus 16 and bus 19 under base load, 105% base load, and 110% base load conditions respectively. For each of these fault conditions, generator 4 (G4) and generator 5 (G5) became unstable.

Table 4.2a: Wavelet entropies of d8 for a line 16-19 fault for base load condition

Cycle	G1	G2	G3	G4	G5	G6	G7	G8	G9	G10
1	0.0004	0	0.0001	0.0022	0.0038	0.0002	0.0001	0	0	0.0001
2	0.0005	0	0.0001	0.0019	0.0026	0.0004	0.0001	0	0	0
3	0.0005	0	0.0002	0.0016	0.002	0.0005	0.0001	0.0001	0	0

Table 4.2b: Wavelet entropies of d8 for a line 16-19 fault for 105% base load condition

Cycle	G1	G2	G3	G4	G5	G6	G7	G8	G9	G10
1	0.0001	0	0	0.0019	0.0035	0	0.0001	0	0	0.0003
2	0	0.0001	0	0.0017	0.0024	0	0.0001	0	0	0.0002
3	0	0.0001	0	0.0014	0.0018	0	0.0001	0	0	0.0002

Table 4.2c: Wavelet entropies of d8 for a line 16-19 fault for 110% base load condition

Cycle	G1	G2	G3	G4	G5	G6	G7	G8	G9	G10
1	0.0002	0.002	0	0.0017	0.0033	0.0002	0.0001	0	0	0.0002
2	0.0002	0.0032	0.0001	0.0015	0.0022	0.0003	0.0001	0	0	0.0001

3	0.0003	0.0049	0.0001	0.0013	0.0017	0.0004	0.0001	0	0	0.0001

The WEs of G4 and G5 which went out of step are noted to be reducing throughout the three cycles while those of the other generators which were stable either increase or remain the same.

Contrary to the above observations, the WEs of a few stable generators somewhat decreased throughout the data cycles. However, for such generators, the WEs of the 3rd cycle were found to be less than or equal to 0.001. This value came about following a comparison made between the 3rd cycle WEs of stable and unstable generators.

Based on the above findings, an algorithmic framework for predicting generator OS conditions was developed. Figure 4.4depicts a flowchart of the proposed wavelet analysis-based generator OS prediction scheme.

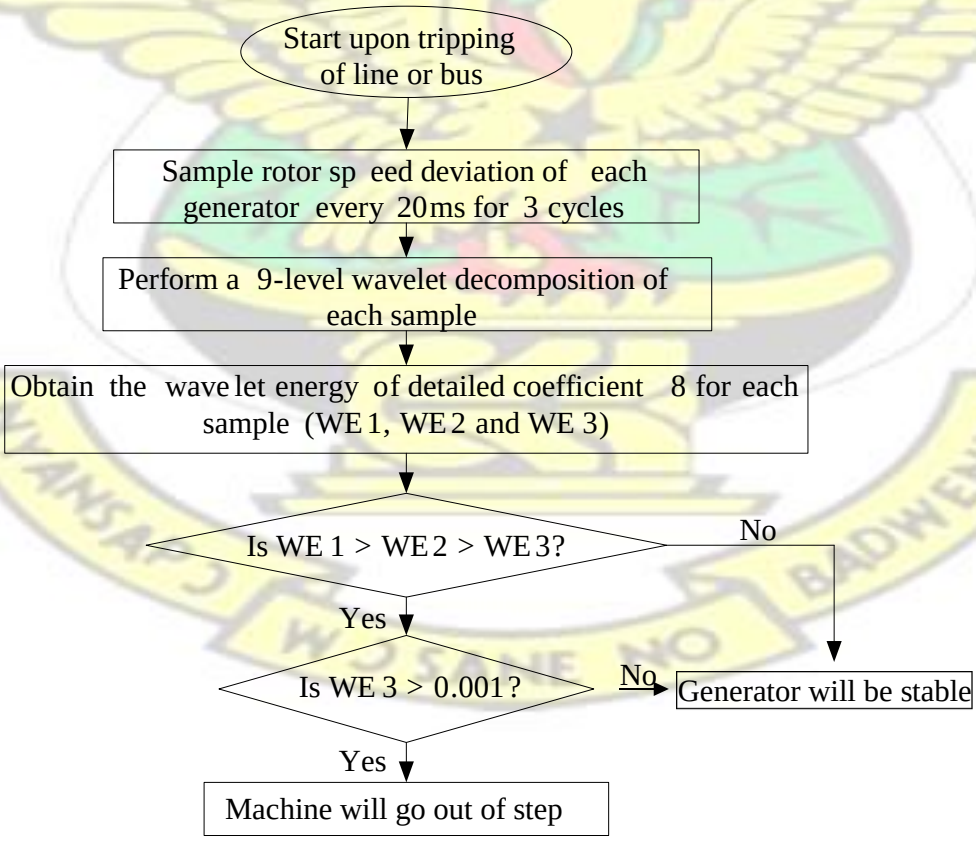

Figure 4.4: Flowchart of wavelet analysis-based out-of-step prediction scheme

The algorithm is initialized upon the tripping of a line or bus. The rotor speed deviation of each generator is sampled every cycle (20ms) for three consecutive cycles. The samples are then decomposed to 9-levels using the Daubechies 4 mother wavelet. The wavelet entropies (WEs) of detail coefficient 8 are then obtained for each sample. The stability status of each generator is predicted by comparing the WEs obtained for the three consecutive cycles. A generator is predicted to be stable if the WEs do not decrease progressively or decrease progressively but the WE of the 3rd cycle is not greater than 0.001. A generator is predicted to go out of step if the WE decreases progressively and the WE of the 3rd cycle is also greater than 0.001.

4.8 **Predicting the Transient Stability Status of Individual Generators using an Artificial Neural Network**

The input data required for the proposed scheme is the maximum rotor speed deviation of each generator in accordance with (4.3). A three-layered MLPNN with biaseswas used in this scheme. The MLPNN was implemented in MATLAB. The choice was informed by the fast decision making capability of multi-layer perceptrons (MLPs). The input layer had one neuron with a linear transfer function (*purelin*). The hidden layer had two neurons with hyperbolic tangent sigmoid transfer functions (*tansig*). The output had one neuron with a *purelin* transfer function. Linear transfer functions are frequently used for input and output layer neurons while non-linear transfer functions are employed for hidden layer neurons [99, 100]. Non-linearity in the hidden layer makes MLPs more effective [101]. Sigmoidal transfer functions are the most commonly used non-linear transfer function [100,101].

Figure 4.5 shows the architecture of the MLPNN.In Figure 4.5, the maximum rotor speed deviation (MSD) is the input *x*to an MPLNN where w_{ij} is the weight between neurons *i* and *j*, w_{i0} is the weight of the bias of neuron *i*, and *O* is the output of the neural network. The output *O* is expected to be either 1 or 0. An output of 0 indicates that the generator will be stable while an output of 1 indicates that the generator will go out of step.The biases have a constant input of 1.

The values of the weights are obtained from the training of the MLPNN.

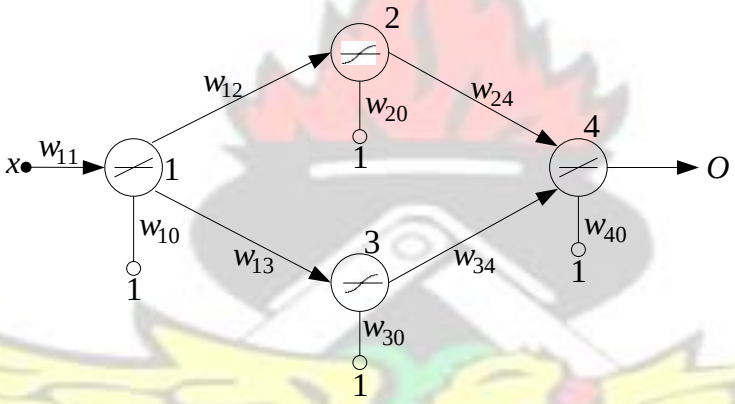

Figure 4.5: Architecture of MLPNN for generator OS prediction

The output, O, of the MLPNN can be determined as follows:

The output, y_1, of neuron 1 is given by:

$$y_1 = f(xw_{11} + w_{10}) = xw_{11} + w_{10} \tag{4.15}$$

The output, y_2, of neuron 2 is given by:

$$y^2 = f(y^1 w^{12} + w^{20}) = \frac{e^{2(y_1 w_{12} + w_{20})} - 1}{e^{2(y_1 w_{12} + w_{20})} + 1} = \frac{e^{2(xw_{11} + w_{10} w_{12} + w_{20})} - 1}{e^{2(xw_{11} + w_{10} w_{12} + w_{20})} + 1} \tag{4.16}$$

The output, y_3, of neuron 3 is given by:

$$\frac{e^{2(y_1 w_{13} + w_{30})} - 1}{e^{2(y_1 w_{13} + w_{30})} + 1} \quad \frac{e^{2(xw_{11} + w_{10} w_{13} + w_{30})} - 1}{e^{2(xw_{11} + w_{10} w_{13} + w_{30})} + 1}$$

$$y^3 = f\left(y^1 w^{13} + w^{30}\right) = \frac{e^{2\left(y_1 w_{13} + w_{30}\right)} - 1}{e^{2\left(y_1 w_{13} + w_{30}\right)} + 1} \quad (4.17)$$

The output,*O*, of MLPNN is thus given by:

$$O = f\left(y_2 w_{24} + y_3 w_{34} + w_{40}\right) = y_2 w_{24} + y_3 w_{34} + w_{40} \quad (4.18)$$

Hence,

$$O = w_{24}\frac{e^{2\left(x w_{11} + w_{10}\right)\left(w_{12} + w_{20}\right)} - 1}{e^{2\left(x w_{11} + w_{10}\right)\left(w_{12} + w_{20}\right)} + 1} + w_{34}\frac{e^{2\left(x w_{11} + w_{10}\right)\left(w_{13} + w_{30}\right)} - 1}{e^{2\left(x w_{11} + w_{10}\right)\left(w_{13} + w_{30}\right)} + 1} + w_{40} \quad (4.19)$$

The MLPNN was trained with 10 input data consisting of 5 maximum speed deviation data for OS conditions and 5 maximum speed deviation data for stable conditions. The maximum speed deviation data for generators that went out of step were distinct from those of stable generators; this permitted the use of such minimal training data.

For example, Table 4.3presents the maximum rotor speed deviation (MSD) of each generator within the 1st cycle after the tripping of bus 28 following a three-phase fault on it. For this fault condition, generator 9 went out of step. It can be observed that generator 9 has distinctively higher maximum speed deviation than the others which remained in synchronism. Table 4.4 also summarizes the maximum rotor speed deviation of each generator withinthe 1st cycle after the tripping of the line between bus 6 and bus 11. Generators 2 and 3 which went out of step had distinctively higher MSDs than the generators that remained in synchronism.

Table 4.3: Maximum rotor speed deviations for a fault on bus 28

Gen.	1	2	3	4	5	6	7	8	9	10
MSD	0.0001	0.0003	0.0007	0.0009	0.0009	0.0008	0.001	0.0014	0.0074	0.001

Table 4.4: Maximum rotor speed deviations for a line fault between buses 6 and 11

Gen.	1	2	3	4	5	6	7	8	9	10
MSD	0.0002	0.0094	0.0106	0.0023	0.0023	0.0022	0.0026	0.002	0.002	0.0022

The MLPNN was trained to give an output of '1' if a generator will pull out of step and '0' if it will be stable. The training was done using the Levenberg-Marquardt back-propagation technique. Figure 4.6 shows a flowchart of the proposed OS prediction scheme. Each generator is assigned one MLPNN to predict its stability status.

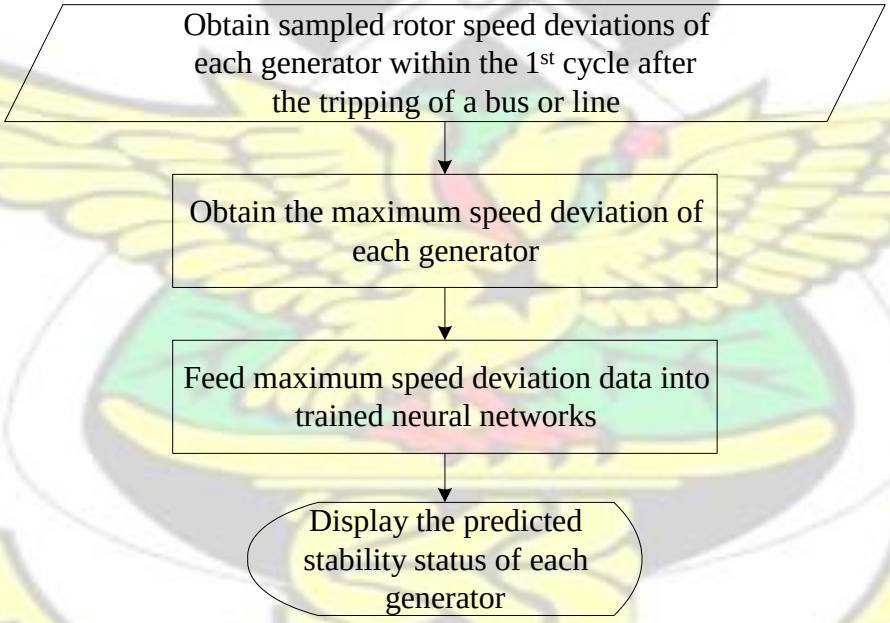

Figure 4.6: Flowchart of ANN-based OS prediction scheme

The algorithm is initialized after the tripping of a line or bus following a disturbance. The rotor speed deviation of each generator is sampled within the first cycle and the maximum speed

deviation is obtained. The maximum speed deviation of each generator is then used as inputsto assigned MLPNNs which predict the stability status of each generator.

4.9 **Prediction of Transient Stability Status using an Artificial Neural Network**

The input data requiredforthe proposed scheme is the sum of the maximum rotor speed deviations (SMSDs) of the generators of the system in accordance with (4.4). A feed forward multilayer perceptron neural network (MLPNN) with three-layers and biases was again used as the decision making tool to predict the transient stability status of the system. The input layer had one neuron with a linear transfer function (purelin). The hidden layer had two neurons with hyperbolic tangent sigmoid transfer functions (tansig). The output had one neuron with a *purelin* transfer function. The architecture of the MLPNN is shown in Figure 4.7.In Figure 4.7, the sum of maximum rotor speed deviations (SMSD) of the generators is the input x to an MPLNN where w_{ij} is the weight between neurons i and j, w_{i0} is the weight of the bias of neuron i, and O is the output of the neural network. The output O is expected to be either 1 or 0. An output of 1 shows that the system will be transient unstable while an output of 0 indicates that the system will maintain transient stability. The value of O can be determined using (4.19).

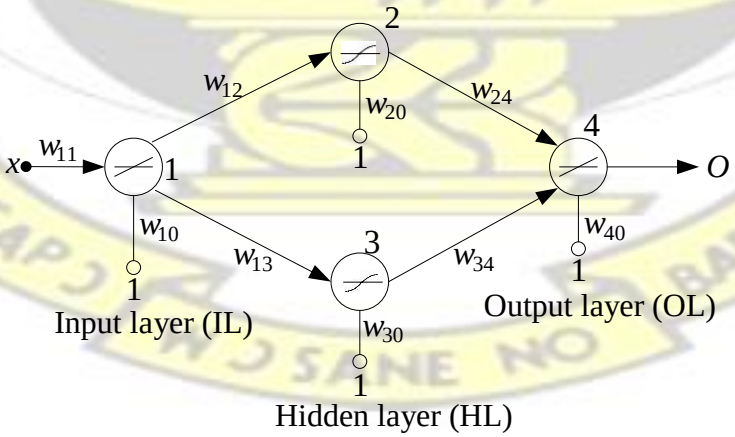

Figure 4.7: Architecture of MLPNN for predicting transient stability status of system

The sum of maximum rotor speed deviation data from five transient stable cases and five transient unstable cases were used to train the MLPNN. The clear distinction between the transient stable data as against the transient unstable data permitted the use of such small volume of training data. For example, Table 4.5presentsSMSD dataobtained within the 1st cycle after the tripping of various lines following three-phase faults. These fault conditions led to system instability. Table 4.6presents SMSDs for stable conditions obtained within one cycle after the tripping of various lines following three-phase faults. A study of the SMSDs for the various cases shows that cases which led to transient instability have a much higher SMSD value compared to cases which did not result in transient instability.

Table 4.5: Sum of maximum speed deviations for various line faults (unstable cases)

Bus-Bus	11-6	10-13	13-10	13-14	22-21
SMSDs	0.0324	0.0326	0.0313	0.0312	0.0283

Table 4.6: Sum of maximum speed deviations for various line faults (stable cases)

Bus-Bus	11-6	10-13	13-10	13-14	22-21
SMSDs	0.0047	0.0047	0.0045	0.0045	0.0041

The MLPNN was trained to give an output of '1' if the system will become transient unstable and '0' if the system will maintain stable operation. The MLPNN was trained using the Levenberg-Marquardt back-propagation technique. A flowchart of the transient stability status prediction scheme is shown inFigure 4.8.

The algorithm is initialized after the tripping of a line or bus following a disturbance. The rotor speed deviation of each generator is sampled within the first cycle and the maximum speed deviations are obtained. The obtained maximum speed deviations are then summed and used as input to a trained MLPNN which predicts the stability status of the system.

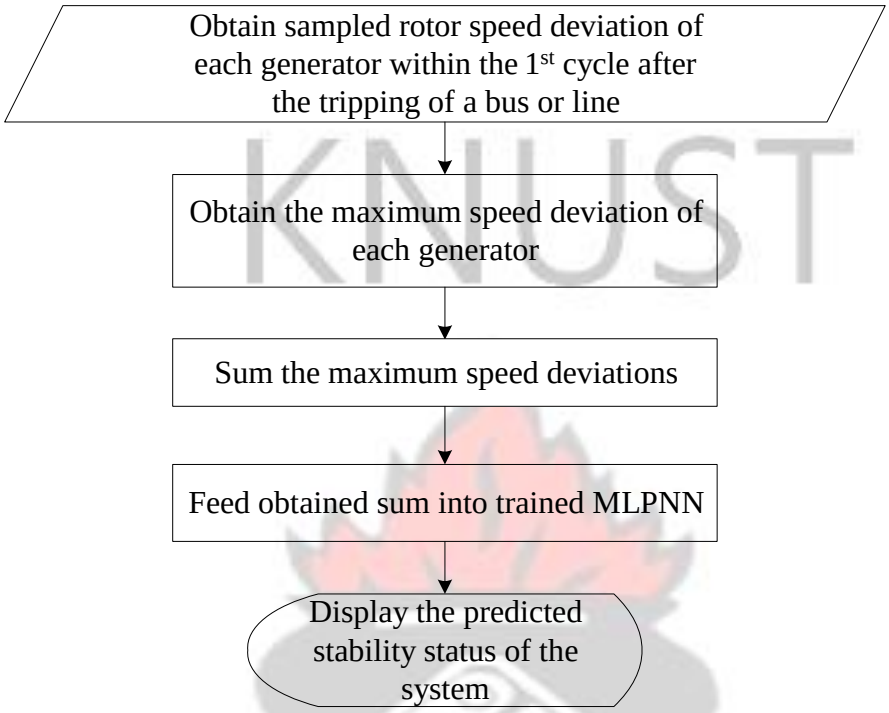

Figure 4.8: Flow chart of proposed transient stability status prediction scheme

4.10 **Prediction of Generator Coherency Groupings for Controlled Islanding**

Three rotor speed deviation related data as specified by (4.8), (4.9), and (4.10) are used as input data by the scheme. The proposed prediction scheme for coherent generator groupsutilises the output of the scheme proposed in Section 4.8 that predicts the stability status of each generator following a disturbance.The coherent generator groups prediction scheme places all generators predicted to be transient stable in one coherent group called group 'S'. The scheme then focuses on only generators which are predicted to go out of step and determines whether they will belong to the same out of step group or different groups.Two multilayer perceptron neural networks namely MLPNN1 and MLPNN2 were trained for the prediction of coherent generator groups. The prediction is done in three stages. MLPNN1 is responsible for the prediction of coherent groups in the first stage while MLPNN2 is responsible for the second and third stages. Both MLPNN1 and

MLPNN 2 have the same architecture. The architecture of the neural networks is shown in Figure 4.9.Each MLPNN had 3 neurons in the input layer, 4 neurons in the hidden layer, and 1 neuron in the output layer. The input and output neurons had 'purelin' transfer functions while the neurons in the hidden layer had 'tansig' transfer functions.In Figure 4.9, x_1 is the maximum speed deviation of the reference generator in a coherent group, x_2 is the of maximum speed deviation of a generator which is to be placed in a coherent group, and x_3 is the absolute value of the difference between x_1 andx_2.*O* is the output of the neural network, which is expected to be either 1 or 0. An output of 1 means that the generators will be in different coherent groups, while an output of 0 means that the generators will be in the same coherent group.

KNUST

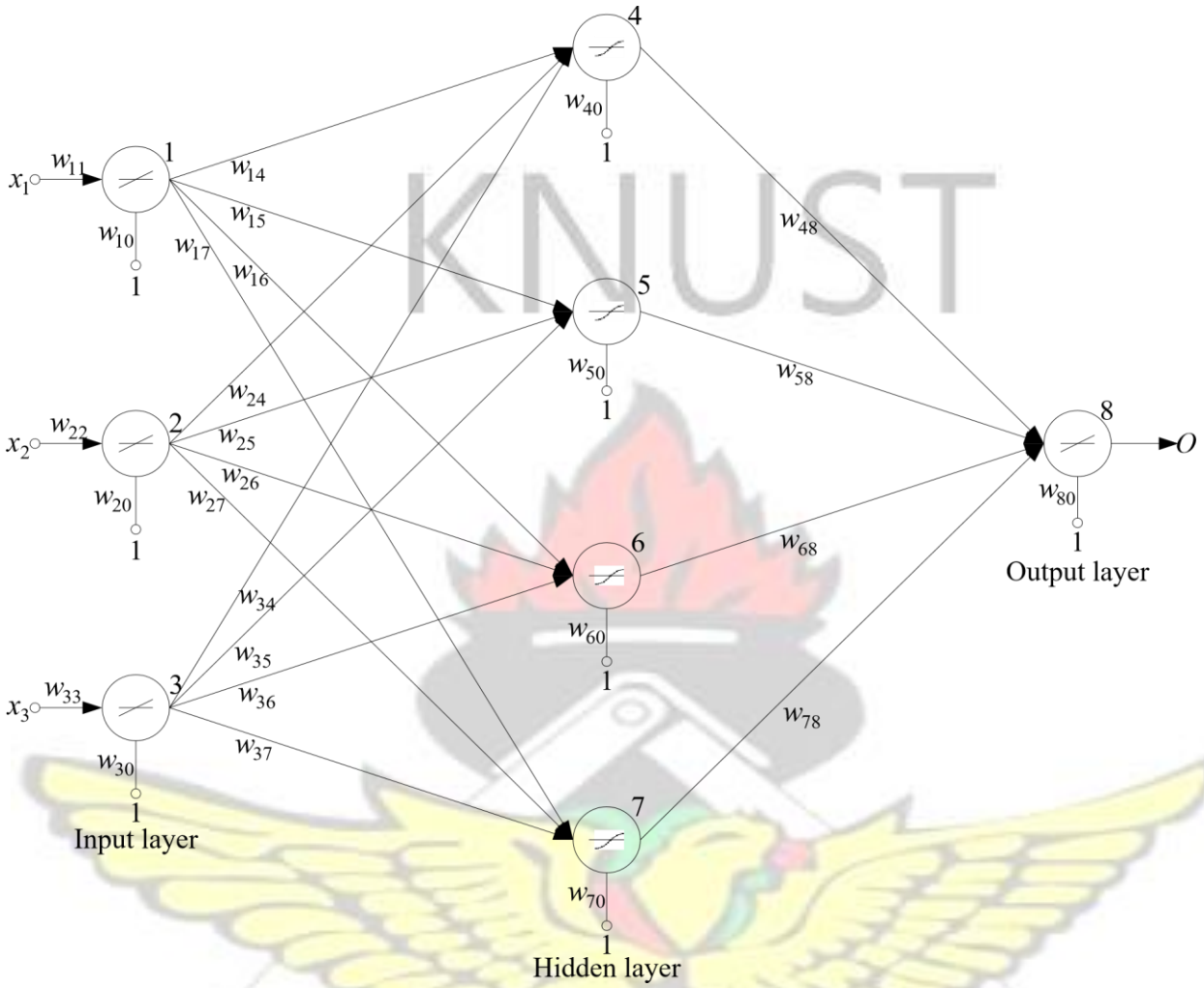

Figure 4.9: Neural network architecture of coherency prediction scheme

The output, O, of the neural network can be determined as follows:

The output, y_1 of neuron 1 is given by:

$$y_1 = f(x_1 w_{11} + w_{10}) = x_1 w_{11} + w_{10} \tag{4.20}$$

The output, y_2 of neuron 2 is given by:

$$y_2 = f(x_2 w_{22} + w_{20}) = x_2 w_{22} + w_{20} \tag{4.21}$$

The output, y_3 of neuron 3 is given by:

$$y_3 = f(x_3 w_{33} + w_{30}) = x_3 w_{33} + w_{30} \quad (4.22)$$

The output, y_4 of neuron 4 is given by:

$$y_4 = f(y_1 w_{14} + y_2 w_{24} + y_3 w_{34} + w_{40}) = \frac{e^{2(y_1 w_{14} + y_2 w_{24} + y_3 w_{34} + w_{40})} - 1}{e^{2(y_1 w_{14} + y_2 w_{24} + y_3 w_{34} + w_{40})} + 1} \quad (4.23)$$

The output, y_5 of neuron 5 is given by:

$$y_5 = f(y_1 w_{15} + y_2 w_{25} + y_3 w_{35} + w_{50}) = \frac{e^{2(y_1 w_{15} + y_2 w_{25} + y_3 w_{35} + w_{50})} - 1}{e^{2(y_1 w_{15} + y_2 w_{25} + y_3 w_{35} + w_{50})} + 1} \quad (4.24)$$

The output, y_6 of neuron 6 is given by:

$$y_6 = f(y_1 w_{16} + y_2 w_{26} + y_3 w_{36} + w_{60}) = \frac{e^{2(y_1 w_{16} + y_2 w_{26} + y_3 w_{36} + w_{60})} - 1}{e^{2(y_1 w_{16} + y_2 w_{26} + y_3 w_{36} + w_{60})} + 1} \quad (4.25)$$

The output, y_7 of neuron 7 is given by:

$$y_7 = f(y_1 w_{17} + y_2 w_{27} + y_3 w_{37} + w_{70}) = \frac{e^{2(y_1 w_{17} + y_2 w_{27} + y_3 w_{37} + w_{70})} - 1}{e^{2(y_1 w_{17} + y_2 w_{27} + y_3 w_{37} + w_{70})} + 1} \quad (4.26)$$

The output of the neural network, O which is the output of neuron 8 is given by:

$$O = f(y_4 w_{48} + y_5 w_{58} + y_6 w_{68} + y_7 w_{78} + w_{80}) = y_4 w_{48} + y_5 w_{58} + y_6 w_{68} + y_7 w_{78} + w_{80} \quad (4.27)$$

MLPNN1 and MLPNN2 were each trained using the Levenberg-Marquet training algorithm.

MLPNN1 was trained to give an output of '0' if the generator to be classified will be coherent with reference generator 'ref 1'. Reference generator 'ref 1' is the generator with the highest MSD value in the second stage. MLPNN1 gives an output of '1' if the generator to be classified will not be coherent with 'ref 1'. MLPNN 2 was trained to give an output of '0' if the generator to be classified will be coherent with reference generator 'ref 2'. Reference generator 'ref 2' is the generator with the highest MSD value in the third stage. MLPNN 2 gives an output of '1' if the generator to be classified will not be coherent with 'ref 2'. MLPNN1 was trained using data from two transient unstable conditions. MLPNN2 was trained with data from one transient unstable condition.

A flowchart of the proposed coherency prediction scheme is shown in Figure 4.10. The coherency prediction scheme is activated when a generator or system is predicted to be transient unstable following a disturbance. The scheme obtains the predicted stability status of each generator and sorts the generators into generators predicted to be stable and those predicted to be unstable. The generators predicted to be stable are all placed in a classified coherent group 'S', while the generators predicted to be unstable are placed in an unclassified coherent group 'U'. The scheme stops when only one generator is found in U. That generator is put in coherent group C_0. When more than one generator is found in U, the scheme sets a variable *j* to zero and obtains the maximum speed deviation (MSD) of each generator in U, in the 5^{th} cycle after the tripping of a line or bus following a disturbance. *j* is a positive integerwhich indicates various coherent groups. The generator with the highest MSD value is placed in a classified coherent group 'C_j' and made the reference generator'ref($jmod2+1$)' in the group, The MSD of 'ref($jmod2+1$)'is used as input $x_1$of MLPNN($jmod2+1$) for the placement of all other generators found in unclassified group U. For each of the other generators in U, its MSD is used as input x_2 of

MLPNN(j*mod*2+1) for the placement of that generator in classified group'C_j'. MLPNN(j*mod*2+1) determines whether a generator in U has to be added to group C_j or belongs to a different group. *j* is incremented when U still has a generator or generators. The scheme ends when no generator is found in U.

KNUST

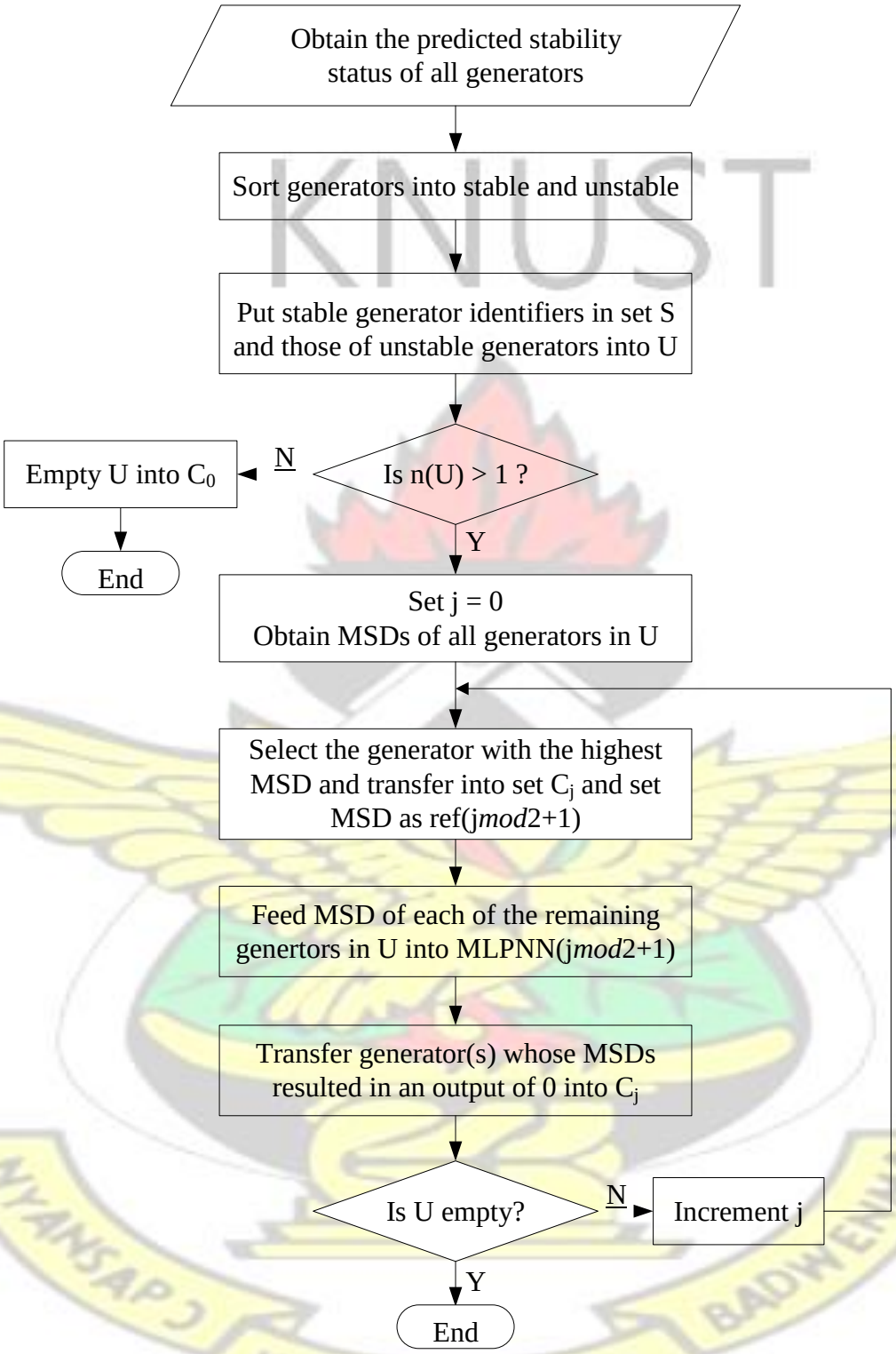

Figure 4.10: Flowchart of proposed prediction scheme for coherency grouping

Chapter 5 RESULTS AND ANALYSIS

5.1 **Wavelet Transform-based Generator Out-of-Step Prediction Scheme**

Data from 54 fault cases were used to test the proposed wavelet transform-based generator outof-step (OS) prediction scheme. Forty four of the 54 cases resulted in generator OS conditions while the remaining 10 cases had all generators remaining stable.

Figure 5.1 shows machine rotor angles for a three-phase fault at bus 26 for a base load case. The fault was applied at time $t = 0.1s$ and the line was tripped after 5 cycles ($t = 0.2s$). From the rotor angle plots, generator 9 became unstable. The corresponding plot of rotor speed deviations is shown in Figure 5.2.

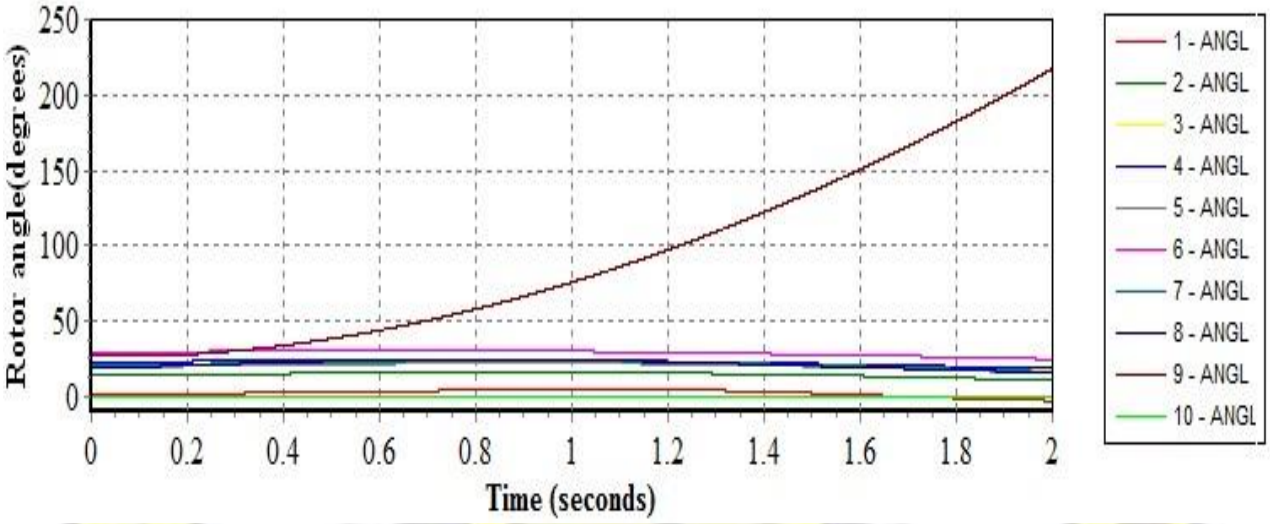

Figure 5.1: Rotors angels for a three-phase fault at bus 26

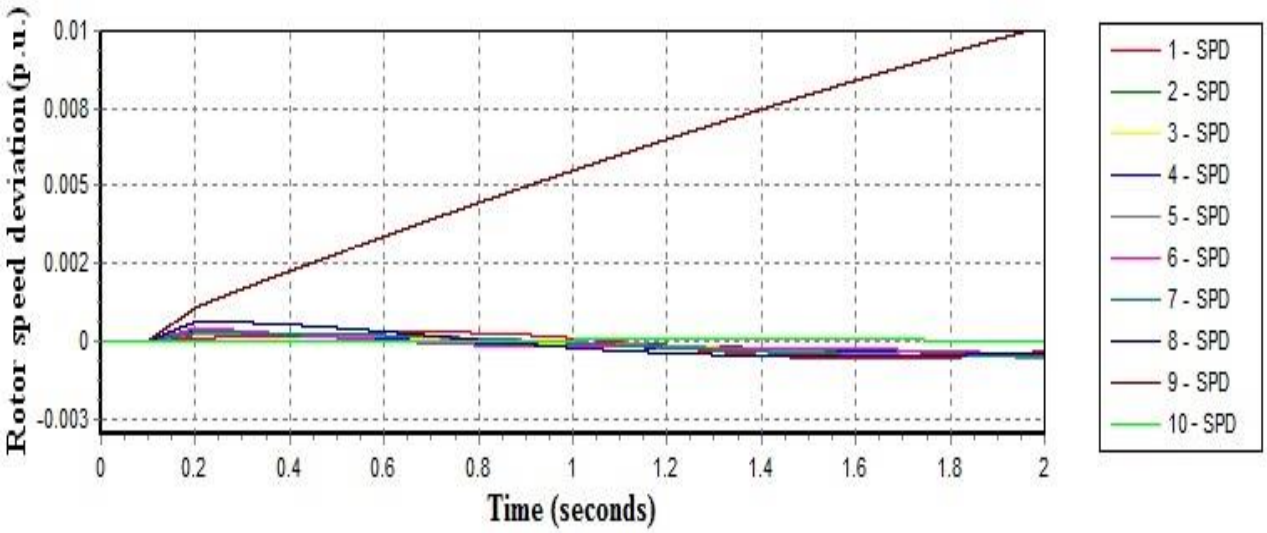

Figure 5.2: Rotor speed deviations for a three-phase fault at bus 26

The time window for the capture of rotor speed deviation data for the wavelet analysis-based transient stability status prediction scheme is the first 3 cycles after the tripping of a bus or line following a disturbance. It is observed from Figure 5.2 that the speed deviations of generator 9 which went out of step are much higher than those of the generators which remained in synchronism. Also, Figure 5.3 shows rotor angles for a three-phase fault on the line between bus 16 and bus 19 for a base load case. Here, generators 4 and 5 went out of step. The corresponding plot of rotor speed deviations is shown in Figure 5.4.

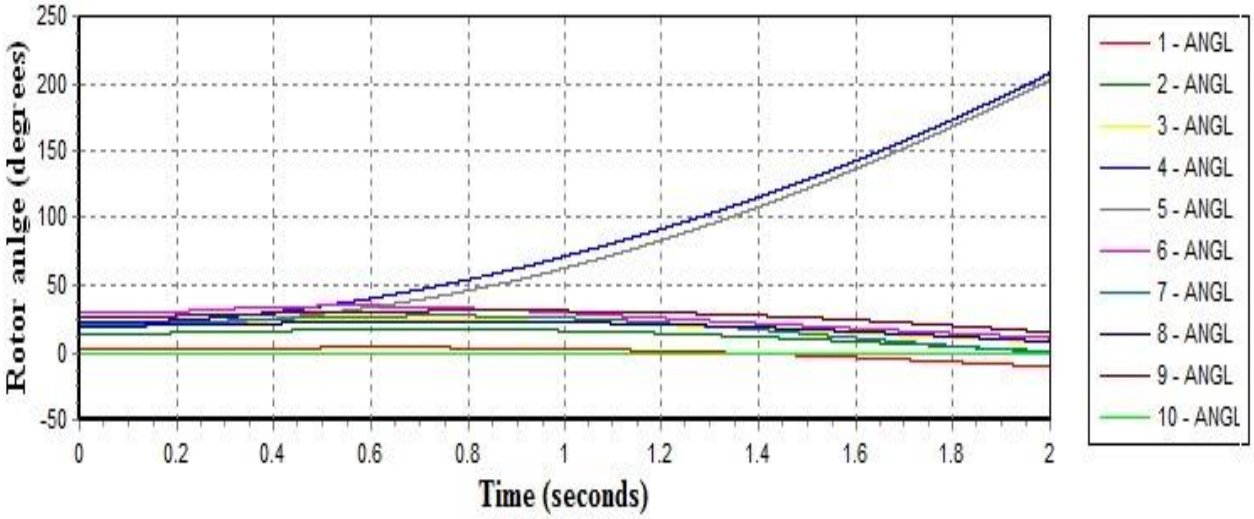

Figure 5.3: Rotors angles for a three-phase fault on the line between bus 16 and 19

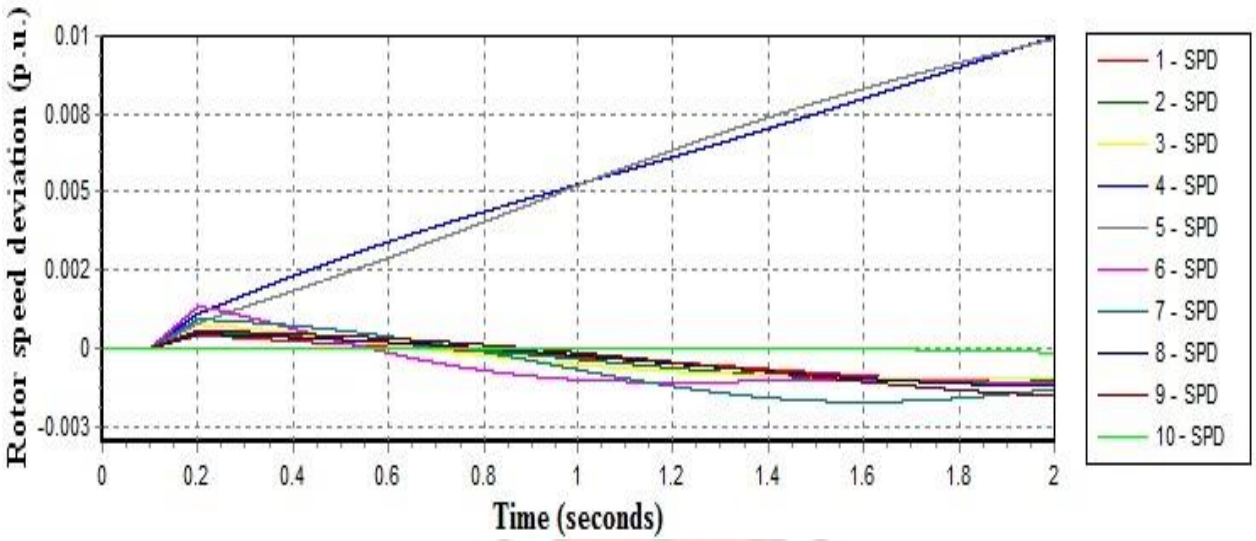

Figure 5.4: Rotor speed deviations for a three-phase fault between line 16 and 19

Similar rotor angle and rotor speed deviation plots were observed for the other system conditions that were simulated. The above speed deviation plots show that even before out of step conditions arise, speed deviations of generators that go out of step are higher than those that remain stable.

Table 5.1 presents the number of generators that went out of step in each of the 44 fault conditions that led to some generators going out of step. For 36 of the 44 unstableconditions, only 1 generator went out of step in each case. In 4 of the 44 unstable conditions, 2 generators each went out of step. In the remaining 4 of the fault cases, 4 generators each went out of step.

Thus a total of 60 individual generator OS cases arose from the 44 transient unstable conditions.

Table 5.1: Number of OS generators for various simulated faults

No.	Number of fault cases	Number of generators that went out of step in each case	Total number of OS cases
1	36	1	36
2	4	2	8
3	4	4	16

For each fault condition, the proposed scheme predicts the stability status of each of the 10 generators. Thus for the 44fault conditions which resulted in some generatorsgoing out of step, a total of 440 (that is 44 fault conditions multiplied by 10 generators)individual generator states had to be predicted. The 440 generator states comprised 60 generator OSstates and 380 stable generatorstates. Table 5.2 presents details of the predictions made by the proposed scheme for the 60 generator OS states. Table 5.3 also presents details of the predictions made by the proposed scheme for the 380 stable generator states.

Table 5.2: Test results of proposed scheme for various generator OS conditions

No.	No. of faults	No. OS predictions required	No. of Correct predictions	No. of Wrong predictions	Error(%)
1	36	36	36	0	0
2	4	8	8	0	0
3	4	16	8	8	50

Table 5.3: Test results of proposed scheme for various stable generator states

No.	No. of faults	No. stable predictions required	No. of Correct predictions	No. of Wrong predictions	Error(%)
1	36	324	324	22	6.8
2	4	32	32	0	0
3	4	24	24	0	0

For each of the 36 fault simulations which resulted in one generator each becoming unstable, the proposed scheme predicted all 36 unstable generator states with 100% accuracy. Also, the proposed scheme predicted all unstable generator conditions with 100% prediction accuracy for each of the 4 fault conditions which resulted in 2 generators each becoming unstable. However, for each of the 4 simulations which had 4 generatorseach becoming unstable, only two out of the four unstable generators states were predicted correctly in each case. Thus the algorithm is limited in predictions involving four unstable generators. However, in terms of predicting the transient

stability status of a system, the prediction accuracy will be 100%.Also, the prediction accuracy of the proposed scheme for the 380 stable generator states with 44 faults that resulted in some generators going out of step was found to be 94.2%.

For the 10 fault conditions which resulted in all generators becoming stable, the algorithm had to make a total of 100 predictions, all indicating stable generator states. 3 out of the 100 generator states were predicted wrongly. Thus the prediction accuracy of theproposed scheme for faults which resulted in all generators remaining stable was found to be 97%.

5.2 **Generator Out-of-Step Prediction using Rotor Speed Deviation and Multilayer Perceptron Neural Network**

Ninety five three-phase faults were simulated to test the proposed rotor speed deviation and MLPNN-based generator OS prediction scheme. Sixty one of the 95 faults resulted in various generator OS conditions while the remaining 34 faults resulted in all generators remaining stable. All stable cases had fault durations of 0.1s (5 cycles) while OS conditions were obtained for faults lasting between 0.7s(35 cycles) and 0.9s (45 cycles).Figure 5.5 shows a plot of machine rotor angles for a three-phase fault on bus 28, for a base load condition. The fault was applied at 0.1s and lasted for 0.7s after which the bus was disconnected resulting in generator 9 going out of step. All other machines remained in synchronism for the aforementioned fault condition. The corresponding plot of rotor speed deviation is shown in Figure 5.6.

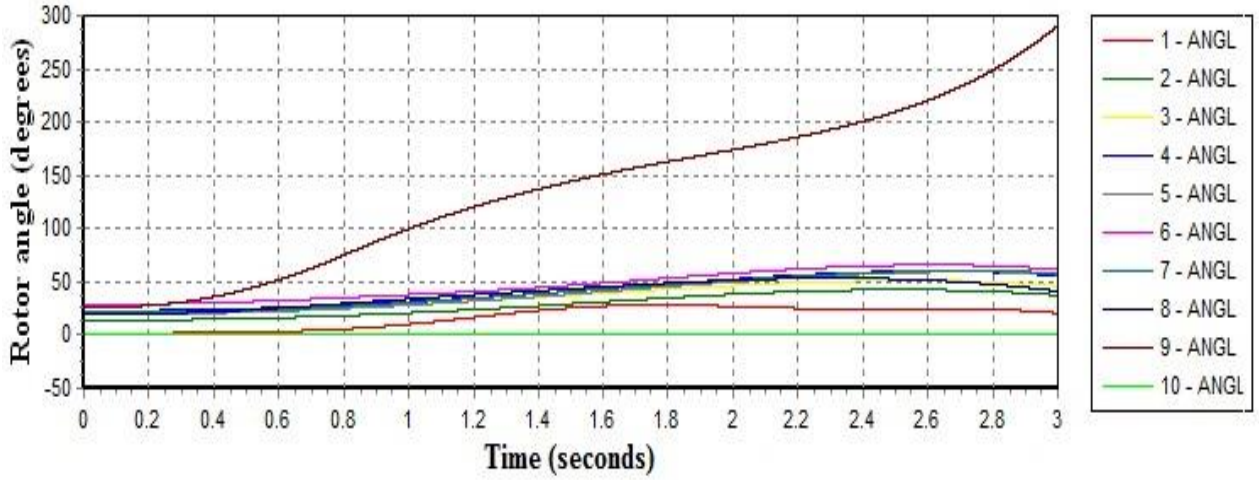

Figure 5.5: Rotor angles for a three-phase fault on bus 28

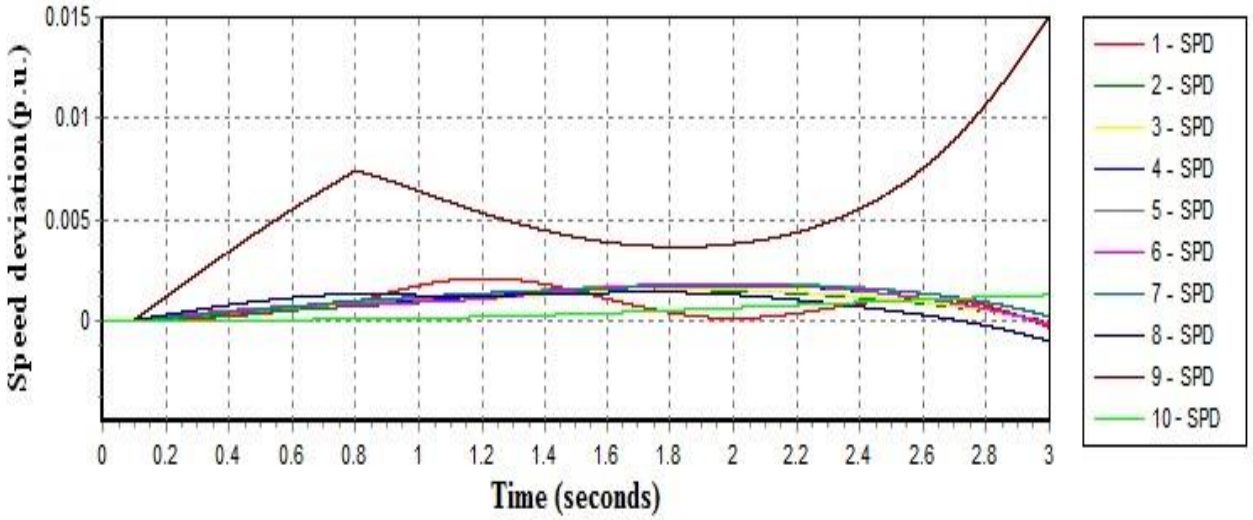

Figure 5.6: Rotor speed deviations for a three-phase fault on bus 28

Also, Figure 5.7 shows rotor angles for a three-phase fault between buses 6 and 11 for 105% of base load condition. The fault was applied at 0.1s and lasted for 1s. This resulted in generators 2 and 3 going out of step. All other generators remained in synchronism. Figure 5.8 shows the corresponding plot of rotor speed deviations.

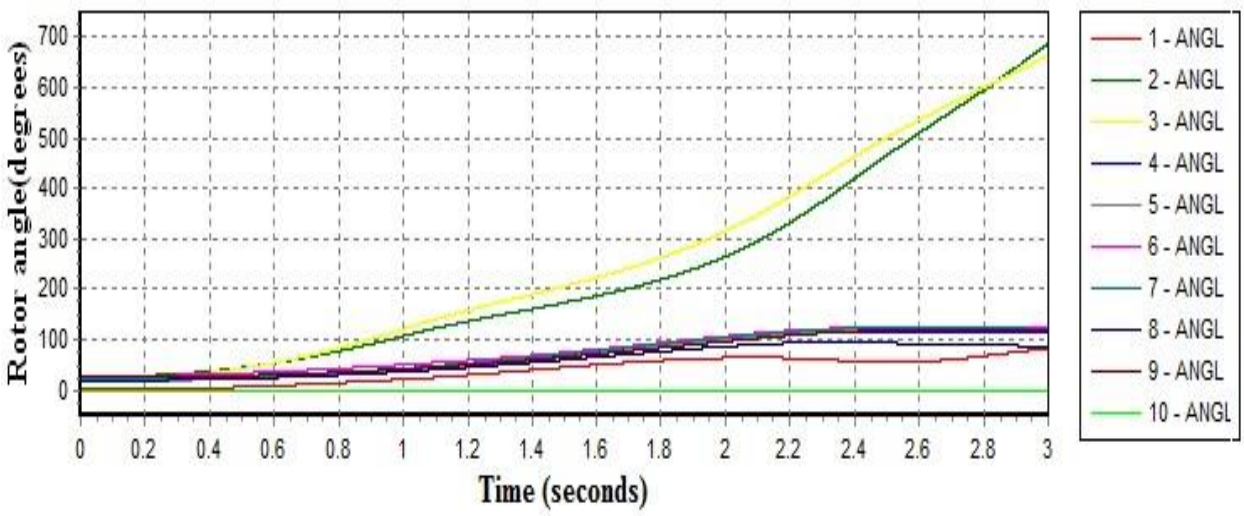

Figure 5.7: Rotor angles for a three-phase fault on the line between bus 6 and bus11

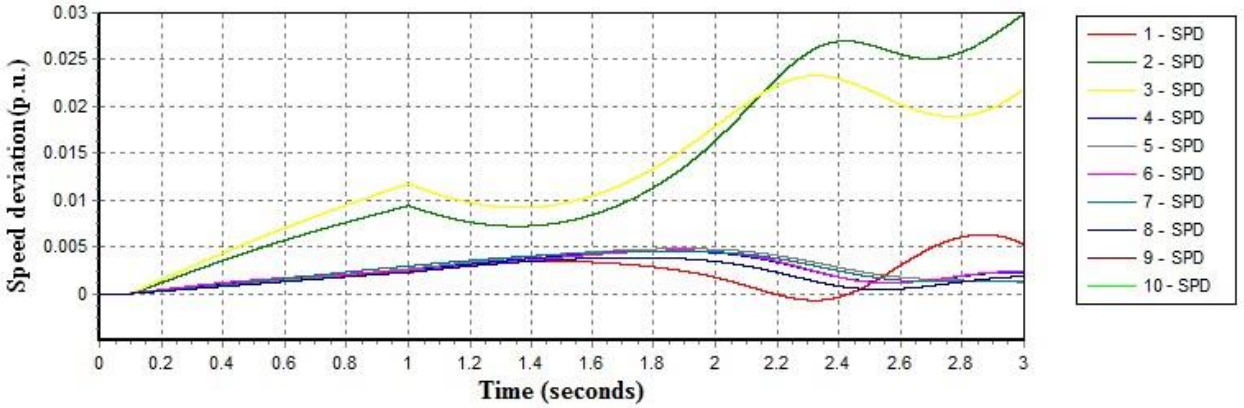

Figure 5.8: Rotor speed deviations for a fault on line between buses 6 and 11

It can be observed from Figure 5.6 and Figure 5.8 that within the first cycle after the tripping of a line or bus, the maximum speed deviations of the generators that went out of step are higher than those of the generators that remained stable. Similar waveforms were observed for the other fault conditions simulated.

The training performance of the MLPNN used is shown in Figure 5.9.

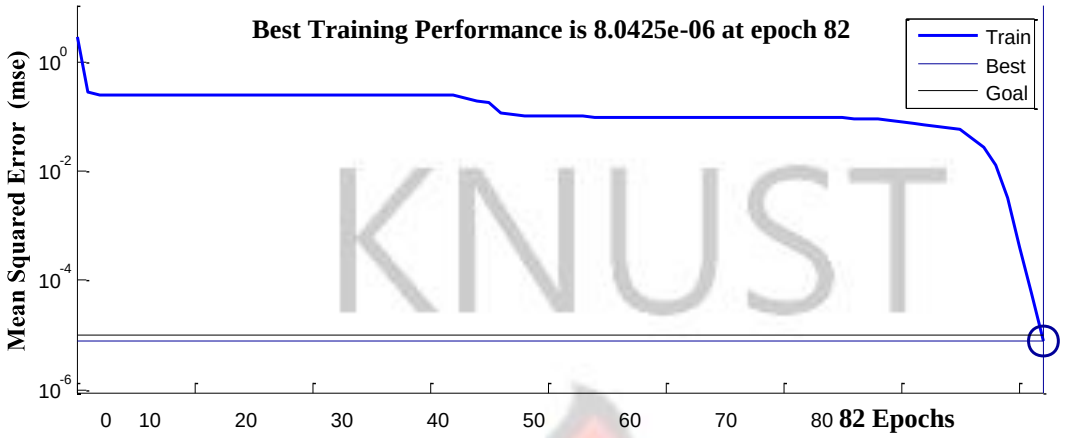

Figure 5.9: Training performance of MLPNN for out-of-step prediction

Table 5.4: Weights and Biases of MLPNN for generator OS prediction

Weight values			Bias values		
x – Input layer	Input layer – Hidden layer	Hidden layer- Output layer	Input layer	Hidden Layer	Output layer
w_{11} 120.9797	w_{12} 7.6581e^{05} w_{13} 121.0394	w_{24} 2.2658 w_{34} 0.500	b_{10} 0.7135	b_{20} 0.0592 b_{20} 3.0738	b_{40} 0.6340

Table 5.4 presents the weights and biases obtained after the training of the MLPNN.Table 5.5 presents sample calculation of how the output of the trained MLPNN is obtained using (4.15) – (4.19) for a given input MSD.

Table 5.5: Sample calculation of output of MLPNN for generator OS prediction

Input (MSD)	State	y_1	y_2	y_3	O
0.0014	stable	-0.59254	-0.0591	-1	0.000273
0.0009	stable	-.060464	-0.0591	-1	0.000275
0.0094	unstable	0.0423687	-0.0592	1	2.000097
0.0106	unstable	0.568862	-0.0592	1	2.000072

From Table 5.5, it can be observed that for the stable generator states where the output of the MLPNN was expected to be 0 for both cases, the MLPNN gave outputs of 0.000273 and

0.000275. Also whereas the outputs for the unstable generator states were each expected to be 1, the MLPNN gave outputs of 2.000097 and 2.000072. A similar situation is observed in digital communication networks, where the received bits have some deviation with respect to the sent bits. In these networks, the Transistor-Transistor Logic (TTL) standard is usually used in the receiving equipment to detect the received bits. This standard is also used to determine the output status of the MLPNN [5].

$$O_j \geq 0.8 \text{ or } O_j \leq 1 \text{ (Out of step)} \tag{5.1}$$

$$O_j \leq 0.2 \text{ or } O_j \geq 0 \text{ (Stable)} \tag{5.2}$$

Where: O_j is the output of the MLPNN.

In the digital communication networks, if the value of a received bit is in the range of 0.2 to 0.8, it is considered as a missing bit. Besides, if a "1" bit is received in the range of 0 to 0.2 or a "0" bit is received in the range of 0.8 to 1 it is considered an error bit, which is a worse incorrect case than the missing bit. This interpretation for the error and missing bits is also used for the output of the MLPNN.

Thus from (5.1) and (5.2), the outputs of the MLPNN in Table 5.5 can be interpreted as 0 for the stable states and 1 for the unstable states.

Each generator was assigned one MLPNN to predict its stability status. Thus for every fault condition simulated, 10 MLPNN independent predictions were made. Therefore for the 61 fault conditions that resulted in OS conditions, there were a total of 610 MLPNN predictions. Table 5.6presents details of the number of out of step predictions that were expected in the 61 fault conditions. A total of 88 individual generator OS predictions were expected out of the 610

predictions. The remaining 512 predictions were expected to be predictions indicating stable generator states.

Table 5.6: Number of generators involved in OS cases

No.	No. of system OOS cases	No.of OS generators per case	No. of OS predictions required
1	38	1	38
2	21	2	42
3	2	4	8
Total	61		88

The trained MLPNN responded to the 88 OS cases with 100% accuracy while the response to the 512 stable generator cases was found to be 98.05% accurate. The 340 MLPNN predictions made for the 34 fault conditions which had all 10 generators remaining in synchronism were 100% accurate.

5.3 **Prediction of System Transient Instability using Rotor Speed Deviations and Multilayer Perceptron Neural Network**

This scheme was also tested with data from the 95 fault conditions used to test the rotor speed deviation and MLPNN-based generator OS prediction scheme. Figure 5.10 shows the training performance of the MLPNN used.

The trained MLPNN predicted the 61 system transient instability cases presented to it with 100% accuracy. The responses to the 34 system transient stability cases were also 100% accurate.

Best Training Performance is 9.1357e-06 at epoch 58

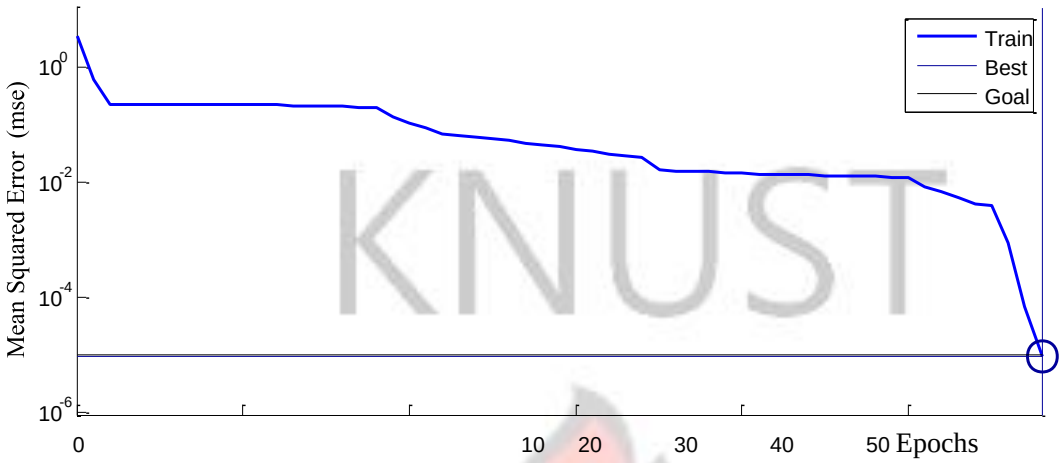

Figure 5.10: Training performance of MLPNN for transient stability status prediction

5.4 **Prediction of Coherent Generator Groupings**

Data from 117 transient unstable fault conditions was used to test the proposed scheme that predicts coherent generator groups that will be formed following transient instability. Figure5.11 shows the rotor angles of the ten generators for a three-phase fault between lines 5 and 8 which lasted for 1s (50 cycles). The loading was a base load condition.

KNUST

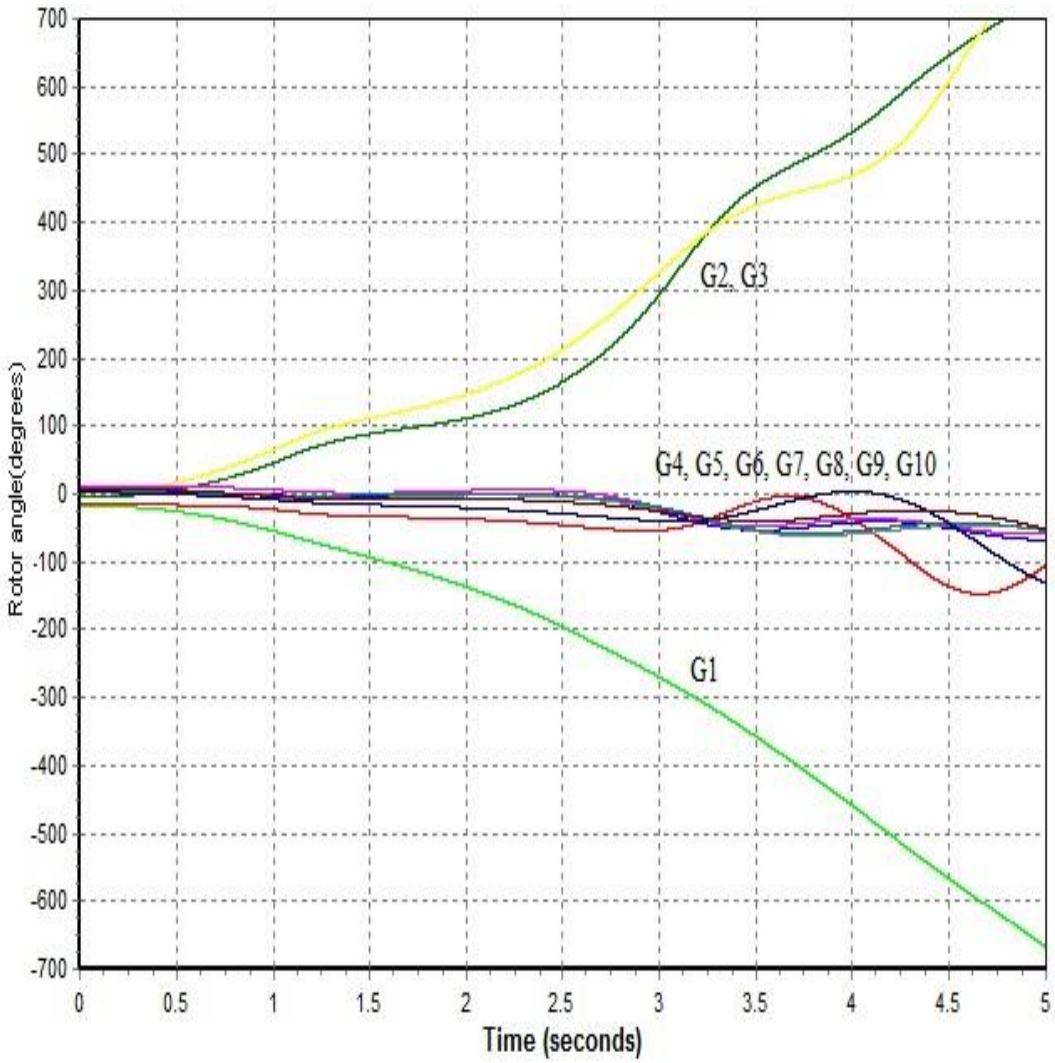

Figure5.11: Rotor angles of generators for a three-phase fault between lines 5 and 8

Three coherent groups resulted from this simulation. It can be observed from Figure 5.11 that generators 2 and 3 form one coherent group. Generators 4, 5, 6, 7, 8, 9, and 10 form another coherent group. Generator 1 stands alone. The corresponding plot of rotor speed deviations is shown in Figure 5.12. It can be seen from Figure 5.12 that the rotor speed deviations of the generators in each coherent group, immediately following the tripping of the line (at 1.1 seconds), are quiet close to each other. However, the speed deviations for different machines belonging to different coherent groups are clearly distinct. For example, whereas the speed deviations of

generators 2 and 3 which form the first coherent group are much greater than 0.005, those in the second coherent group which comprises generators 4, 5, 6, 7, 8, 9 and 10 are lower than 0.005. Also, the speed deviation of generator 1 which forms the third group is much lower than 0.001. Additionally, the difference between the speed deviations of generators in a coherent group is much lower than that between generators belonging to different coherent groups. Similar trends were observed for the other simulations that were carried out. Thus, the plots from the simulations corroborate what has been demonstrated theoretically that the speed deviations of the various generators in a system can be used to predict coherent generator groups following a disturbance.

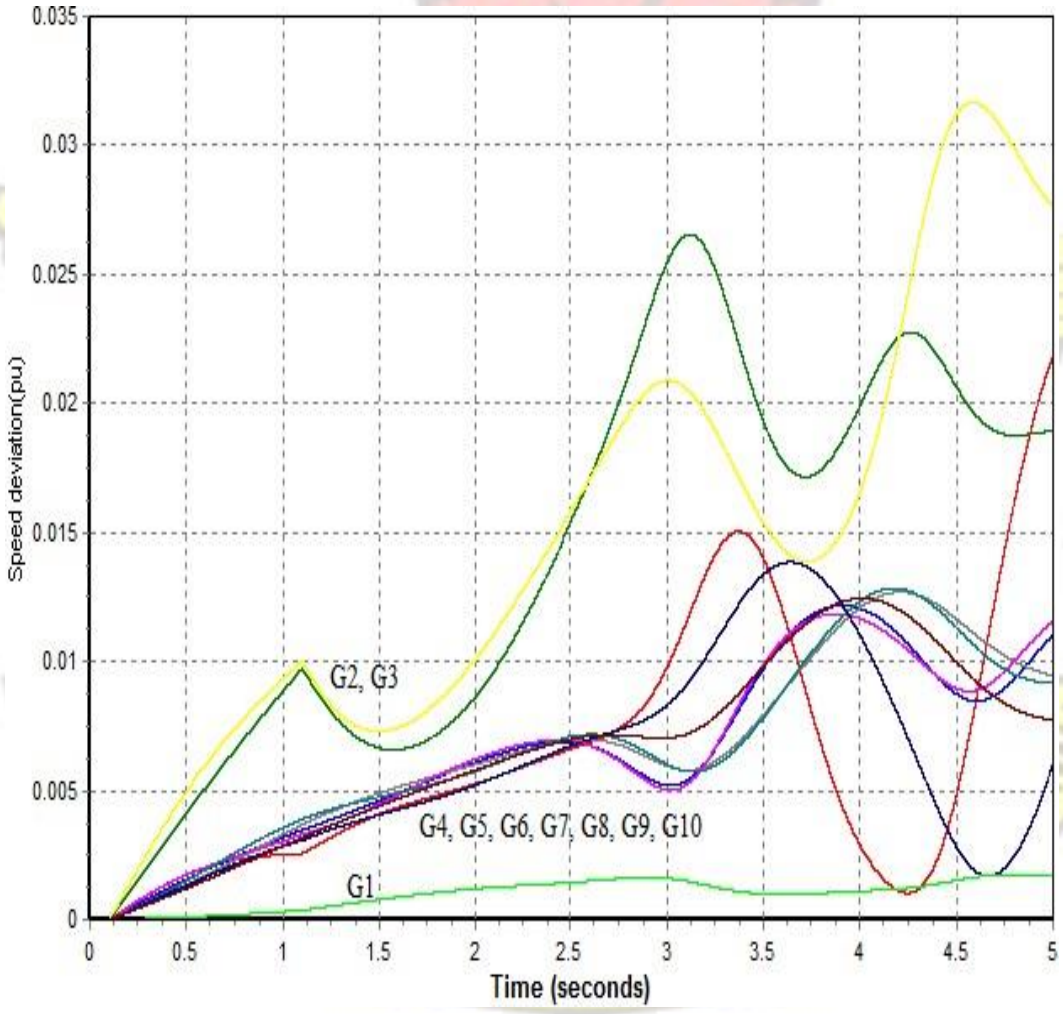

Figure5.12: Rotor speed deviations of generators for a three-phase fault between lines 5 and 8

Table 5.7presents the number of coherent groups that were formed in the 117 fault conditions simulated.

Table 5.7: Number of coherent groups formed for various fault conditions

No.	Number of fault conditions	Number of coherent groups for each condition
1	83	2
2	31	3
3	3	4

Figure 5.13 and Figure 5.14 show training performance curves for MLPNN1 and MLPNN2respectively.

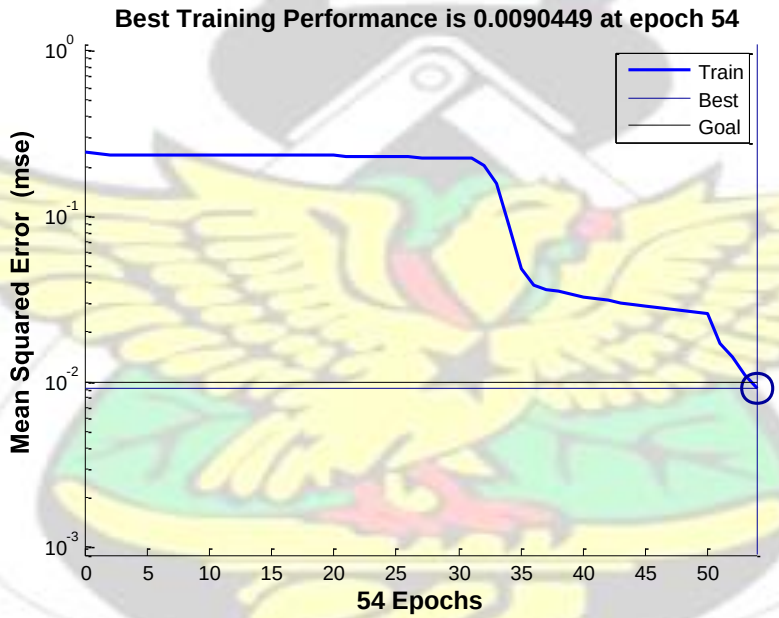

Figure 5.13:Training performance of MLPNN 1

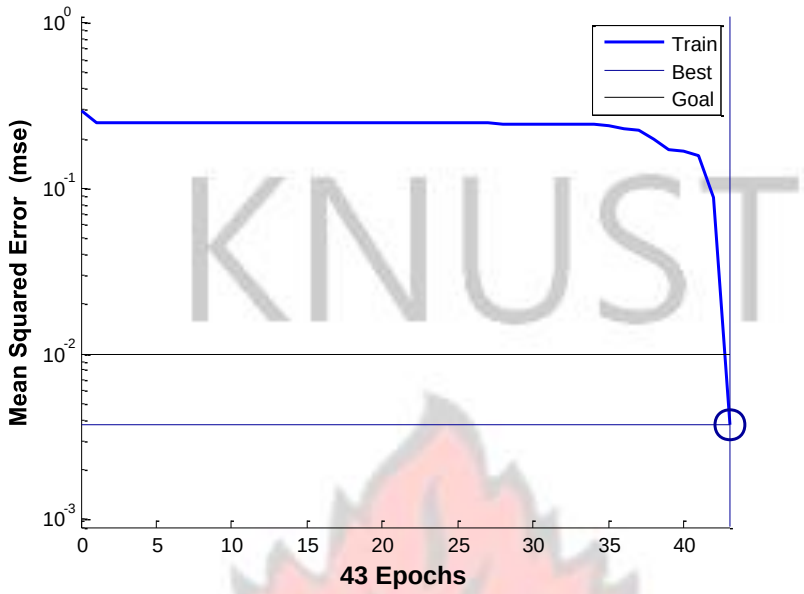

Figure 5.14:Training performance of MLPNN 2

Table 5.8 presents the coherent groups formed for a three-phase fault on the line between buses 5 and 8. The rotor angle and speed deviation plots are shown in figures 5.12 and 5.13 respectively.

Table 5.8: Formed coherent groups for a fault on the line between buses 5 and 8

Group name	Generators
A	1
B	2 and 3
C	4, 5, 6, 7, 8, 9 and 10

In the first stage of the proposed grouping algorithm, generators in group C were placed in coherent group S. The generators in groups A and B were placed in unclassified group U1.In the second stage of the algorithm, generator 3 which had the highest MSD(that is 0.0088) was made the reference generator, 'ref1'. Generator 3 was thus placed in classified unstable group C1. The scheme then determined whether or not generators 1 and 2 were in group C1.

Generator 1 did not belong to group C1 so MLPNN1 was required to give an output of '1', which it did. Generator 2 belonged to group C1 and as expected,MLPNN1 gave an output of '0'.The algorithm ended at the second stage after placing generator 1 in group C2. Table 5.9presents the responses of MLPNN1.

Table 5.9: MPLNN1 responses to a fault on the line between bus 5 and bus 8

Generator no.	MSD	Desired MLPNN1 output	Actual MLPNN1 output
1	0.0005	1	1
2	0.0085	0	0

Table 5.10presentsthe coherent groups formed for a three-phase fault on bus 4 for 80% base load condition. For this condition, four coherent groups were formed.

Table 5.10: Formed coherent groups for a three-phase fault on bus 4

Group name	Generators
A	1
B	2
C	4, 5, 6 and 7
D	3, 8, 9 and 10

In the first stage of the proposed algorithm, the generators in D were placed in stable coherent group S. The generators in A, B and C were placed in unclassified unstable group U1. In stage two, generator 7 was made ref1 and placed in group C1. Table 5.11presents the responses of MLPNN1. MLPNN1 gave outputs of '0' each when fed with MSD data of generators 4, 5 and 6, indicating that they belonged to the same coherent group as generator 7. MLPNN1 gave outputs of '1' when fed with MSD data for generators 1 and 2, indicating that they do not belong to the same coherent group as 7. Generators 1 and 2 were subsequently placed in unclassified unstable group U2. In stage three, generator 2 was made

'ref 2' and placed in classified group C2. MLPNN2 was then employed to determine whether or not generator 1 belonged to the same group as 2. MPLNN2 gave an output of '1' as required showing that the two generators belonged to different coherent groups.

Table 5.11: MLPNN1 responses to a three-phase fault on bus 4

Generator no.	MSD	Desired MLPNN1 output	Actual MLPNN1 output
1	0.0004	1	1
2	0.0034	1	1
4	0.0062	0	0
5	0.0072	0	0
6	0.0079	0	0

Similar responses were obtained for the other fault conditions. There were however, some grouping errors. Table 5.12 presents the generator placement prediction accuracy of the proposed scheme for the 117 fault conditions simulated.

Table 5.12: Prediction accuracy of proposed coherent grouping scheme

No.	No. of faults	No. of coherent groups per fault	Prediction accuracy
1	83	2	92.77%
2	31	3	89.03%
3	3	4	53.33%

KNUST

Chapter 6

CONCLUSIONS

6.1 **Overview**

In this work,comprehensive predictive schemes for improving power system operation following a large disturbance have been developed. The schemes make use of rotor speed deviation as the only power system input parameter. Wavelet transform and multilayer perceptron neural networks were used for signal processing and decision making respectively. The schemes predict the transient stability status of a system following a disturbance and also indicate specific generators that will go out of step.For a system that will be transient unstable, the coherent generator groups that will be formed are also predicted.

6.2 **Contributions**

Firstly, a wavelet transform-based generator out-of-step prediction scheme has been developed. In this scheme, the wavelet entropies contained in detail 8 coefficients obtained three consecutive cycles after the tripping of a bus or line are used. Test results of the scheme show 8.8% prediction error.

Secondly, a multilayer perceptron neural network-based scheme that predicts the transient stability status of a power system has been developed. The scheme responded to 61 transient unstable cases with 100% accuracy. Also, the response to 34 transient stable cases was 100% accurate.

Thirdly, a scheme that predicts generators that will go out of step following a transient disturbance has been developed. The scheme was tested using 95 fault conditions. The prediction accuracy for the proposed scheme was 98.05%.

Lastly, a scheme that predicts coherent generator groups that may be formed after a disturbance has been proposed. This scheme uses two multilayer perceptron neural networks. The prediction accuracy ofthis scheme for 117 fault conditions which resulted in the formation of coherent generator groups was 90.43%.

All the four schemes use rotor speed deviation as inputs thus demonstrating also the potential of speed deviation as a power system input signal for the prediction of transient instability conditions. The use of speed deviation which can be measured in the field makes the schemes easy to implement. The use of only one input parameter also makes the schemes simple to implement. The schemes are also accurate in their predictions.Finally, given the early period of data capture, quick data processing, and the speedy response of decision making tools used, the schemes are expected to give fast responses.

6.3 **Future Work**

The following additional studies are recommended:

(a) Improving the prediction accuracy of the coherent generator prediction scheme. Such a study may vary the data window for extracting the rotor speed deviations or explore other power system input parameters. Other decision making tools such as decision trees may also be investigated.

(b) Development of an adaptive islanding scheme based on the proposed coherent generator group prediction scheme. This study will determine the splitting boundaries for various islands taking inputs from the proposed coherency prediction scheme.

(c) Development of a scheme to predict when actual out-of-step begins during disturbances. Such a scheme will provide advance information on when system splitting should take place.

KNUST

KNUST

REFERENCES

1. Frimpong, E. A., Okyere, P. Y., and Anto, E. K. (2009). Adaptive single-Pole autoreclosure scheme based on standard deviation and wave energy. Journal of Electrical Engineering, 9(4): 61-68.
2. Amjady N. (2005). Application of a new fuzzy neural network to transient stability prediction. IEEE Power Engineering Society General Meeting, 1: 636-643.
3. Al-Tallaq K. N. and Feilat E. A. (2005).Online detection of out-of-step operation based on prony analysis-impedance relaying. Proceedings of the 5th WSEAS Int. Conf. on Power Systems and Electromagnetic Compatibility, 55-60.
4. Trodden, P. A., Bukhsh, W. A., Grothey, A. and McKinnon, K. I. M. (2012). MILP islanding of power networks by bus splitting, IEEE Power and Energy Society General Meeting.
5. Akuoko, S. et al (2012). Investigation into the causes of the three total system collapses in the Ghana power system, Draft Final report for Public Utilities Regulatory Commission (PURC).
6. Amjady, N. and Majedi, S. F. (2007). Transient stability prediction by a hybrid intelligent system, IEEE Transactions on Power Systems, 22(3): 1275-1283.
7. Amjady, N. and Ehsan, M. (1997). Transient stability assessment of power systems by a new estimating neural network, Can. J. Elect. Comp. Eng., 22(3): 131-137.
8. Brown,H. E.,Happ,H. H., Person,C. E., and Young, C. C. (2009). Transient stability solution by an impedance matrix method, IEEE Transactions on Power Apparatus and Systems, 84(12): 1204-1214.

9. Jones, G. A. (2009). Transient stability of a synchronous generator under conditions of bangbang excitation scheduling, IEEE Transactions on Power Apparatus and Systems, 84(1): 114121.
10. Pai, M. A.Energy function analysis for power system stability,Kluwer Academy Publishers, Norwell, Massachusetts, 1989.
11. Garcia, G.,Benussou, J. and Berbuche, M. (1992). Pattern recognition applied to transient stability analysis of power systems with modeling including voltage and speed regulation", Proceedings of Institute of Electrical Engineers, 139(4): 321-325.
12. Miranda, V.,Fidalgo, J. N.,Pecas Lopes, J. A. and Almedia, L. B. (1995). Real time preventive actions for transient stability enhancement with a hybrid neural networkoptimization approach, IEEE Transactions on Power Apparatus and Systems, 10(2): 10291035.
13. Yorino, N.,Saito, T.,Kamei, Y. and Sasaki, H. (2007). A new method for transient stability analysis, Electrical Engineering in Japan, 159(3): 26-33.
14. Abdelaziz,A.Y., Irving, M.R., Mansour, M.M., El-.Arabaty, A.M. andNosseir, A.I. (1996) Adaptive detection of generator out-of-step Conditions in power systems using an artificial Neural network, Proceedings of UKACC International Conference on control, 1:1407-1412.
15. Wang, L., Girgis, A. A. (1997). A new method for power system transient instability detection. IEEE Transactions on Power Delivery, 12(3): 1082-1089.
16. Guo, H.-Z., Xie, H., Zhang, B.-H., Yu, G.-L, Li, P., Bo, Z. -Q and Klimek, A. (2010). Study on power system transient instability detection based on wide area measurement system, European Transactions on Electrical Power, 20:184–205.
17. Guo, H.-Z., Xie, H., Zhang, B.-H., Yu, G.-L, Li, P., Bo, Z. -Q and Klimek A. (2008). Power System Transient Instability Detection Algorithm Based on Real Time Measurement,

Proceedings of Asia Pacific Conference on Circuits and Systems, IEEE, 631-634.

18. Xie, H., Zhang, B., Zou, B.-g., Bo Z.-q., Yu, G.-L and Li, L. (2007). Real time transient instability detection with partial wide-area measurement information, Power Engineering Society General Meeting, 2007, IEEE, 1-7.
19. Rajapakse, A. D., Gomez, F., Nanayakkara, O. M. K. K., Crossley, P. A. and Terzija, V. V. (2010). Rotor angle stability prediction using post-disturbance voltage trajectory patterns, IEEE Transactions on Power Systems, 25(2): 945-956.
20. Ebrahimpour, R., Abharian, E. K., Moussavi, S. Z. and MotieBirjandi, A. A. (2010). Transient stability assessment of a power system by mixture of experts, International Journal of Engineering, 4(1): 93-104
21. Ebrahimpour, R. andAbharian, E. K. (2009). An improved method in transient stability assessment of a power system using committee neural networks, International Journal of Computer Science and Network Security, 9(1): 119-124.
22. Wahab, N. I. A., Mohamed, A. and Hussain, A. (2007). Method in transient stability assessment of a power system using probabilistic neural network, Journal of Applied Sciences Research, 3(11): 1267-1274.
23. Yamashita, K., and Kameda, H. (2004). Out-of-Step Prediction Logic for Wide-Area Protection Based on an Autoregressive Model, IEEE PES Power Systems Conference and Exposition, 1: 307 – 312.
24. Kundur, P., Paserba J., Ajjarapu V., Andersson, G., Bose, A., Canizares, C., Hatziargyriou, N., Hill, D., Stankovic, A., Taylor, C., Cutsem, T. V. and Vittal V. (2004). Definition and Classification of Power System Stability, IEEE Transactions on Power Systems, 19(2): 13871401.

25. Gomez, F.,Rajapakse A., Annakkage, U., Fernando, I. (2011). Support Vector MachineBased Algorithm for Post-Fault Transient Stability Status Prediction Using Synchronized Measurements, IEEE Transactions on Power Systems, 26(3):1474-1483.
26. Liu, C. W.,Su, M. C.,Tsay, S. S., and Wang,Y. J. (1999) "Application of a novel fuzzy neural network to real-time transient stability swings prediction based on synchronized phasor measurements". IEEE Trans. Power App. Syst., 14(2): 685-692.
27. Rovnyak, S., Kretsinger, S., Thorp, J. and Brown D.(1994).Decision trees for real-time transient stability prediction.IEEE Transactions on Power Systems, 9(3): 1417-1426.
28. Morioka, Y., Tomiyama, K., Arima, H., Sawai, R., Omata, K., Matsushima, T., Takagi, K., Ishibashi, A. and Saito, H. (1993). System separation equipment to minimize power system instability Using generator's angulajx-velocity measurements. IEEE Transactions on Power Delivery, 8(3): 941-947.
29. Rebizant, W. and Feser, K. (2001). Out-of-step protection with AI methods, IEE Seventh International Conference on Developments in Power System, 298-298.
30. Rebizant, W. (2000). ANN based detection of OS conditions in power system. 12th International conference on Power System Protection, 51-56.
31. Amraee,T. andRanjbar, S. (2013). Transient Instability Prediction Using Decision Tree Technique. IEEE Transactions on Power Systems, 28(3): 3028-3037
32. Kamwa, I., Varennes, Q. C., Samantaray, S.R. and Joos, G. (2009). Development of rulebased classifiers for rapid stability assessment of wide-area post-disturbance records. IEEE Transactions on Power Systems, 24(1): 258-270.
33. Aggarwal, R. K., Johns, A. T., Song, Y. H., Dunn, R. W. and Fitton, D. S. (1994). Neuralnetwork based adaptive single-pole autoreclosure technique for ehv transmission systems.IEEProceedings on Generation, Transmission and Distribution, 141(2): 155-160.

34. E. A. Frimpong, P. Y. Okyere and E. K. Anto (2010). Adaptive single-pole autoreclosure scheme based on wavelet transform and multilayer perceptron, Journal of Science and Technology, 30(1): 102-110.

35. D. S. Fitton, R. W. Dunn, R. K. Aggarwal, A. T. Johns and A. Bannett, "Design and implementation of an adaptive single pole autoreclosure technique for transmission lines using artificial neural networks", IEEE Trans. on Power Del., vol. 11, no. 2, pp. 748-756, 1996.

36. Li, M., Pal, A., Phadke, A. G, Thorp, S. J. (2014). Transient stability prediction based on apparent impedance trajectory recorded by PMUs. International Journal of Electrical Power & Energy Systems, 54: 498–504.

37. Pakdel, Z. (2011). Intelligent instability detection for islanding prediction. PhD dissertation submitted to the Virginia Polytechnic Institute and State University.

38. Senroy, N. and Heydt, G. T. (2006). A conceptual framework for the controlled islanding of interconnected power systems. IEEE Transactions on Power Systems, 21(2): 1005-1006.

39. You, H., Vittal, V. and Wang X. (2004). Slow Coherency-Based Islanding IEEE Transactions on Power Systems, 19(1): 483-491.

40. Avdaković, S., Bećirović, E., Nuhanović, A. and Kušljugić, M. (2014), Generator coherency using the wavelet phase difference approach, IEEE Transactions on Power Systems, 29(1): 271-278.

41. Tang, K. and Venayagamoorthy, G. K. (2014). Online coherency analysis of synchronous generators in a power system. IEEE PES Innovative Smart Grid Technologies Conference (ISGT), 1-5.

42. Senroy, N. (2008). Generator Coherency Using the Hilbert–Huang Transform, IEEE Transactions on power systems, 23(4): 1701-1708.

43. Jonsson, M., Begovic, M. andDaalder (2008). A New Method Suitable for Real-Time Generator Coherency Determination, IEEE Transactions on Power Systems, 19(3): 14731482.

44. Aghamohammadi, M.R. and Tabandeh, S. M. (2012). Online Coherency Identification Based on Correlation Characteristics of Generator Rotor Angles, IEEE International Conference on Power and Energy (PECon), 499-504.

45. Yang S., Zhang B., Su, F. and Bo, Z. (2012). A Real-time Identification Scheme of Coherent Generators based on the WAMS information, 2014 International Conference on Power System Technology (POWERCON 2014), 388-394.

46. Feng, K., Zhang, Y. Liu, Z., Li Ting, Ma, H. (2012). A Wide Area Information Based Online Recognition of Coherent Generators in Power System. Power System Technology, 38(8): 2082-2086.

47. Wei, J., Kundur, D. and Butler-Purry, K. L. (2015). A Novel Bio-Inspired Technique for Rapid Real-Time Generator Coherency Identification. IEEE Transactions on Smart Grid, 6(1): 178-188.

48. Susuki, Y. and Mezic´, I. (2011). Nonlinear Koopman Modes and Coherency Identification of Coupled Swing Dynamics. IEEE Transactions on Power Systems, 26(4): 1894-1904.

49. Susuki, Y. and Mezic´, I. (2011). Correction to "Nonlinear Koopman Modes and Coherency Identification of Coupled Swing Dynamics". IEEE Transactions on Power Systems, 26(4): 2584.

50. Wang, X., Vittal, V. andHeydt, G.T. (2005)Tracing generator coherency indices using the continuation method: A novel approach. IEEE Transactions on Power Systems, 20(3): 15101518.

51. Ariff, M. A. M. and Pal, B. C. (2013),Coherency Identification in Interconnected Power System - An Independent Component Analysis Approach, IEEE Transactions on Power Systems, 28(2): 1747-1755.

52. Hart, D. G., U, D., Gharpure V., D., Karlsson, D., and Kaba, M. (2001). "PMUs – A new approach to power network monitoring" (http://www05.abb.com/global/scot/scot296.nsf/veritydisplay/2d4253f3c1bff3c0c12572430075caa7/$file/editorial_2001_04_en_pmus_-_a_new_approach_to_power_network_monitoring.pdf), (Accessed 23/07/2014).

53. Abdelaziz A. Y., Ibrahim, A. M. and Hasan, Z. G. (2012).Phasor Measurement Units for Out of Step Detection. 8th International Conference on Electrical Engineering (ICEENG), 1-21.

54. Satyanarayana, K., Prasad, B.K.V. and Rajesh, G. (2011). Transient stability enhancement of power system using intelligent technique. International Journal of Advanced Engineering Research and Studies, 1(1): 10-14.

55. Torrence, C. and P. Compo, G. P. (1998). A Practical Guide to Wavelet Analysis. Bulletin of the American Meteorological Society, 79(1): 61-78.

56. McGarry., K. J, Wermter, S. and MacIntyre, J. (1999). Knowledge Extraction from Radial Basis Function Networks and Multi-layer Perceptrons. International Joint Conference on Neural Networks, Washington D.C. 1-4.

57. Kavousifard, A. and Samet, H. (2011). Consideration effect of uncertainty in power system reliability indices using radial basis function network and fuzzy logic theory. Neurocomputing, 74(17): 3420-3427.

58. Angel, A. D., Glavic, M., and Wehenkel, L. (2007). Using Artificial Neural Networks to Estimate Rotor Angles and Speeds from Phasor Measurements. Neurocomputing, 70(16-18): 2668-2678.

59. Frimpong, E. A. and Okyere, P. Y. (2010). Forecasting the Daily Peak Load of Ghana Using Radial Basis Function Neural Network and Wavelet Transform. Journal of Electrical Engineering, 10(1): 15-18.
60. Power Systems Transient Stability – A Grand Computing Challenge
61. McDonald, M. et al. (2005). Power Swing and Out-of-Step Considerations on Transmission Lines, IEEE PSRC WG D6.
62. Senroy, N. and Heydt, G. T. (2006). A Conceptual Framework for the Controlled Islanding of Interconnected Power Systems, IEEE Transactions on Power Systems, 21(2): 1005-1006.
63. You, H., Vittal,V. and Yang, Z. (2003). Self-Healing in Power Systems: An Approach Using Islanding and Rate of Frequency Decline-Based Load Shedding. IEEE Transactions on Power Systems, 18(1): 174-181.
64. Custem, T. V. and Vournas, C. Voltage stability of electric power systems, Springer Science & Business Media, 1998, 8-9.
65. Kundur, P. Power System Stability and Control. McGraw-Hill, Inc., 1994, 17-27, 128-131, 827-832.
66. Sadat, H. Power Systems Analysis. Tata McGraw-Hill Publishing Company Limited, New Delhi, 2002, 460-464.
67. Smith, G. and Sun, K. (2009). A Controlled System Separation Scheme and Related Dynamic Studies for New York State Transmission System Using Synchrophasors, Electric Power Research Institute,1-7.
68. Liu, C.-W. and Thorp, J. (1995).Application of Synchronised Phasor Measurementsto Realtime Transient Stability Prediction, IEE Proceedings on Generation, Transmission and Distribution, 142(4): 355-360.

69. Nagrath, I. J. and Kothari, D. P. Power System Engineering. Tata Mcgraw-Hill Publishing Compay Limited, New Delhi,

70. Venkatasubramanian, V. M. and Ajjarapu, Ajjarapu. (2010). Real-Time Security Assessment of Angle Stability Using Synchrophasors, Power Systems Engineering Research Center, Document 10-10.

71. Wilkinson, W.A. and Cox, M.D. (1998). Discret Wavelet Analysis of Power System Transients. IEEE Transactions on Power Systems, 11(4): 2038-2044.

72. Fernándes, R. M. C. and Rojas, H. N. D. An Overview of Wavelet Transform Applications in Power Systems. 14th PSCC, Servilla, Session 01, Paper 6: 1-8.

73. Lee, D. T. L. and Yamamoto, A. (1994). Wavelet Analysis: Theory and Application. Hewlett-Packard Journal, 44-52.

74. Kim, C. H. and Aggarwal, R. (2000). Wavelet transforms inpower systems, Part 1 General introduction to thewavelet transforms, Power Engineering Journal, 81-87.

75. Chanda, D., Kishore, N.K. and Sinha, A.K. (2004). A wavelet multiresolution-based analysis for location of the point of strike of a lightning. IEEE Transactions on Power Systems, 19(4): 1727-1733.

76. Buckheit, J., Chen, S. Donoho, D., Johnstone, I. and Scargle, J. (2005). About WaveLab. NASA-Ames Research Center, Version 850, 1-39.

77. Pittner, S. and Kamarthi, S. V. (1999). Feature Extraction from Wavelet Coefficients for Pattern Recognition Tasks. IEEE Transactions on Pattern Analysis and Machine Intelligence, 21(1): 83-88.

78. Chanda, D., Kishore, N.K. and Sinha, A. K. (2003). Application of Wavelet Multiresolution Analysis for Classification of Faults on Transmission lines. Conference on Convergent Technologies for the Asia-Pacific Region, IEEE, 4: 1464-1469.

79. Youssef, O. A. S. (2002). New algorithm to phase selection based on wavelet transforms. IEEE Transactions on Power Delivery, 17(4): 908-914.

80. Uyar, M., Yildirim, S. and Gencoglu, M. T. (2008). An Effective Wavelet-Based Feature Extraction Method for Classification of Power Quality Disturbance Signals. Electric Power Systems Research 78: 1747–1755

81. Song, Y. H. and Yu, I. K. (1998). Wavelet Analysis and Neural Network based Adaptive Single-pole Autoreclosure Scheme for EHV Transmission Systems. Electrical Power and Energy Systems, 20(7): 465-474.

82. Gershenson, C. (2001). Artificial Neural Networks for Beginners, Formal Computational Skills Teaching Package, COGS,University of Sussex, UK.

83. Momeni, A., Maleki, S. and Khajeh, K. (2014). Analysts' Equity Forecasts Using of Multilayer Perception (MLP), Advances in Environmental Biology, 8(1): 207-211.

84. Devaraja, D., Yegnanarayanab, B. and Ramara, K. (2002). Radial Basis Functions for Fast Contingency Ranking. International Journal of Electrical Power & Energy Systems, 24(5): 387-393.

85. Karami, A. (2008). Radial Basis Function Neural Network for Power System Transient Energy Margin Estimation. Journal of Electrical Engineering & Technology, 3(4), 468-475.

86. A. N., Fathian, M. and Gholamian, M. R. (2012). Using MLP and RBF Neural Networks to Improve the Prediction of Exchange Rate Time Series with ARIMA. International Journal of Information and Electronics Engineering, 2(4): 543-546.

87. Memarian1, H. and Balasundram, S. K. (2012). Comparison between Multi-Layer Perceptron and Radial Basis Function Networks for Sediment Load Estimation in a Tropical Watershed. Journal of Water Resource and Protection, 4: 870-876.

88. Özkan, C. K. and Erbek, F. S. (2003). The Comparison of Activation Functions forMultispectral Landsat TM Image Classification, Photogrammetric Engineering & Remote Sensing, 69(11): 1225–1234.

89. Yu, H. and Wilamowski, B. M. Industrial Electronics Handbook, Intelligent Systems, CRC press, 2011, 12-1 to 12-15

90. Behbahani, H. H., Zanganeh, A, Abdi, B. (2014). Transient Stability Assessment of Power Systems using Support Vector Machine (SVM) with Distributed Generation Units. Indian Journal of Science Research, 1(2): 20-27.

91. Rudnick, H., Patino, R.I. and Brameller, A. (1981). Power-System Dynamic Equivalents: Coherency Recognition via the Rate of Change of Kinetic Energy, IEE Proceedings, 128(6): 325-333.

92. Power System Simulator for Engineers, PSS®E University Edition, 2013.

93. Song Y. (2009): Design of Secondary Voltage and Stability Controls with Multiple Control Objectives. PhD. Dissertation, School of Electrical and Computer Engineering, Georgia Institute of Technology, Georgia, USA.

94. Dobson, I. et al (1999). Avoiding and Suppressing Oscillations, Final report for PSerc project.

95. MATLAB® R2013a, MathWorks Company, 2013.

96. Rosso, O. A., Blanco, S., Yordanova, J., Kolev, V., Figliola, A., Schürmann, M. and Başar, E. (2001). Wavelet entropy: a new tool for analysis of short duration brain electrical signals. Journal of Neuroscience Methods, 105: 65-75.

97. Shrivastava, S., Jain, S. and Nema, R.K. (2012): Wavelet Entropy: Application in Islanding Detection.WSEAS Transactions on Power Systems, 7(3):126-136.

98. He, Z., Gao, S., Chen, X., Zhang, J., Bo, Z. and, Qian, Q. (2011).Study of a new method for power system transients classification based on wavelet entropy and neural network, Electrical Power and Energy Systems, 33: 402-410.

99. Dorofki, M., Elshafie, A. H., Jaafar, O., Karim, O. A. and Mastura, S. (2012). Comparison of artificial neural network transfer function abilities to stimulate extreme runoff data. International Conference on Environment, Energy and Biotechnology (IPCBEE), Singapore, 33: 1-6.

100. Duch, W. and Jankowski, N. (1999). Survey of neural transfer functions. Neural Computing Survey, 2: 163-212.

101. Karlik, B. and Oglac, A. V. (2015). Performance analysis of various activation functions in generalised MLP architectures of neural networks. International Journal of Artificial Intelligence and Expert Systems, 1(4): 111-122.

Appendix A – IEEE 39-BUS TEST SYSTEM INFORMATION

A1- General Information and Snapshot of the IEEE 39-bus Test System

The IEEE 39-bus test system also known as the New England test system is a widely used test system for transient stability studies. It is a 10-machine system with 39 buses. The generators and loads in the system represent the aggregation of many generators and load feeders connected to the same node. Generator 1 represents a large system. The system parameters adopted in the simulations carried out in this study were obtained from a dissertation written by Song [90].

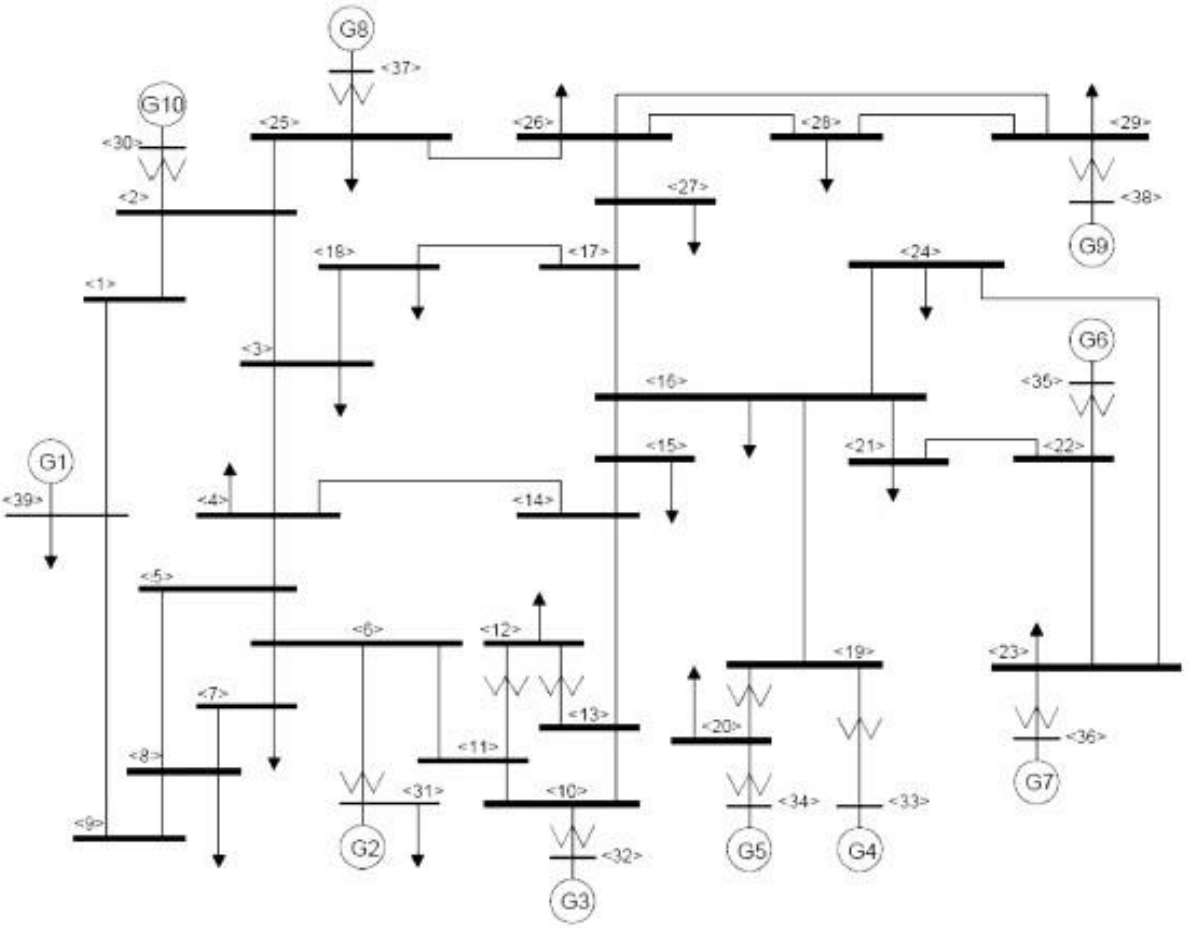

Figure A1: Snapshot of IEEE 39-bus test system

A2 - **Steady-state Modelling Information of the IEEE 39-bus System**

I – ***Lines and Transformers***

The line data for this system is shown in the Table A1. Table A2 also presents transformer tap data. All values are given on the same system base MVA of 100MVA.

Table A1: Transmission line data for IEEE 39-bus test system

From bus	To bus	R	X	B
1	2	0.003500	0.041100	0.698700
1	39	0.001000	0.025000	0.750000
2	3	0.001300	0.015100	0.257200
2	25	0.007000	0.008600	0.146000
3	4	0.001300	0.021300	0.221400

3	18	0.001100	0.013300	0.213800
4	5	0.000800	0.012800	0.134200
4	14	0.000800	0.012900	0.138200
5	6	0.000200	0.002600	0.043400
5	8	0.000800	0.011200	0.147600
6	7	0.000600	0.009200	0.113000
6	11	0.000700	0.008200	0.138900
7	8	0.000400	0.004600	0.078000
8	9	0.002300	0.036300	0.380400
9	39	0.001000	0.025000	1.200000
10	11	0.000400	0.004300	0.072900
10	13	0.000400	0.004300	0.072900
13	14	0.000900	0.010100	0.172300
14	15	0.001800	0.021700	0.366000
15	16	0.000900	0.009400	0.171000
16	17	0.000700	0.008890	0.134200
16	19	0.001600	0.019500	0.304000
16	21	0.000800	0.013500	0.254800
16	24	0.000300	0.005900	0.068000
17	18	0.000700	0.008200	0.131900
17	27	0.001300	0.017300	0.321600
21	22	0.000800	0.014000	0.256500
22	23	0.000600	0.009600	0.184600
23	24	0.002200	0.035000	0.361000
25	26	0.003200	0.032300	0.513000
26	27	0.001400	0.014700	0.239600
26	28	0.004300	0.047400	0.780200
26	29	0.005700	0.062500	1.029000
28	29	0.000000	0.015100	0.249000

Table A2: Transform tap data for IEEE 39-bus test system

From bus	To bus	Magnitude	Angle
2	30	1.0250	0.00
6	31	1.0700	0.00
10	32	1.0700	0.00
11	12	1.0060	0.00
12	13	1.0060	0.00
19	20	1.0600	0.00
19	33	1.0700	0.00
20	34	1.0090	0.00
22	35	1.0250	0.00

23	36	1.0000	0.00
25	37	1.0250	0.00
29	38	1.0250	0.00

KNUST

II – ***Loads and Generators***

Table A3 presents bus load data. This data served as the base load. Table A4 presents generator steady state data for base case.

Table A3: Steady state load data for base case

Bus	Active power(MW)	Reactive power(MVAr)
3	322.0000	2.4000
4	500.0000	184.0000
7	233.8000	84.0000
8	522.0000	176.0000
12	7.5000	88.0000
15	320.0000	153.0000
16	329.0000	32.3000
18	158.0000	30.0000
20	628.0000	103.0000
21	274.0000	115.0000
23	247.5000	84.6000
24	308.6000	-92.2000
25	224.0000	47.2000
26	139.0000	17.0000
27	281.0000	75.5000
28	206.0000	27.6000
29	283.5000	26.9000
31	9.2000	4.6000
39	1104.0000	250.0000

Table A4: Steady state generator data for base case

Bus	Voltage (pu)	Active power(MW)	Reactive power(MVAr)
30	1.0475	250.0000	145.0375
31	0.9820	0.0000	206.3611
32	0.9831	650.0001	206.0271
33	0.9972	632.0002	109.1180
34	1.0123	508.0001	167.0703
35	1.0493	650.0001	211.3163

36	1.0635	560.0001	100.5535
37	1.0278	539.9999	0.7260
38	1.0265	830.0000	22.7317
39	1.0300	1000.0000	87.6621

KNUST

A3 – **Dynamic Modelling of the IEEE 39-bus Test System**

I–***GENROU model equations***

The modelling equations of the GENROU generator model are:

$$T_{do}\frac{dE'_q}{dt} = -E_q + (X_d - X_d)I_d + E_{fd} \quad \text{(A1)}$$

$$T_{do}\frac{dE'_d}{dt} = -E_d + (X_q - X_l)I_q \quad \text{(A2)}$$

$$T_{qo}\frac{dE'_q}{dt} = -E_d + (X_q - X_l)I_q \quad \text{(A3)}$$

$$T_{qo}\frac{dE'_q}{dt} = -E_d + (X_q - X_l)I_q \quad \text{(A4)}$$

$$\omega = \omega_{sn} \quad \text{(A5)}$$

$$\frac{}{d \quad l} \qquad \frac{}{d \quad l} \qquad q \quad l \tag{A6}$$

X_q□□□□□X_{ql}□ $_{q\,d}$ □□ X_q□ □ X_d□□□□$I_d\ I_q$

□ □ *I* □

X_q *X* □

II - ***IEEE type 1 exciter equations*** (A7)

The model equations of IEEE type 1 exciter are:

(A8)

$$T_E E\text{?}_{fd} \text{□□} \square K_E \square S_E \square E_{fd} \square\square E_{fd} \square V_R \tag{A9}$$

$$T_F R\text{?}_f \text{□□} R_f \square K_F E_{fd}$$

? K_A

$$T_A V_R \text{□□} V_R \square \frac{}{} \square R_f \square K_F E_{fd} \square K_A \square V_{ref} \square V_T \square$$

$$2Hn\text{?} \square 1 \frac{}{} n \square P_M \square D_n \square \square_d \square \square X_l E_q \square I_q \square X_d \square\square\square XX_d \square\square_d I_d \square \frac{}{} XX_q \square\square \square\square XX_l E_d \square I_d$$

□ *X* □ *X* *X* □

T_F

III – ***Generator data***

The GENROU generator model in PSSE was adopted for the study. The parameters for the twoaxis model of the synchronous machines are shown in Table A5. All values are given on the same system base of 100MVA.

KNUST

Table A5: Dynamic data of generator models for IEEE 39-bus test system

Bus	30	31	32	33	34	35	36	37	38	39
T'do	10.200	4.7900	6.7000	5.6600	7.3000	5.400	5.6700	5.7000	6.5600	7.0000
T"do	0.0600	0.0600	0.0600	0.0600	0.0600	0.060	0.0600	0.0600	0.0600	0.0600
T'qo	0.2000	1.5000	0.4100	1.5000	0.4000	0.440	1.5000	1.5000	1.5000	0.7000
T"qo	0.0500	0.0500	0.0500	0.0500	0.0500	0.050	0.0500	0.0500	0.0500	0.0500
H	42.000	34.500	24.300	26.400	34.800	26.00	28.600	35.800	30.300	500.00
D	2.0000	2.0000	2.0000	2.0000	2.0000	2.000	2.0000	2.0000	2.0000	2.0000
Xd	0.1000	0.2106	0.2900	0.2950	0.2540	0.670	0.2620	0.2495	0.2950	0.0200
Xq	0.0690	0.2050	0.2800	0.2920	0.2410	0.620	0.2580	0.2370	0.2820	0.0190
X'd	0.0310	0.0570	0.0570	0.0490	0.0500	0.132	0.0436	0.0531	0.0697	0.0060
X'q	0.0800	0.0587	0.0911	0.1860	0.0814	0.166	0.1660	0.0876	0.1700	0.0080
X"d	0.0200	0.0420	0.0300	0.0380	0.0300	0.080	0.0320	0.0400	0.0430	0.0040
Xl	0.0125	0.0298	0.0280	0.0322	0.0224	0.054	0.0295	0.0304	0.0350	0.0030

IV – ***Exciter data***

The IEEET1 exciter model in PSSE was used for the study. Table A6 presents the exciter data.

Table A6: IEEET1 exciter data for IEEE 39-bus test system

Bus	30	31	32	33	34	35	36	37	38	39
TR	0.000	0.000	0.000	0.0000	0.000	0.0000	0.000	0.0000	0.000	0.0000
KA	40.000	40.00	5.000	40.000	5.000	40.000	5.000	5.0000	6.200	5.0000
TA	0.0200	0.020	0.020	0.0200	0.020	0.0200	0.060	0.0600	0.050	0.0600
VRMAX	10.000	10.50	1.000	6.5000	1.000	10.000	1.000	1.0000	1.000	1.0000
VRMIN	-10.00	-10.5	-1.000	-6.500	-1.00	-10.000	-1.00	-1.000	-1.00	-1.000
KE	1.000	1.00	-0.047	1.000	-0.0419	1.000	-0.525	-0.0198	-0.633	-0.0485
TE	0.785	1.40	0.5280	0.730	0.4710	0.785	0.500	0.5000	0.405	0.2500
KF	0.030	0.03	0.0845	0.030	0.0754	0.030	0.080	0.0800	0.057	0.0400
TF	1.000	1.00	1.2600	1.000	1.2460	1.000	1.000	1.0000	0.500	1.0000
Switch	0.000	0.00	0.0000	0.000	0.0000	0.000	0.000	0.0000	0.000	0.0000
E1	0.750	0.75	0.7500	0.750	0.7500	0.750	0.750	0.7500	0.750	0.7500
SE(E1)	0.670	0.62	0.0720	0.530	0.0640	0.670	0.080	0.1300	0.660	0.0800
E2	1.100	1.10	1.1000	1.100	1.1000	1.100	1.100	1.1000	1.100	1.1000
SE(E2)	0.910	0.85	0.2820	0.740	0.2510	0.910	0.314	0.3400	0.880	0.2600

V – ***Stabilizer data***

The PSS2A stabilizer model in PSSE was used for the study. Table A7 presents the definitions of the various parameters can be found in the PSSE library.

Table A7: Data for PSS2A stabilizer for IEEE 39-bus test system

Bus	30	31	32	33	34	35	36	37	38	39
TW1	10.0	10.0	10.0	10.0	10.0	10.0	10.0	10.0	10.0	10.0
TW2	0.00	0.00	0.00	0.00	0.00	0.00	0.00	0.00	0.00	0.00
T6	0.00	0.00	0.00	0.00	0.00	0.00	0.00	0.00	0.00	0.00
TW3	2.00	2.00	2.00	2.00	2.00	2.00	2.00	2.00	2.00	2.00
TW4	0.00	0.00	0.00	0.00	0.00	0.00	0.00	0.00	0.00	0.00
T7	0.00	0.00	0.00	0.00	0.00	0.00	0.00	0.00	0.00	0.00
KS2	0.00	0.00	0.00	0.00	0.00	0.00	0.00	0.00	0.00	0.00
KS3	0.00	0.00	0.00	0.00	0.00	0.00	0.00	0.00	0.00	0.00
T8	0.50	0.50	0.50	0.50	0.50	0.50	0.50	0.50	0.50	0.50
T9	0.10	0.10	0.10	0.10	0.10	0.10	0.10	0.10	0.10	0.10
KS1	1.00	0.50	0.50	2.00	1.00	4.00	7.50	2.00	2.00	1.00
T1	1.00	5.00	3.00	1.00	1.50	0.50	0.20	1.00	1.00	5.00
T2	0.05	0.40	0.20	0.10	0.20	0.10	0.02	0.20	0.50	0.60
T3	3.00	1.00	2.00	1.00	1.00	0.50	0.50	1.00	2.00	3.00
T4	0.50	0.10	0.20	0.30	0.10	0.05	0.10	0.10	0.10	0.50
VSTMAX	0.20	0.20	0.20	0.20	0.20	0.20	0.20	0.20	0.20	0.20
VSTMIN	-0.20	-0.20	-0.20	-0.20	-0.20	-0.20	-0.20	-0.20	-0.20	-0.20

VI – ***Turbine governor data***

The turbine governor model in PSSE used for the study was TGOV1. Table A8 presents data for the TGOV1

Table A8: TGOV1 turbine governor data for IEEE 39-bus test system

Bus	30	31	32	33	34	35	36	37	38	39
R	0.05	0.05	0.050	0.050	0.050	0.050	0.050	0.050	0.050	0.100
T1	0.40	0.40	0.400	0.400	0.400	0.400	0.400	0.400	0.400	0.800
VMAX	1.00	1.00	1.000	1.000	1.000	1.000	1.000	1.000	1.200	1.500
MIN	0.00	-0.05	-0.05	-0.05	-0.050	-0.05	-0.05	-0.05	-0.05	-0.05
T2	1.50	1.50	1.500	1.500	1.500	1.500	1.500	1.500	1.500	1.500
T3	5.00	5.00	5.000	5.000	5.000	5.000	5.000	5.000	5.000	5.000

Dt	0.00	0.00	0.000	0.000	0.000	0.000	0.000	0.000	0.000	0.000

KNUST

Appendix B – MATLAB M-FILES FOR NEURAL NETWORK TRAINING

M-files written in MATLAB for the execution of various tasks have been presented below. The definition of the various terms can be found in the neural network toolbox for MATLAB.

I – **M-file for training of multilayer perceptron artificial neural network (MLPNN) for generator out of step prediction scheme**

```
P=[0.0118 0.0141 0.0072 0.0072 0.0059 0.0055 0.0035 -0.0001 0.0030 0.004];
net=newff([-1 1],[1 2 1],{'purelin' 'tansig' 'purelin'}); T=[1 1 1 1 1 0 0 0 0 0];
net.trainParam.epochs=600; net.trainParam.goal=1e-5;
net.trainParam.min_grad=0; net.trainParam.max_fail=10;
net.trainParam.mu=0.001; net.trainParam.mu_max=1e10;
net=train(net,P,T);
```

II – **M-file for training of MLPNN for prediction of transient stability status of a power system**

```
P=[0.0324 0.0326 0.0155 0.0165 0.0047 0.0019];
net=newff([-1 1],[1 2 1],{'purelin' 'tansig'
'purelin'}); T=[1 1 1 1 0 0];
net.trainParam.epochs=600;
net.trainParam.goal=1e-5;
net.trainParam.min_grad=0;
net.trainParam.max_fail=10;
net.trainParam.mu=0.001;
net.trainParam.mu_max=1e10;
net=train(net,P,T);
```

III – **M-file for training of MLPNN 1 for the prediction of coherent generator groups** P=[x1c1 x1c2 x1c3 x1c4 x1c5 x1c7 x20c1 x20c3];

```
net=newff([0 0.1;0 0.1;0 0.1],[3 4 1],{'purelin' 'tansig'
'purelin'}); T=[1 1 0 0 0 1 1 1]; net.trainParam.epochs=600;
net.trainParam.goal=0.01; net.trainParam.min_grad=0;
net.trainParam.max_fail=10;
net.trainParam.mu=0.001; net.trainParam.mu_max=1e10;
net=train(net,P,T);
```

KNUST
NYANSAPO WO SANE NO BADWENHWA